UNIVERSITY OF CALIFORNIA MERCED

Life Cycle Greenhouse Gas Emissions of Electricity Generated from Solar Updraft Towers

A Thesis submitted in partial satisfaction of the requirements
for the degree of Master of Science

in

Mechanical Engineering

By

Farhana Sharmin

The committee in charge:

Professor Marie-Odile Fortier, Chair
Professor Abel Chuang
Professor Jeanette Cobian-Iñiguez

2021

The Thesis of Farhana Sharmin is approved, and it is acceptable
in quality and form for publication on microfilm and electronically:

Professor Marie-Odile Fortier, Chair

Professor Abel Chuang, Thesis Committee Member

Professor Jeanette Cobian-Iñiguez, Thesis Committee Member

University of California, Merced

2021

ACKNOWLEDGEMENT

This thesis would not be possible without the teaching and guidance of the faculty at the University of California Merced. I would especially like to thank Dr. Marie-Odile Fortier for serving as my patient and helpful academic advisor; Dr. Abel Chuang for teaching Fuel Cell Fundamentals, Modeling, and Diagnostic, Convective Heat and Mass Transfer and serving on my thesis committee; and Dr. Jeanette Cobian-Iñiguez for teaching Fundamentals - Wildfire Dynamics and her kind service on my committee. The incredibly helpful staff members at UC Merced were also the people I would like to thank.

I am grateful to all the authors whose published works and other resources I found immensely helpful while completing this thesis. Most importantly, I'd like to express my gratitude towards my mother, other family members, and friends who supported me mentally and emotionally throughout this whole process to make it possible for me to earn this Master's degree.

TABLE OF CONTENTS

LIST OF ILLUSTRATIONS

LIST OF TABLES

Abstract

Life cycle greenhouse gas emissions of electricity generated from solar updraft towers, Farhana Sharmin, Master of Science in Mechanical Engineering, University of California Merced, 2021, Marie-Odile Fortier.

The solar updraft tower power plant (SUTPP) is a technology that combines wind and solar energy and has been proposed for future utility-scale installation in arid climates such as the southwestern United States. To assess its potential global warming impact and compare its life cycle greenhouse gas (GHG) emissions against alternative electricity sources, a geospatial life cycle assessment (LCA) was performed for a solar updraft tower energy system for ten different case study locations in five states in the Southwest United States: Arizona, California, Nevada, New Mexico, and Texas. This is the first study to incorporate location-specific solar radiation, ambient temperature, and thermal energy storage in the soil at 1-hour time intervals into an LCA model of this technology to calculate its electricity generation and life cycle GHG emissions. Scenarios were also developed modeling solar photovoltaic (PV) panel coverage on a small percentage of the collector area to determine how much the life cycle impacts vary for a solar updraft tower system with and without PV. Without PV incorporated into the system, the total life cycle GHG emissions ranged from 29.74 g CO_{2eq}/kWh electricity to 33.82 g CO_{2eq}/kWh electricity for the 10 locations, and when 2.0% of the collector area is covered by solar PV panels, the total life cycle GHG emissions ranged from 30.36 g CO_{2eq}/kWh electricity to 34.36 g CO_{2eq}/kWh electricity. The site-by-site comparison demonstrates that the climate change impacts with solar PV were generally slightly higher than the stand-alone SUTPP systems for every studied location. Sensitivity analyses show that the operational lifetime of the system is the single most sensitive variable for both the stand-alone system and the hybrid system. For the stand-alone system, turbine efficiency is the next most sensitive parameter and for the hybrid system, the next most sensitive parameters are performance ratio followed by turbine efficiency. This study suggests that the potential life cycle GHG emissions from SUTPPs can be notably lower than fossil fuel (~15 times lower than natural gas and ~31 times lower than coal) and so implementation of SUTPPs may reduce global warming impacts of electricity generation in the southwest regions of the US.

Keywords: Life cycle assessment, solar updraft tower, solar PV, southwestern US, greenhouse gas emission, electricity generation model

CHAPTER-01

INTRODUCTION

1. Introduction

1.1. Solar Updraft Tower Power Plant (SUTPP)

As concerns about harmful greenhouse gas emissions as well as the depletion of fossil fuel-based resources have risen, many nations have taken necessary measures for transitioning to renewable energy to mitigate climate change. Novel and sustainable energy technologies that can utilize abundant natural resources can contribute towards this goal (Mazzeo et al., 2020). One promising technology that requires further study is a solar updraft tower power plant (SUTPP). SUTPP technology combines two major renewable energy sources simultaneously: wind and solar energy, and is comprised of three main components that are the collector, the tower, and the turbines (Figure 01) (Nizetic et al., 2008). Incident solar radiation on the collector surrounding the tower heats the air underneath, causing it to flow and rise into the central tower. A turbine located near the bottom of the tower rotates as the hot air flows into the tower, and the rotational mechanical energy is subsequently converted to electrical energy (Schlaich et al., 2005).

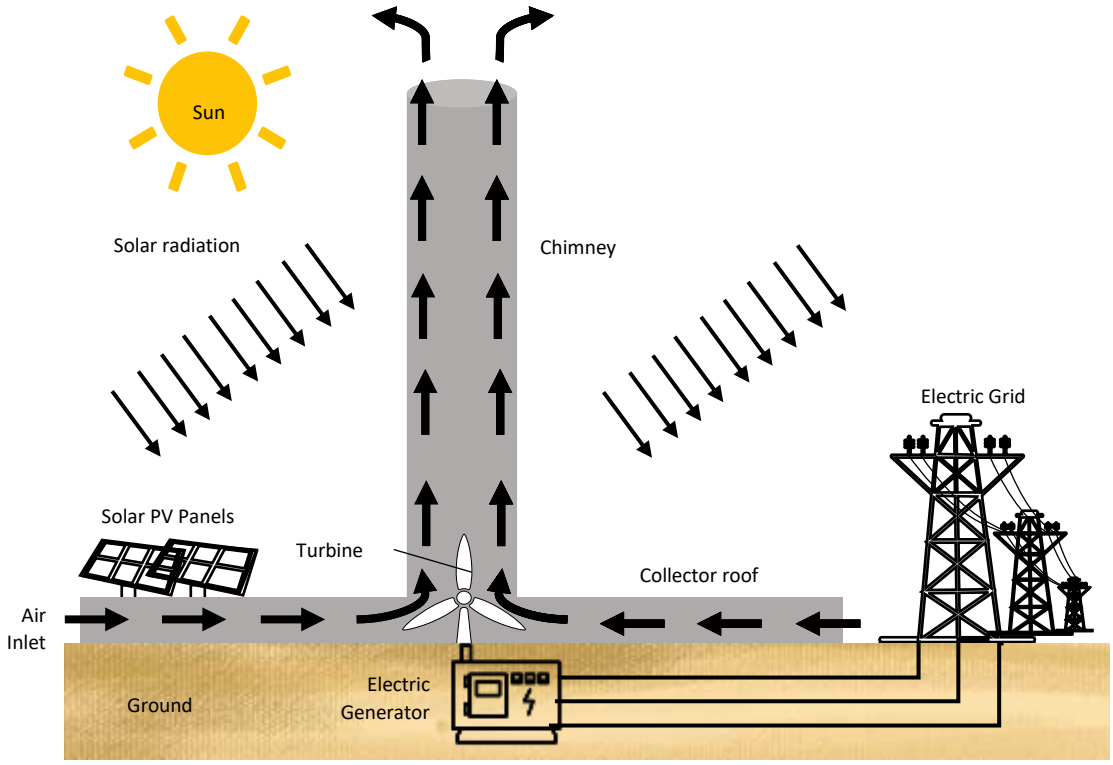

Figure 01: Schematic diagram of the working principle of solar updraft tower inspired from Nizetic et al., (2008) (Nizetic et al., 2008).

Building a solar updraft tower of even 1,000 m in height can be possible as there are already stable structures that are close to this height (Schiel & Schlaich, 1996). It is

believed that the lifespan of a reinforced concrete tower like this can exceed up to 100 years in a dry climate, although it is not yet established as a realistically achievable lifetime for large concrete towers (Schiel & Schlaich, 1996). There have been previous prototypes that have informed improvements to SUTPP design and materials. Between 1982 and 1989, the experimental plant in Manzanares, Spain, operated for about 15,000 hours (Schiel & Schlaich, 1996), but ultimately, the cables rusted due to corrosion, and the chimney broke and fell in a storm (Francesca Lupi et al., 2011).

It was also found that a solar chimney's performance is primarily determined by the types of materials that can be used for the collector roof, and therefore, different materials, designs, and building methods for the roof were tested in the prototype at Manzanares (Francesca Lupi et al., 2011). Another finding from this prototype was that resistance to wind action was the most influential factor in the tower design. A study performed by Francesca Lupi et al., (2015) found that applying stiffening rings along the tower can enhance the structural stability, decreasing the effects of structural stress from wind (F Lupi et al., 2015).

Still, in a solar updraft tower, the turbine blades themselves normally do not face any critical loading. This makes the components structurally simple and long-lasting. The turbines generally have a lifespan of 25 years (Schiel & Schlaich, 1996), which is comparable to other renewable energy systems. SUTPPs do not require water for cooling purposes, unlike concentrated solar power (CSP) plants that also use solar radiation as an energy source. CSP plants are also well-suited for utility-scale electricity generation in hot desert lands, though they typically have minimal water resources (Van Blommestein & Mbohwa, 2013).

Despite these potential advantages over CSP, SUTPP towers can be high-rise and the collector areas can be much larger relative to CSP plants. A prototype in Jinshawan, Mongolia, that started with an average power output of only 200 kW had a 200 m high chimney and a collector area of 196,270 m^2, operated till 2013. Before shutting down, this project aimed to ultimately expand it to a much larger system that would be capable of delivering 27.5 MW power output, occupying a total of 2.78 million m^2 area of a desert (Al-Dabbas, 2012; Ming et al., 2007; Nizetic et al., 2008). Previously a different but similar case study performed in Northwestern China concluded that with a chimney height of 200 m and chimney diameter of 10 m, SUTPP can produce 110-190 kW of electric power (Nizetic et al., 2008).

Although the idea of the SUTPP was first proposed in 1903, the only installations thus far have been prototypes: the original prototype of 50 kW installed in Spain in 1982, the 200 kW prototype installed in Mongolia in 2009, a similarly-sized prototype in Northwestern China, and a 800 W prototype in Baghdad, Iraq(Al-Dabbas, 2012; Bernardes, 2004; Chaichan et al., 2018; Francesca Lupi et al., 2011; Nizetic et al., 2008). No SUTPP has yet been installed at a commercial scale. In 2010, there was a plan of constructing two 200 MW solar updraft towers in Arizona that was never implemented (Al-Dabbas, 2012). Similarly, The government of Namibia approved a proposal for a 400

sMW solar updraft tower with a tower of 1.5 km height and 280m diameter inside which crops were planned to be grown, but it has not yet been put into action (Al-Dabbas, 2012). Before utility-scale installations of SUTPPs are planned, the carbon footprint of this technology must be determined using life cycle assessment (LCA). LCA is a holistic, quantitative, and widely used method for measuring environmental impacts along the life cycle of a given system that is crucial to estimating the long-term sustainability of a system (Chang et al., 2014).

1.2. Contribution of This Study:

There have not been many LCAs performed on SUTPPs (Bernardes, 2004; Van Blommestein & Mbohwa, 2013; Zongker, 2013). Thus far, existing LCAs on SUTPPs were carried out for European and East Asian conditions, but climatic conditions vary between locations, which can lead to different electricity generation over the lifetime of a SUTPP and subsequently, different amounts of life cycle greenhouse gas emissions per kWh from even the same scale technology. Bernardes (2004) compared the life cycle impacts of a 50 kW SUTPP with a 194.6 m high tower against different renewable energy resources for a state in Germany. It was a theoretical study that was done by using a mathematical model involving a non-linear approximation method to scale up the solar updraft tower power system hypothetically to 5 MW, 30 MW, and 100 MW capacity systems. This study showed that increasing the power capacity from 5 MW to 100 MW reduced the CO_2 emissions from 170 to 70 g CO_{2eq}/kWh. However, that study was not site-specific and did not investigate the impacts of climatic factors like solar radiation and temperature on LCA results (Bernardes, 2004).

Van Blommestein & Mbohwa (2013) focused their study on the prototype in Manzanares, Spain, and determined that the life cycle greenhouse gas emissions associated with the SUTPP located at Manzanares were around 25.9 g CO_{2eq}/kWh, with the manufacturing and the construction phases comprising the majority of emissions while the operational and end of the life stages have minimal impact (Van Blommestein & Mbohwa, 2013). This carbon footprint is comparable to the emissions from wind energy systems (Dolan & Heath, 2012; Liu & Barlow, 2016; Zongker, 2013). Similar to the Bernardes (2004) study, this LCA concluded that scaling up the capacity increases electricity output, leading to a substantial decrease in the emissions per unit of electrical energy (Bernardes, 2004). This study also showed minimal geographic specificity in its calculation approach. The electricity output model in their LCA only had one climatic variable, global horizontal radiation, which was not varied over space and time (Van Blommestein & Mbohwa, 2013).

Also in 2013, Zongker and Ahmed performed an LCA of SUTPPs in which they tested different types of power plant construction designs for the same location to compare their resulting life cycle greenhouse gas emissions (Zongker, 2013). That study concluded that solar updraft towers have a lower global warming potential (GWP) than solar photovoltaics. Additionally, it was found that the construction process has

comparatively lower impacts and the GWP can be recovered within only 1.8 to 3.4 years of operation. The biggest contributors were the collector followed by the tower, the turbine, and the generator system (Zongker, 2013). Other studies like Niemann et al., (2009) focused heavily on design consideration and service life rather than the climatic conditions and mentioned that with a lifetime between 80 to 120 years, the CO_2 emissions can be reduced to around 10 g CO_{2eq}/kWh of electricity generation. However, this estimated lifetime is only based on the design of the structure, not based on the mechanical and electrical performance of the SUTPP energy system (Niemann et al., 2009).

In addition to these LCAs, there have been studies on the potential electricity generation by SUTPPs in selected climates. Nizetic et al., (2008) studied the feasibility of a SUTPP for the Mediterranean climate and chose two locations in Croatia for their analysis (Nizetic et al., 2008). This study used the Schiel & Schlaich (1996) model that uses incident global solar radiation and ambient temperature as environmental parameters to calculate electricity generation (Schiel & Schlaich, 1996). For a solar updraft tower power plant with a chimney height of 550 m and a collector diameter of 1250 m, the prediction was that a power plant of this size would produce 2.8 to 6.2 MW of power, where the average annual electricity generation would range between 4.9 and 8.9 GWh of electricity per year in the average Mediterranean climatic conditions. However, using the actual climatic data like temperature and solar radiation of their selected locations: Split and Dubrovnik in Croatia, in their model their calculation showed a solar updraft tower of that size would be able to generate from 5.0 to 6.0 GWh of electricity per year on average where their considered lifespan of the power plant was between 20 years and 40 years (Nizetic et al., 2008). This analysis was done using the general metrological data like temperature and solar radiation that are needed for the Schlaich model, for Split and Dubrovnik in Croatia, not for any actual prototype (Nizetic et al., 2008; Schiel & Schlaich, 1996).

There have been numerous pilot-scale or small-scale laboratory setups for studying solar updraft tower technology in different parts of the world (Afonso & Oliveira, 2000; Aurybi et al., 2006; Choi et al., 2015; Haaf et al., 1983). However, despite having suitable conditions for the performance of this technology in the Southwest part of the US, there has not been any study performed for this climatic condition, let alone any LCA to determine the environmental impacts of SUTPPs for this geographic location.

As of 2014, the Bureau of Land Management (BLM) administered a massive amount of land in the southwestern United States for several solar energy projects due to the highly favorable conditions for solar energy, available public and private lands, and ease of transportation and infrastructural development (Grippo et al. 2015). According to a study on climatology on solar irradiance from 2019, the southwestern part of the US has the lowest ratio of diffused to direct solar radiation and the lowest level of cloud coverage in the US, meaning a very high amount of direct solar radiation with clear sunlight exposure (Kafka & Miller, 2019). Arizona, California, Nevada, New Mexico, and Texas

are particularly well-suited for SUTPP technology with a 15-year average direct solar irradiance of approximately 5 kWh/m^2 to 9 kWh/m^2 (Kafka & Miller, 2019).

Furthermore, SUTPP installations present a unique opportunity to combine different types of solar electricity generation systems and increase renewable energy harnessed per unit area of land occupied as the collectors can be partially covered with solar photovoltaics (PV). Eryener & Kuscu (2018) worked on the experimental performance of a hybrid solar updraft tower and solar PV prototype, where PV modules cover 42% of the transpired solar collector area (Eryener & Kuscu, 2018). In this analysis, the turbine power was 200 W whereas the total photovoltaic capacity on 42% of the 110 m^2 collector area was 7420 W, and the average recorded power of the system was 5215 W (Eryener & Kuscu, 2018). Over an observation period of 18 months, a roughly 2% increase in efficiency in the hybrid system was measured compared to a stand-alone solar updraft tower system (Eryener & Kuscu, 2018). Their reported solar power utilization efficiencies of the hybrid system were between 16% and 18% which seems to be almost a hundred times more efficient than the solar power conversion efficiency of conventional solar updraft tower systems that are currently or were previously in action (Eryener & Kuscu, 2018).

This study presents the first geographically specific LCA for a utility-scale SUTPP modeled in the Southwest US. Previous studies of the life cycle greenhouse gas emissions from solar updraft tower systems relied on laboratory scale models or prototypes and the results obtained from them cannot be easily scaled up for utility-scale power plants and also are not applicable for different parts of the world (Al-Kayiem & Aja, 2016; Choi et al., 2015; Kasaeian et al., 2017; F Lupi et al., 2015). The purpose of this study is to investigate the cradle-to-grave life cycle greenhouse gas emissions associated with SUTPP generating electricity in the Southwest US region, using several locations as case studies. This study also accounts for the nighttime electricity generation caused by the heat stored in the soil under the collector (dos Santos Bernardes, 2013; Göğüş, 2006; Guo et al., 2016). This analysis uses location-specific solar radiation, soil temperature, ground temperature, and ambient temperature to determine the overall electricity output and the carbon footprint of this technology, and so with proper data sources, this model can be applied to other parts of the world if the environmental data is available as well. Not only that, the model is built in a way that makes it convenient to change different parameters as needed, allowing it to be flexible to new information gathered over time on this emerging technology.

CHAPTER-02

METHODS

2. Methods

2.1 Life Cycle Assessment (LCA)

Life cycle assessment (LCA) is considered the most standardized, established, and system-oriented tool for measuring the potential environmental impacts of a system or product, or service utilizing a life cycle perspective (Jolliet et al., 2003; Kim et al., 2019). LCA follows the International Organization for Standardization (ISO) 14040 and 14044 standards and is intended to be used for comparative analyses (Finkbeiner et al., 2006; Standardization, 2006). LCA involves defining goals and scope, analyzing inventory, assessing various impacts, and interpreting stages (Jolliet et al., 2003; Kim et al., 2019). ISO 14040 suggests an iterative route for performing LCA, meaning that the results and interpretations may lead to further modifications and refining of the system, data, and approaches for new iterations of an LCA model (Finkbeiner et al., 2006; Gathorne-Hardy, 2013a).

Life cycle impacts include contributions from various sources and processes like raw materials, transportation, manufacturing, assembly, operational activities, and end-of-life management. All the contributing effects are aggregated to represent the impact of a certain product or service or system throughout its life cycle (Guinée & Lindeijer, 2002). Generally, LCA results of different systems and technologies that provide the same function are comparable to each other, and so LCA results for one energy system can be compared to any other energy system when scaled to the same functional unit (M. W. Ryberg et al., 2016). Further discussion on the functional unit for the studied system can be found later in this paper.

2.2. Goal and Scope Definition

The goal and scope definition phase of a life cycle assessment (LCA) study requires the purpose of the study and decisions regarding the details of the system (Curran, 2017). The purpose of this study is to assess the global warming potential of electricity generated by a solar updraft tower power plant (SUTPP) and compare the findings with other renewable and non-renewable energy systems suitable for the Southwestern United States (US). This analysis takes into account the geospatial aspects of this technology and the results are intended to be used for assessing the sustainability of establishing this technology in suitable geographic locations with arid climates and warm weather with abundant exposure to solar radiation (Berardy & Chester, 2017). The intended audience of this LCA study is the scientific community, policymakers, regulators, and individuals and businesses planning to install renewable energy projects with lower life cycle greenhouse gas emission emissions. The overall step by step processes involved in this study can be best described by the flow chart shown in figure 02.

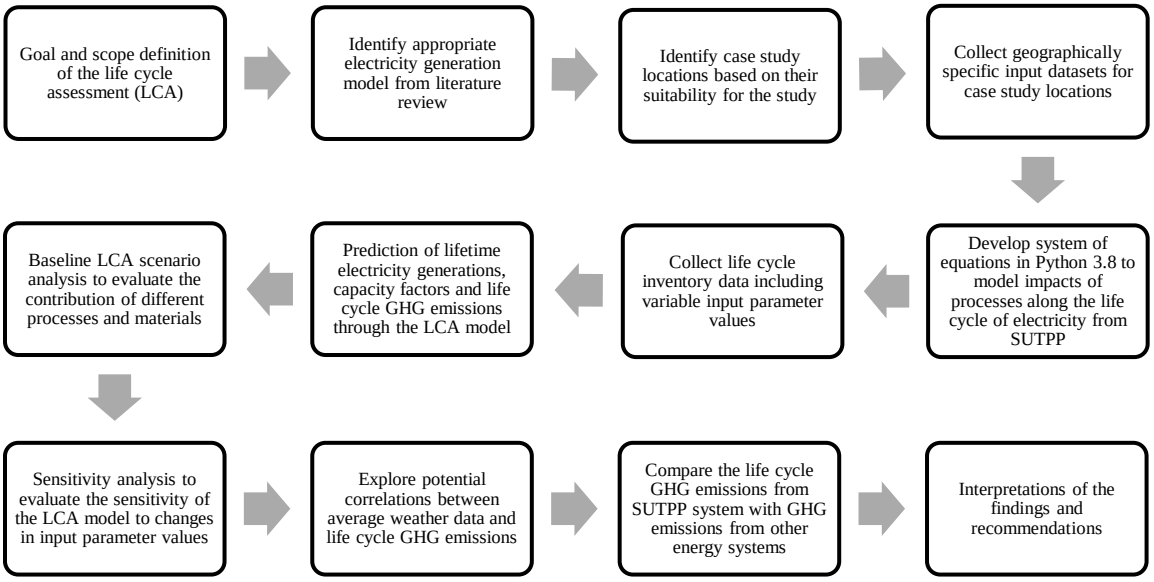

Figure 02: Flowchart of the steps involved in this life cycle assessment study.

The EPA TRACI 2.1 life cycle impact assessment method was used to assess the life cycle climate change impacts of all the processes analyzed in the study (Morelli et al., 2018; M. Ryberg et al., 2014). Global warming potential was chosen as the sole impact category because a primary goal of installations of novel renewable energy sources like SUTPPs is reducing the climate change impacts of energy provision (Ludin et al., 2018).

A cradle-to-grave scope was used in this study because for a renewable energy system of this size, the end of life management would be of interest to its target audience (Góralczyk, 2003; Ludin et al., 2018). An LCA model for a utility-scale SUTPP was developed for this analysis, as past studies have shown how larger scales can translate to higher environmental sustainability for SUTPP technology (Nizetic et al., 2008; Van Blommestein & Mbohwa, 2013). This LCA study is geographically based in the southwestern United States, with case studies modeled for 10 locations (Figure 03). The selection of the locations was based on the appropriateness of climates under a few selected classes of Level 3 ecoregions of the continental United States: the Mojave Basin and Range, Sonoran Desert, Arizona/New Mexico Mountains, Arizona/New Mexico Plateau, Madrean Archipelago, Chihuahuan Desert, Edwards Plateau, and Southern Texas Plains/Interior Plains and Hills with Xerophytic Shrub and Oak Forest. (*Southwest USA Landscapes - Deserts*, n.d.). These ecoregions cover several areas of Arizona, California, Nevada, New Mexico, Texas, and Utah.

Figure 03: Approximate point locations showing the geographic sites of the case study

The next criteria for the case study locations selected were the availability of solar radiation and ambient temperature data at a fine-scale interval. Only locations with weather data at 1-hour increments from quality-controlled environmental datasets from the National Oceanic and Atmospheric Administration (NOAA) were considered (Diamond, Karl, Palecki, Baker, Bell, Leeper, Easterling, Lawrimore, Meyers, & Helfert, 2013). The selection of the datasets from NOAA first involved reviewing the data quality. The locations that included incomplete, impossible (e.g., negative or beyond realistic ranges), or null values for solar radiation and temperature data were excluded from the analyses in this study. Because the LCA model developed for this study used hourly environmental data to constitute conditions for a representative year, the datasets that had missing or unworkable values were completely excluded since methods like interpolation to fill in the data gaps may lead to misleading interpretations of the results. The year 2020 was selected as a representative year for this analysis. The raw datasets from 2020 were extracted from the NOAA website and converted into data tables in Microsoft Excel. A thorough inspection was performed to see whether there are any discrepancies in the data and the workable complete datasets were transferred into a text file in order for them to be accessed and used by the LCA model in Python code (Bell et al., 2013; Diamond, Karl, Palecki, Baker, Bell, Leeper, Easterling, Lawrimore, Meyers, & Helfert, 2013).

Only 10 locations had their complete set of hourly data for the year 2020, available on the NOAA website, and were within the selected Level 3 ecoregions in the southwest US. The selected studied scenarios that met the criteria were: Elgin, Tucson, Williams, and Yuma in Arizona; Stovepipe Wells in California; Las Cruces and Socorro in New Mexico; Mercury in Nevada; and Monahans and Panther Junction in Texas. It should be clarified that these selected locations do not represent the specific future sites for building utility-scale SUTPPs, but they merely represent the regions with very similar climate in the southwest due to the availability of climatic data at the NOAA website since two of these sites are located in preserved National Park areas (Death Valley National Park, CA and Big Bend National Park, TX).

2.3 Functional Unit

LCAs scale their results to a functional unit, that is constituted by the function of the system at any given time (Kim et al., 2019). As the function of SUTPPs is to provide useful electrical energy, the functional unit was chosen for this study is 1 kWh of electricity provided to the grid. This functional unit is consistent with the vast majority of electricity generation LCAs and enables the comparison of the results in units of kilograms of CO_{2eq} emitted per kWh of net electricity generated. Previous LCAs of solar updraft tower systems have also set functional units like 1 MWh or 1 GWh of electricity output, which are just the larger scale of this same functional unit (Van Blommestein & Mbohwa, 2013; Zongker, 2013).

2.4 Life cycle inventory and system description

A commercial-scale SUTPP system that has similar dimensions to that described in (Schlaich et al., 2005) was modeled in this study with slight modifications to meet the design criteria. The SUTPP system in this study is comprised of a 10 MW turbine and generator and transmission cables of the same capacity. The SUTPP has a tower height of 550 m, a tower diameter of 200 m, a tower thickness of 0.25 m, a collector diameter of 1250 m, and a collector glass thickness of 0.005 m, with a graded depth into the ground of 1.0 m (Schlaich et al., 2005). The average lifetime of the SUTPP modeled in this LCA is 25 years to reflect the typical design lifespan of an installed SUTPP. Van Blommestein & Mbohwa's (2013) analysis from 2013 has used 30 years as their service period to be studied (Van Blommestein & Mbohwa, 2013).

The raw materials used in the production, treatment, and machining of the materials, manufacturing, and assembly of the components, construction, operation, and maintenance, and end-of-life management of the materials were all included in the LCA model. LCAs of concentrated solar power (CSP) systems that have a similar system boundary show that transportation has minimal contribution to the overall climate change impact (Alhaj & Al-Ghamdi, 2019; Corona et al., 2014). Therefore, “market for” inventories from Ecoinvent 3 were used instead of measuring distances and modeling transportation impacts separately because they include a global average transportation

impact. Similar to the LCAs of CSP systems where the physical system boundary ends at the diameter of the outermost series of mirror placement (Burkhardt III et al., 2012); (Ko et al., 2018), the electricity transmission is modeled only to the outer edge of the collector and subsequent distribution is not included in the system boundary. The complete system diagram illustrating the cradle-to-grave process flows is shown in Figure 04.

All the required information needed for a turbine of 10 MW capacity that can be used for solar updraft tower system is not yet available and so the relevant components of a 10 MW wind turbine were used as a proxy (Penghua Guo et al., 2017; Sethuraman et al., 2017). For the 10 MW SUTPP, the mass of a single blade of a 10 MW wind turbine was obtained from Sethuraman (2017) as 24.928 tonnes and there are 3 blades in the turbine (*MHI Vestas Offshore V164-10.0MW - 10,00 MW - Wind turbine*, n.d.; Sethuraman et al., 2017). The turbine rotor diameter was 164.0 m and the swept area of 21,124.0 m^2 would fit as placed at the bottom of the 31,416 m^2 tower. The materials used to manufacture the blades were glass fiber (65-75%) and epoxy resin composites (25-35%) (Mishnaevsky Jr & Favorsky, 2011). The nacelle material was not considered as inventory in this study since for a Solar Updraft Tower system it is not applicable unlike wind power systems (MHI Vestas Offshore V164-10.0MW - 10,00 MW - Wind turbine, n.d.).

The total weight of the turbine blades and the weight of the generator were used to compute the amount of material used in the manufacturing and construction of the power plant using the average material percent composition. Turbine blade manufacturing involves resin infusion technology whereas epoxy resin goes through injection molding or vacuum-assisted resin transfer molding (Mishnaevsky et al., 2017), which were also modeled as part of the analysis.

The generator is comprised of steel, copper, and a permanent magnet. The required material for this 10 MW generator is 54 t of iron, 9 t of copper, 4.96 t of permanent magnet (Sethuraman et al., 2017). A 66,000 V synchronous direct-drive permanent magnet generator was used for the 10 MW turbine generator system in the SUTPP (MHI Vestas Offshore V164-10.0MW - 10,00 MW - Wind turbine, n.d.). The generator is manufactured through processes such as punching and bending of steel sheets, fabrication or grinding, powder coating, heat treatment, and finally assembly (Manufacturing Process | Powerline :: Kirloskar Green Generator Manufacturer in North East India, n.d.). These were also included in the LCA model. The electric cables that are used in the system are comprised of plastic, copper, and aluminum (Jensen, 2019).

The fractions of materials that are recycled instead of landfilled were obtained from external industry sources, as were the required machining and treatment processes for the metals and plastics needed for the component manufacturing. Generally, 90% of copper is recycled at the end of life (Copper Development Association, 2019). For aluminum, steel, and plastic, the recycled material percentage was around 51.0%, 40.5%, and 8.5%, respectively (Janajreh et al., 2015). Turbine blades themselves are not recycled at the end of their lives and the materials are recycled separately. A huge portion of turbine blade materials, mainly glass-fiber and epoxy, are supposed to be recycled (up to 45-50%), and the remaining waste created from them would be considered inert waste.

Theoretically, 80% of the turbine materials could be recovered (Cousins et al., 2019). Table 1 represents the life cycle "market for" inventories that were integrated into the Python-based LCA model.

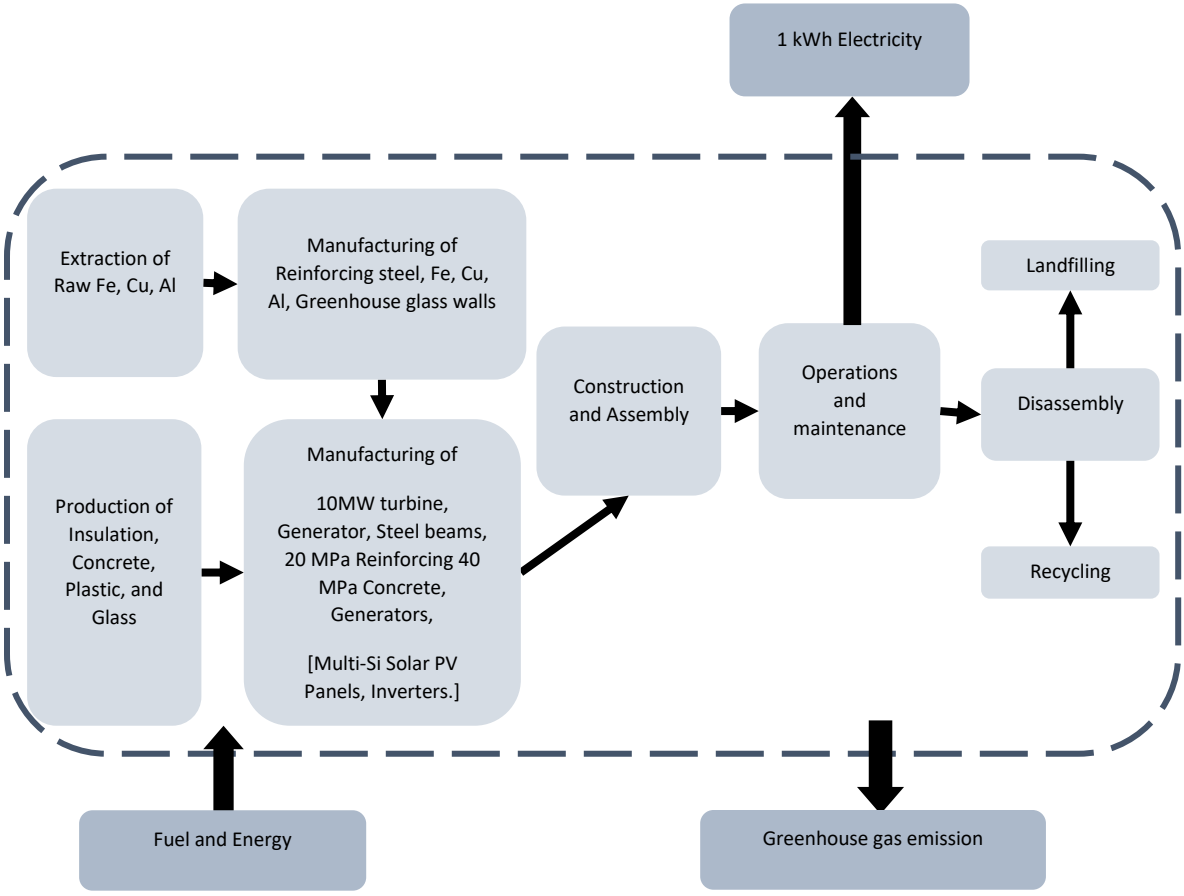

Figure 04: Cradle-to-grave system diagram of the modeled SUTPP system (Materials mentioned within third bracket [ ] are applicable for only the SUTPP- Solar PV Hybrid system).

In the life cycle inventory phase sometimes water usage is reported depending on the type of the system, type of use, source of water, etc. It is especially important when ecotoxicity is being considered as an impact category in the analysis and the LCA points to a potential concern due to water usage in the area unlike our case (Pfister et al., 2009; Schiel & Schlaich, 1996). Chaichan et al., (2018) found that the transparency of solar collector systems play an important role in their prototype of 4 m tall, 10 m diameter collector solar updraft tower's performance in the heavily dusty atmosphere of Baghdad, Iraq where sand and dust storms are very frequent (Chaichan et al., 2018; Sissakian et al., 2013). Depending on how close the washing periods are, they observed a 2% to 5%

efficiency improvement for their 800 W capacity solar updraft tower system based in Iraq (Chaichan et al., 2018).

The sand and dust deposition along with the sand and dust storm are very frequent and harsh in Baghdad, Iraq and so dust deposition can be a major concern for a location similar to that (Sissakian et al., 2013). The dust depositions and dust storms in the southwestern United States are much tamer and occur mostly during certain times during the summer and fall seasons unlike in Iraq where dust deposition is an all-year-round occurrence. Moreover, the dust deposition in the winter and spring seasons was found to be negligible compared to summer and fall dust deposition for eastern Colorado Plateau and Mojave–southern Great Basin (Reheis & Urban, 2011; Sissakian et al., 2013). The overall dust particle size for the southwest US (10 μm to 53 μm) was also found to be much larger than the average dust particle size in Iraq (2 μm to 3.5 μm) making it harder to blow in the wind (Abdulla et al., 1988; Reheis & Urban, 2011). And so based on the lower severity of dust in our studied locations, dust deposition impact was not a part of the analyses, and water usage impact to clean the dust deposition on top of the collector glass was also excluded.

Table 01: Life cycle inventories characterized through EPA TRACI and extracted from SimaPro to be used in this LCA. All chosen inventories are from the Ecoinvent 3 database (except for end-of-life management of copper, which is from an LCA of Copper tube and sheet (The Copper Development Association, 2019)), "market for" inventories, and APOS (at point of substitution). All are either labeled RoW (rest of world) or GLO (global) and (S) stands for the system.

Materials and Processes	Units
Aluminum scrap production, RoW APOS S	kg CO_{2eq}/kg
Copper production, primary, RoW APOS S	kg CO_{2eq}/kg
Cast iron production, GLO APOS S	kg CO_{2eq}/kg
Engineering Steel production, RoW APOS S	kg CO_{2eq}/kg
Three conductor cable production, GLO APOS S	kg CO_{2eq}/m
Greenhouse glass walls production, RoW APOS S	kg CO_{2eq}/m^2
20MPa concrete production, RoW APOS S	kg CO_{2eq} /m^3
40MPa concrete production, RoW APOS S	kg CO_{2eq}/m^3
Epoxy resin production, RoW APOS S	kg CO_{2eq}/kg
Sand production, quarry operation, RoW APOS S	kg CO_{2eq}/kg
Cable yarding, RoW APOS S	kg CO_{2eq}/hour
Construction machine operation using diesel, RoW APOS S	kg CO_{2eq}/hour
Waste brick treatment, RoW APOS S	kg CO_{2eq}/kg
Waste 20MPa concrete disposal, RoW APOS S	kg CO_{2eq}/kg
20Mpa Concrete recycling, RoW APOS S	kg CO_{2eq}/kg
Waste Reinforced concrete 40MPa disposal, RoW APOS S	kg CO_{2eq}/kg

Reinforced concrete 40Mpa recycling, RoW APOS S	kg CO_{2eq}/kg
Waste glass disposal, unsorted, RoW APOS S	kg CO_{2eq}/kg
Plastic production, RoW APOS S	kg CO_{2eq}/kg
Glassfibre production, polyester resin, GLO APOS S	kg CO_{2eq}/kg
Permanent magnet, for electric motors, GLO APOS S	kg CO_{2eq}/kg
Glass disposal, unsorted, RoW APOS S	kg CO_{2eq}/kg
Steel disposal, RoW APOS S	kg CO_{2eq}/kg
Steel recycling, RoW APOS S	kg CO_{2eq}/kg
Iron disposal, RoW APOS S	kg CO_{2eq}/kg
Iron recycling, RoW APOS S	kg CO_{2eq}/kg
Plastic disposal, RoW Cut-off S	kg CO_{2eq}/kg
Plastic recycling, RoW APOS S	kg CO_{2eq}/kg
Composite waste disposal, RoW APOS S	kg CO_{2eq}/kg
Composite waste chemical recycling, RoW APOS S	kg CO_{2eq}/kg
Aluminum scrap disposal, RoW APOS S	kg CO_{2eq}/kg
Aluminum recycling, RoW APOS S	kg CO_{2eq}/kg
Copper End of the Life	kg CO_{2eq}/kg
Forging steel, GLO APOS S	kg CO_{2eq}/kg
Hot rolling steel, GLO APOS S	kg CO_{2eq}/kg
Impact extrusion steel, GLO APOS S	kg CO_{2eq}/kg
Impact extrusion aluminum, GLO APOS S	kg CO_{2eq}/kg
Sheet rolling aluminum, GLO APOS S	kg CO_{2eq}/kg
Sheet rolling copper, GLO APOS S	kg CO_{2eq}/kg
Wire drawing copper, GLO APOS S	kg CO_{2eq}/kg
Multi-Si PV panel production, GLO APOS S	kg CO_{2eq}/m^2
Multi-Si PV panel recycling, GLO APOS S	kg CO_{2eq}/m^2
Multi-Si PV panel disposal, RoW APOS S	kg CO_{2eq}/kg (1.0 kg/10.4 m^2)
Inverter (18 Pieces for 9000 kW), GLO APOS S	kg CO_{2eq}/piece (500 kW each)

2.5. SUTPP electric power generation model selection

The literature on existing SUTPP electricity generation models was reviewed to select the best fit to calculate electricity generation by a SUTPP based on location-specific environmental data within the LCA model (Table 2). Several different models have been developed in other studies to determine electricity generation for SUTPP technology, which were based on different types of construction designs and different scales of the system.

Table 02: Studied electric power generation models for solar updraft tower power plants that include (a) solar radiation; (b) pressure drop rate; (c) ambient temperature; (d) wind or air flow rate, and (d) heat stored in the soil as inputs or intermediates for calculating electric power generation from solar updraft tower systems.

Study	Geographic locations	Solar Radiation	Pressure drop rate	Ambient Temperature	Air flow rate	Heat Stored in Soil
Alfonso et. al. 2000	Portugal	✔	✔		✔	
(Ayub et al., 2018) [a]	Bangladesh	✔	✔		✔	
(Bernardes, 2004)	Manzanares, Spain	✔		✔		
(Gannon & von Backstro¨ m, 2000)	South Africa	✔		✔		
(G. Li et al., 2019) [b]	China	✔	✔	✔		✔
(Francesca Lupi et al., 2011) [a]	Manzanares, Spain	✔	✔		✔	
(F Lupi et al., 2015)	Aswan, Egypt	✔		✔		
(Mehla et al., 2019)	Panchkula, India	✔	✔	✔		
(Ming et al., 2007)	Jinshawan, Mongolia	✔	✔		✔	
(Niemann et al., 2009) [c]	Manzanares, Spain	✔				
(Nizetic et al., 2008)	Split and Dubrovnik, Croatia	✔		✔		
(Padki & Sherif, 1999)	Florida, US	✔		✔		
(Penghua Guo, Wang, Li, et al., 2016)	Yinchuan, China	✔		✔	✔	✔
(S. Li, 2017)	Jinshawan, Mongolia	✔	✔		✔	
(Van Blommestei	Manzanares, Spain	✔		✔		

n & Mbohwa, 2013)						
(von Allwörden et al., 2018)	Winnipeg, Canada	✔		✔	✔	
(Zhou & Xu, 2016)	Yinchuan, China	✔	✔	✔		✔
(Zongker, 2013)	Manzanares, Spain	✔		✔		

In certain studies, the SUTPP scale of the model was too small for this analysis. For example, (Mehla et al., 2019) performed an analysis for a prototype with only a 1.78 m tall tower and a collector of 1.78 m diameter, and (Ayub et al., 2018) modeled a chimney height of 2.1 m and a collector diameter of 1.8283 m. (Aurybi et al., 2006), (Anderson et al., 2015), (Joneydi Shariatzadeh et al., 2015), and (Tian et al., 2020) also modeled small-scale prototypes that are not well matched to our studied system. Some other studies developed models for novel designs for the power plant that is beyond the scope of this LCA, including a floating solar chimney (Papageorgiou, 2011) and an inflatable solar chimney (Chi et al., 2015) Consequently, their electricity generation models were not selected for integration into this LCA model.

Similarly, electricity generation models designed for hybrid (but not hybridized with solar PV) SUTPP systems were not selected. These include models that incorporate an external heat source or integrate high-temperature fuel cells with the conventional SUTPP system (Eryener & Kuscu, 2018; Kasaeian et al., 2017; Kiwan & Salim, 2020; Singh et al., 2020; Tian et al., 2020). Studies that include a secondary system like waste-to-energy (Habibollahzade et al., 2018) or water purification systems (Mustafa et al., 2014) within the conventional power plants were also excluded for being out of the scope for this paper.

Next, the necessary environmental inputs were considered in further narrowing the pool of potential electricity generation models to incorporate in this LCA. (von Allwörden et al., 2018) demonstrated that a collector with a sloped field can change the power output drastically especially in the high latitude regions, but they did not find any strong correlation between air humidity and power output from their one-dimensional fluid dynamic model. Therefore, humidity is established to be not an influencing factor in power generation by a SUTPP. Temperature and air velocity were the two most important factors for power generation in their study.

(Choi et al., 2015) found pressure difference to be another influencing factor along with solar irradiation, ambient temperature, and air velocity inside the chimney. Pressure drops are mainly found to be responsible for frictional losses. However, none of the reviewed models cite any mathematical equation to derive the values of air velocity and temperature inside the solar chimney from the environmental conditions outside of the tower. With no means to measure these exact values directly from a utility-scale

SUTPP (which has yet to be implemented at this scale), it is not possible to ascertain geographically and temporally specific values for these parameters from other climate data. (Padki & Sherif, 1999) set constant values for the ambient air density and the air density inside the chimney.

(S. Li, 2017) studied the effects of wind loading on SUTPPs which were heavily focused on material properties like stiffness and bonding behavior, and a direct correlation between power generation and wind loading has yet to be discovered. (Afonso & Oliveira, 2000), which mainly studied the structural and thermal efficiency of solar chimneys in Portugal, also excluded wind effects due to their unpredictable nature in the region. (Adarsh & Menon, 2014) included mass flow rate through the collector area as another important influencing factor for the electrical performance of SUTPP with a sloped collector roof. Temperature and solar irradiation were also found in their study as highly influential input parameters, and so an appropriate electricity generation model for this study must include these two variables.

(Peng-hua Guo et al., 2014) performed a comprehensive study showing how power outputs are affected by each of the factors of solar irradiation, ambient temperature, turbine pressure drop, and updraft velocity. However, the results obtained from this numerical model were unlike other studies. They found ambient temperature to be negligible, and solar irradiation and turbine pressure drop also have a considerably lower impact on power generation. Studies like this and (Williams & Waterson, 2008) that focused mainly on the thermal performance of SUTPP, found convection heat and mass transfer to be more influential than the others, which are dependent mainly on ground temperature and pressure difference. Similarly, (Gannon & von Backstro¨ m, 2000) studied various system losses with the SUTPP system using the simulation of a utility-scale power plant, keeping the input solar radiation constant, and found that the main reason for power loss is the drop in mass flow rate and temperature.

Two comparatively recent reviews on SUTPPs, (Kasaeian et al., 2017) and (F Lupi et al., 2015), both used the electricity generation model from the first proposed model in the literature by (Schiel & Schlaich, 1996). The electricity generation model developed by Schiel & Schlaich (1996) fits the design considerations for a utility-scale system and uses environmental inputs like solar radiation and ambient temperature, but it does not account for nighttime electricity generation due to heat stored in the soil under the collector. Other proposed models that are available included input parameters that are less accessible to measure or calculate. For example, the proposed electricity generation model from SUTPPs designed for the Mediterranean region required the enthalpy of inlet air and outlet air of the solar tower (Nizetic et al., 2008).

A different approach was proposed by (J. Li et al., 2012) that uses differential equations to calculate the heat loss and time-lapse inside and outside of the chimney. The experimental data from the Spanish prototype was used, but there is a precedent for using these equations for higher capacity designs as the authors used this same model to calculate the Levelized cost of electricity for a 10-MW solar updraft tower power plant modeled for China (Penghua Guo et al., 2017). This 500-m tall solar updraft tower has

closer approximate dimensions, design, and power generation capacity than any other study with a power generation model that was reviewed.

The study also used hourly meteorological data and soil heat data for the modeled location. The annual electricity generation for this 10 MW plant was estimated to be 40.22 GWh and the capacity factor was around 45% (Penghua Guo et al., 2017). (Penghua Guo et al., 2014) also developed an unsteady theoretical model for the heat stored in the soil. In (Penghua Guo, Wang, Li, et al., 2016), the authors compared the electricity generated from this unsteady simulation model with their previous steady simulation model where the soil was not considered as a natural heat storage component (Zhou et al., 2009). The daily generation was found to be 31.26% higher with the unsteady model for the Spanish prototype of 50 kW capacity (Penghua Guo, Wang, Li, et al., 2016).

To incorporate the increased power generation due to heat storage while taking into account the transient heat transfer in the soil, the concept of thermal efficiency by Göğüş (2006) was implemented with equations representing the steady model from Zhou et al. (2009). (dos Santos Bernardes & Zhou, 2013b; Göğüş, 2006; Penghua Guo, Wang, Li, et al., 2016; Zhou et al., 2009) compares the results of excess power generation caused by soil heat storage for three different types of soils, from which loamy sand comprised of 2.4% clay, 33.2% silt, and 64.4% sand matches the most common type of soil found in the Southwest US (Bell et al., 2013; Soils of the Southwestern US, n.d.). Therefore, the values of density, specific heat and thermal conductivity used in the model were 1587.32 kg m^{-3}, 1464.80 J kg^{-1} K^{-1}, and 1.24 W m^{-1} K^{-1}, respectively, corresponding to this soil type (Penghua Guo, Wang, Li, et al., 2016).

The theoretical steady model that was originally validated for the 50 kW prototype in Manzanares, Spain, and later used to represent the 10 MW plant in Yinchuan, China is described briefly below. This analysis to evaluate the performance of the solar updraft tower system is based on the assumptions that the air follows the ideal gas law and only the buoyancy force is considered inside the chimney (Ming et al., 2007). The pressure difference between air at the chimney base and the ambient air, Δp, was determined using Equation 1.

$$\Delta p = g \int_0^H (\rho_\infty(h) - \rho(h))\, dh \qquad \text{(Equation 1)}$$

where g is the gravitational acceleration of air (9.81 m s^{-2}); $\rho_\infty(h)$ is the density of air at chimney base where h = 0 m, and ρ(h) is the density of air at any altitude h. The air density ρ (in kg m^{-3}) and air specific heat capacity c_p (in J kg^{-1} K^{-1}) can each be represented by an empirical relation to temperature (T, in units of K) that is expressed by Equations 2 and 3 (Ong & Chow, 2003).

$$\rho = 1.1614 - 0.00353\,(T - 300) \qquad \text{(Equation 2)}$$

$$c_p = (1.007 + 0.00004\,(T - 300)) * 10^3 \qquad \text{(Equation 3)}$$

Combining Equations 2 and 3, the pressure difference Δp can be written as in Equations 4 and 5 below. Here, H is the height (in m) where the pressure difference is being calculated.

$$\Delta p = 0.00353\ g \int_0^H (T_\infty(h) - T\ (h))\ dh \quad \text{(Equation 4)}$$

$$\Delta p = 0.00353\ g\ (H - T(H) \int_0^H dT(h) - \int_0^H T_\infty(h) dh) \quad \text{(Equation 5)}$$

$T_\infty(h)$, which represents the temperature at height h (in m), is given by Equation 6.

$$T_\infty(h) = T_{\infty\,in} \quad \gamma_\infty(h) \quad \text{(Equation 6)}$$

where T_∞ in is the temperature of atmospheric air at the collector inlet; γ_∞ is the lapse rate of ambient air. The mass flow rate (in kg/s) of hot air passing through the chimney, m can be calculated with Equation 7.

$$m = \rho_{in} \quad A_c \quad V_{in} \quad \text{(Equation 7)}$$

where A (in m^2) is the cross-sectional area of the chimney, ρ_{in} (in kg m^{-3}) is the density of the chimney inlet airflow; and V_{in} (in m^3/hour) is the rate of the chimney inlet airflow.

The boundary condition is the temperature of the chimney inlet airflow, which is equal to the temperature of the collector outlet airflow, which is calculated using Equation 8.

$$T(0) = T_{\infty\,in} \quad \frac{\pi G \eta_{Coll}}{C_p m} R_{Coll}^2 \quad \text{(Equation 8)}$$

where G (in W m^{-2}) is solar radiation; R_{coll} (in m) is the collector radius; η_{coll} (in %) is collector efficiency.

The temperature at height h or T(h) then becomes

$$T(h) = T_{\infty\,in} \quad - \frac{g}{C_p} h + \frac{\pi G \eta_{Coll}}{C_p m} R_{Coll}^2 \quad \text{(Equation 9)}$$

And consequently, T (H) becomes

$$T(H) = T_{\infty\,in} \quad - \frac{g}{C_p} H + \frac{\pi G \eta_{Coll}}{C_p m} R_{Coll}^2 \quad (K) \quad \text{(Equation 10)}$$

Δp can also be written as

$$\Delta p = 0.00353\ gH\ (\frac{\pi G \eta_{Coll}}{C_p m} R_{Coll}^2 \quad - \frac{g}{2C_p} H + \frac{1}{2} \gamma_\infty H) \quad \text{(Equation 11)}$$

The electric power generated by the turbine generators is calculated as shown in Equation 12, in which η_t is the turbine efficiency (Zhou et al., 2009).

$P_{out} = \eta_t \quad \Delta p \, V \, A_c$ (Equation 12)

The efficiency of thermal energy storage systems is determined using Equation 13 (Göğüş, 2006).

$$\eta = \frac{T - T_0}{T_\infty - T_0}$$ (Equation 13)

Where T is the maximum temperature in the ground during discharging (K), T_0 is the minimum temperature in the ground during discharging (K), and T_∞ is the maximum temperature in the ground at the end of the charging period (K).

The proposed charging period was the time of sunshine approximately from 6:00 am to 6:00 pm (dos Santos Bernardes & Zhou, 2013; Göğüş, 2006). The efficiency of the thermal energy storage system would be factored into the steady model so that it can function as the unsteady model. The final form of output electric power is expressed in Equation 14 (Göğüş, 2006; Peng-hua Guo et al., 2014; Penghua Guo, Wang, Li, et al., 2016; J. Li et al., 2012; Zhou et al., 2009).

$$P_{out} = \frac{T - T_0}{T_\infty - T_0} \eta_t \, 0.00353 \, g \, H \left(\frac{\pi G \eta_{Coll}}{C_p m} R_{Coll}^2 \quad - \frac{g}{2C_p} H + \frac{1}{2}\gamma_\infty H\right) V_c \, A_c$$ (Equation 14)

Initially, this equation was developed to account for the variable temperature difference between the air inside the chimney and air outside whereas most other models assume an average temperature difference between these two. Later it was modified further to account for the unsteady thermal energy that is captured in the soil underneath the collector. This equation was adjusted to allow for the use of hourly data for solar radiation, soil temperature, the maximum and minimum values of ground temperature, and ambient temperature to determine the temperature difference. The obtained power output was multiplied by this time interval to calculate energy harvested, then aggregated to the lifetime of the system (Penghua Guo et al., 2021; Penghua Guo, Wang, Li, et al., 2016).

The total electricity generated during the lifetime of the system was then adjusted to accommodate maintenance activities during which the SUTPP would not be operating. The time of maintenance as a fraction of the total time of operation was based on systems that are similar to the SUTPP, such as CSP systems (Gonzalo et al. 2019). Being a more established energy technology, CSP plants have more detailed operations and maintenance data available (Pérez et al. 2017). Although the maintenance activities of these two systems would vary slightly due to the presence of molten salt as a form of energy storage, they share many maintenance activities (Cohen et al. 1999).

2.6 Hybridizing Solar Updraft Tower with Solar PV

In addition to the SUTPP LCA scenarios, hybrid scenarios that pair SUTPP infrastructure with solar photovoltaics (PV) were modeled and analyzed for the same

sites. In the hybrid scenarios, the solar PV panels are placed on the south edge of the collector facing south with the global optimal tilt that is 75°N and 60°S (Jacobson & Jadhav, 2018). The global optimal tilting for single-axis solar PV panels is the angle at which tracking the radiation can improve the performance such a negligible amount that it causes minimal benefit over the higher investment on a tracking mechanism, and for the southwest United States, this angle is around 30^{o} for optimal electricity generation (Breyer, 2020; Jacobson & Jadhav, 2018). Southwest US states like Arizona, Nevada, New Mexico, and Texas have the highest amount of annual solar radiation at the global optimal tilt (Lave & Kleissl, 2011).

The placing is recommended along the edge of the collector for ease of maintenance (Figure 05). Only 2% of the total collector area was modeled as covered by solar PV for this analysis, to minimize the effects of adding solar PV panels on the SUTPP electricity generation as the influence of solar PV is not accounted for in the selected electricity generation model (dos Santos Bernardes, 2013; Penghua Guo, Wang, Li, et al., 2016). Although it would be possible to cover almost 80% of the collector area with solar PV panels, the heat generated under the panels and the shading provided onto the collector would affect the airflow inside the collector-chimney system (Kiwan & Salim, 2020; Singh et al., 2020). Therefore, covering a higher surface area of the collector would be incompatible with the (Penghua Guo et al., 2021; Penghua Guo, Wang, Meng, et al., 2016) electricity generation model.

For the scenarios integrating solar PV in addition to the SUTPP, three added variable parameters are the performance ratio, the annual degradation rate, and the fraction of solar PV panels recycled. The performance ratio of solar PV panels is characterized by the ratio of measured output to the expected output of the solar PV panels (Deline et al., 2016). The solar PV performance ratio is a key parameter that is crucial for grid-connected solar PV panels (Khalid et al., 2016). The world acceptable average value of performance ratio is 70%, though it varies between 50% and 90% (Quansah & Adaramola, 2019). The highest degradation rate is observed at 1% and the median value is 0.5% annually (Jordan, Silverman, Wohlgemuth, et al., 2017; Jordan & Kurtz, 2013). In addition to the solar PV performance ratio (PR), the electricity generated by a solar PV system (E, in kWh/year) is dependent on the total solar panel area (A, in m^2), the solar panel efficiency (r, unitless), and the average solar radiation on titled panels (G, in W/m^2), and calculated as shown in Equation 15 (Yadav, 2015).

$$E = A \times r \times G \times PR \quad (kWh/year) \qquad \text{(Equation 15)}$$

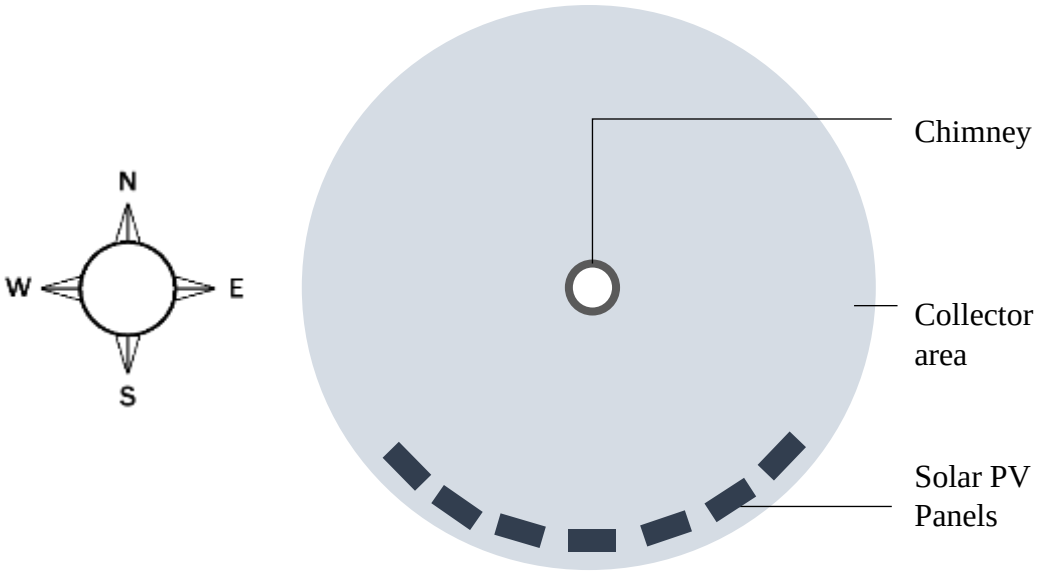

Figure 05: Bird's eye view of a solar updraft tower with solar PV panels placed on the outer edge of the collector.

This electricity generation model is used globally to estimate electricity output from tilted solar PV panels (Deline et al., 2016). The material inventories added to the SUTPP LCA model for the hybrid scenarios were the production of multi-Si solar PV panels, the production of the required number of solar PV inverters, and multi-Si solar PV recycling and disposal (Luo et al., 2018). The 2% covered area of the collector is comprised of multi-Si solar PV panels of 9000 kW capacity (Jacobson & Jadhav, 2018; Khalid et al., 2016). Multi-Si solar cells have higher output performance due to their comparatively lower reflectivity and they cost the least among all the different types of solar PV panels (Y. Jiang et al., 2017). The production of solar PV panels includes all the impacts of cells, glass, back sheet, frame, ribbon, and cross connector, as well as framing tape (Luo et al., 2018).

2.7 Baseline scenario analysis

In this study, we are evaluating life cycle greenhouse gas (GHG) emissions for two scenarios representing stand-alone solar updraft tower energy systems and solar updraft tower-solar PV hybrid energy systems. The baseline LCA scenario analysis yields the life cycle GHG emissions based on baseline input parameter values representing the most common and overall averages for these inputs. Some parameter values may need to be assumed and therefore baseline values may not be the absolute exact values of life cycle GHG emissions in reality. However, making necessary and rational assumptions about variable parameters lead us to better results than completely disregarding them. Also, later in the sensitivity analysis depending on how sensitive a system is to a

particular parameter, the preciseness of the baseline parameters may or may not be identified as crucial to the accuracy of the results (Gathorne-Hardy, 2013b).

2.8 Sensitivity analysis and Monte Carlo analysis

The SUTPP and hybrid SUTPP with solar PV LCA models were developed in Python 3.8 with equations that link to variable parameters (Fortier, 2021). This parametric LCA structure allows for sensitivity analysis and Monte Carlo analysis to be performed and to contribute to the interpretation of LCA results (Raychaudhuri, 2008).

The sensitivity analysis identifies the parameters that the LCA results are most sensitive to. With a realistic range of values set, the sensitivity analysis is performed through one-at-a-time variation of the parameters (Igos et al., 2019); in this case, they are varied to their minimum and maximum values (Table 3). A total of 13 parameters for the SUTPP system and 16 parameters for the SUT-PV hybrid system were varied in this analysis. The obtained ranges represent the realistic range of change but not the precise ranges (Igos et al., 2019; Shirvan et al., 2017). It should be mentioned that if the systems do not seem to be very sensitive to the change of a certain parameter, the preciseness of the ranges is not crucial to the analysis (Shirvan et al., 2017). The sources of these variable parameters are listed in Table 3.

Table 03: Ranges of the variable input parameters to the LCA models with respective sources.

Variable Parameter name	Units	Minimum	Baseline	Maximum	Sources
Operational lifetime	Years	20	25	30	(Attig Bahar et al., 2016; Bernardes, 2004; F Lupi et al., 2015; Niemann et al., 2009; Zhou et al., 2010; Zongker, 2013)
Turbine efficiency	n/a	0.8	0.85	0.9	(Fluri & von Backström, 2008; Gannon & von Backstro¨ m, 2000, 2003; Guo et al., 2016; Li et al., 2012; Von Backström & Gannon, 2004
Performance ratio	n/a	0.5	0.7	0.9	(Khalid et al., 2016; Reich et al., 2012; Yadav, 2004)
Annual degradation	n/a	0.005	0.0075	0.01	Jordan, Silverman, Sekulic, et al., 2017; Jordan, Silverman,

rate					Wohlgemuth, et al., 2017; Jordan & Kurtz, 2013)
Fraction of maintenance time	n/a	0.04	0.05	0.06	(Cohen et al., 1999; Corona et al., 2014; Papaelias et al., 2018)
Fraction of glass walls needing replacement	n/a	0.2	0.25	0.3	(Barou et al., 2018; Gresser, 1985)
Cable yarder operation for assembly	Hours	100	120	140	(Hoffmann et al., 2016; Spinelli et al., 2020)
Cable yarder operation for disassembly	Hours	60	72	84	(Hoffmann et al., 2016; Kamali & Hewage, 2016; Spinelli et al., 2020)
Hours of construction	Hours	300	350	400	(Adedeji et al., 2010; Ayub et al., 2018; Cohen et al., 1999; Haaf et al., 1983; Hatti, 2014; W. Jiang et al., 2012; Kraetzig et al., 2009; Ortiz et al., 2009; Padki & Sherif, 1999; Ruppert et al., 2021; Schlaich et al., 2005; Van Blommestein & Mbohwa, 2013)
Fraction of reinforcing concrete recycled	n/a	0.1	0.225	0.35	(Andersen et al., 2014; Kunieda et al., 2014; Mehta, 1991, 1999; Merli et al., 2020; Noguchi et al., 2011)
Fraction of steel recycled	n/a	0.6	0.75	0.9	(Bowyer et al., 2015; Fenton, 2003; Sethuraman et al., 2017)
Fraction of iron recycled	n/a	0.4	0.45	0.5	(• *U.S. metal recycling rates by type 2019 | Statista*, 2019)
Fraction of plastic recycled	n/a	0.1	0.15	0.2	(Heller et al., 2020; McCormick et al., 2019; Rahimi & García, 2017; Subramanian, 2000)
Fraction of epoxy recycled	n/a	0.1	0.3	0.5	(Andersen et al., 2014; Chen et al., 2019; Cousins et al., 2019; Fonte & Xydis, 2021; Liu & Barlow, 2016; Topham et al., 2019)

Fraction of glass-fiber recycled	n/a	0.1	0.3	0.5	(Andersen et al., 2014; Chen et al., 2019; Cousins et al., 2019; Fonte & Xydis, 2021; Liu & Barlow, 2016; Topham et al., 2019)
Fraction of aluminum recycled	n/a	0.14	0.27	0.4	(Jensen, 2019; Sethuraman et al., 2017)
Fraction of PV panels recycled	n/a	0.7	0.8	0.9	(Ardente et al., 2019; Ashfaq et al., 2017; Chowdhury et al., 2020; Venkatachary et al., 2020)

(Bernardes, 2004) chose an average lifetime of solar chimney power plants to be 30 years and for multi-Si solar PV to be 25 years on average. In this 2004 study, the capacity factors of these power plants were 13.5% and 32.1% for solar chimney and multi-Si solar PV panels, respectively (Bernardes, 2004). However, (Zongker, 2013) found that although the operating lifetime of solar chimneys can extend up to 80 years or more, due to the various components involved in the structure, the lifetime cannot be longer than 30 to 50 years even if the structure is free from any photo-degradation, rain, dust and other disaster-like phenomena (F Lupi et al., 2015; Niemann et al., 2009; Zhou et al., 2010; Zongker, 2013). The upper and lower threshold of the lifetime for the solar updraft tower was thus selected to be 30 and 20 years, respectively, in this LCA model (Attig Bahar et al., 2016; Zongker, 2013).

(Schiel & Schlaich, 1996) first mentioned that the solar chimney turbine efficiency is approximately 80%. The most common turbine efficiency was found to vary from 0.8 to 0.9 both analytically and experimentally (Fluri & von Backström, 2008; Gannon & von Backstro¨ m, 2000, 2003; Penghua Guo, Wang, Li, et al., 2016; J. Li et al., 2012; Von Backström & Gannon, 2004).

(Reich et al., 2012) mentioned that solar PV performance ratio has been reported from 50% to all the way to 90% whereas 70-80% seemed to be the most reported performance ratio for modern technologies. This performance ratio is the product of the performance ratio of the direct current (DC) side (solar PV cells) and alternating current (AC) side (inverter) (Khalid et al., 2016; Reich et al., 2012; Yadav, 2004). The annual degradation rate was reported to vary from 0.5% to 1% per year (Jordan, Silverman, Sekulic, et al., 2017; Jordan, Silverman, Wohlgemuth, et al., 2017; Jordan & Kurtz, 2013).

The solar PV panel's glass recovery rate is around 91% whereas the recovery rate of cadmium and tellurium is 95% to 97%. On a weight basis, at least 65% to 75% of solar PV panel materials are recovered worldwide and on average 80% of those materials are recycled (Chowdhury et al., 2020). About 90% of the recovered solar PV material can be recycled into fully functioning components that are found to last in their second use for another 25 to 30 years (Ashfaq et al., 2017). With a 25 year lifetime, only 10 to 15% of

the solar PV materials go to waste (Ardente et al., 2019; Venkatachary et al., 2020). The average recycling rate was found to be 80 to 83% on a mass basis (Ardente et al., 2019).

Being a novel technology the information about the maintenance time for a 10 MW solar updraft tower power plant was not available. However, concentrated solar power (CSP) plants have a slightly similar structure to the solar chimneys. Although for the CSP plant there is no greenhouse-like structure, there are specialized glass mirrors placed around the tower that need regular cleaning and maintenance. For a CSP plant that covers a similar area, the maintenance time takes up to 5% of the total operational time (Cohen et al., 1999; Papaelias et al., 2018). Although the solar collector does not need an equal amount of cleaning as the glass mirrors of CSP systems, it contains a massive central turbine that needs to be shut down during maintenance and so, it is assumed that the maintenance time for a SUT is more or less similar to a CSP plant covering similar area (Cohen et al., 1999; Corona et al., 2014; Hatti, 2014; Papaelias et al., 2018).

The solar chimney and collector construction details were obtained from (Adedeji et al., 2010; Ayub et al., 2018; Cohen et al., 1999; Haaf et al., 1983; Hatti, 2014; Kraetzig et al., 2009; Ortiz et al., 2009; Padki & Sherif, 1999; Schlaich et al., 2005; Van Blommestein & Mbohwa, 2013). Crane operation details were determined based on a southern China study that found that per scheduled service hour the gross achievable productivity ranges from 2.64 to 3.09 m^3 material being carried (Hoffmann et al., 2016). On the other hand, (Spinelli et al., 2020) found that the productivity rate of automated cable yarders ranged between 8.2 to 13.3 m^3/hour. For a system like a SUTPP, cable yarding operation should take about 100 to 140 hours. The disassembly process normally takes about 40% less time than the assembly process (Kamali & Hewage, 2016). So, it should take about 60 to 84 hours of cable yarding operation to disassemble the tower at the end of its life.

(Ruppert et al., 2021) calculated that a 2 km tall tower with at least 20 cm thick wall will take roughly 1 year to construct with 11 meters/day. However, for a 1 km tall tower, the time would be reduced by 80%, and (W. Jiang et al., 2012) did a similar analysis where they set the construction time as 4 days/floor for a 101 story tall building with a total height of 492 m and a base area of 350,000 m^2. According to these analyses, for a 550 m tall simple hollow tower, the construction time would be more or less 350 hours.

(Gresser, 1985) found that as much as 30% of the greenhouse glass walls might need replacement throughout their lifetime. According to (Barou et al., 2018), 25% of the structural glasses need replacement whereas (Omar et al., 2019) found that the deterioration rate of structural glasses is 24.5%. (McCormick et al., 2019) found that less than 10% of plastics get recycled in the US. As of 1996, it did rise to almost 12% (Rahimi & García, 2017; Subramanian, 2000). (Heller et al., 2020) mentioned in North America and the US this has increased up to 19% and 21% respectively in recent years.

Up to 60% of the high-strength concrete (>40 MPa) or reinforced concrete can be reused at the end of its life (Mehta, 1991, 1999). However, this might be an overestimate because, in reality, it fluctuates around 10 to 15% (Merli et al., 2020; Noguchi et al.,

2011). (Andersen et al., 2014) found that the disposal rate of concrete or brick is 64% and the remaining can be recycled. Still, 90% of the crushed concrete can be used as the base materials for road construction (Kunieda et al., 2014).

Steel, aluminum, copper, and permanent magnet are the main three components of the generator used for electricity generation from a turbine (Sethuraman et al., 2017). In North America, the steel recycling rate has been consistently high (60%-90%) as reported by Steel Recycling Institute (SRI) and U.S. Geological Survey (USGS) (Bowyer et al., 2015). Even in 1998, the recycling rate of steel was as high as 41% (Fenton, 2003). The average recycling rate of aluminum is 27% according to (Jensen, 2019). The recycling rate of rare earth materials is very low at less than 1% and the main components of the permanent magnet in the generator are rare earth materials (Jensen, 2019). So for this study, the recycling rate for permanent magnets was not taken into account.

The turbine structure is comprised of 60 to 65% glass fiber and 32.3 to 40% epoxy resins and adhesives (Fonte & Xydis, 2021; Liu & Barlow, 2016). Although theoretically 80 to 90% of the turbine materials can be recycled, for both glass-fiber and epoxy up to 50% - 55% of the end of the life materials should be considered as waste making the remaining 45% - 50% recyclable (Andersen et al., 2014; Beauson et al., 2021; Topham et al., 2019). Overall depending on the manufacturer, the recycling rate of the composite materials used to manufacture wind turbines varies from 10% to 30% on average (Chen et al., 2019; Cousins et al., 2019; Fonte & Xydis, 2021). For a wind turbine of our current design, at least 35% of the blade and rotor materials should be recycled (Beauson et al., 2021; Mishnaevsky et al., 2017). Although currently wind turbine blades are not recycled for the most part, this system was modeled to be representative of the future conditions assuming the recycling infrastructure and rate would improve. So, a baseline value of 30% recycling rate for blade materials was considered whereas the highest and lowest recycling rate aswas considered 50% and 10% respectively.

Uncertainties might arise from the quality of data, complicated dynamics among the processes of a system, quality of inventories, and similar factors (Baker & Lepech, 2009). To analyze these uncertainties, Monte Carlo analysis was used because it provides statistical data for possible LCA results by combining randomized parameter values within their specified ranges and according to their probability distributions (Wang & Shen, 2013). Monte Carlo simulation looks at the long-term effect of uncertainties in the parameters on the output results (Bonate, 2001). Stochastic modeling like Monte Carlo simulation is a powerful tool to deal with the limitations of the data (Huijbregts et al., 2001). For each scenario, 10,000 Monte Carlo simulations were run in Python 3.8 that selects random values based on a specific distribution type for calculating the stochastic results. The resulting probability distribution of life cycle GHG emissions is generated for each scenario from the Monte Carlo results using Minitab 17.

CHAPTER-03

RESULTS AND DISCUSSION

3. Results and Discussion

3.1. Overall Baseline LCA Results and Electricity Generation by Scenario

This cradle-to-grave LCA of the solar updraft tower power plant (SUTPP) was performed for 10 different locations across 5 different states in the southwestern part of the United States (US), both with and without integration of solar PV, thus yielding 20 LCA scenarios. Figure 06, Figure 07, and Figure 08 represent the differences between the stand-alone SUTPP scenarios and the hybridized SUTPP with 2% collector area solar PV coverage scenarios in all 10 locations in terms of life cycle GHG emissions, calculated lifetime electricity generation, and capacity factors, respectively.

The cutoff power for the SUTPP system without the inclusion of solar PV was its full capacity of 10 MW. The generated electricity values in the LCA model were capped to not exceed this amount of power because it was the maximum power of the turbine as well as the generator. Ultimately, using hourly weather data at each of the 10 sites, the capacity factors calculated ranged from 0.49 to 0.56 for the stand-alone SUTPP and 0.29 to 0.33 for the SUTPP-PV hybrid systems. Thus, with the incorporation of 2% coverage of solar PV with the SUTPP system, the capacity factor was reduced by ~40%. However, the two systems had different capacities, and so the lower capacity factors of the SUTPP-PV hybrid system still equated to slightly higher electricity generation. The average lifetime electricity generation for the stand-alone SUTPP was 1149 GWh, whereas, for the hybrid SUTPP-PV plant, it was 1286 GWh. From Equations 14 and 15, it is clear that electric power generated from both the SUTPP and SUTPP-PV hybrid systems is directly proportional to solar radiation. Although solar PV power generation had no interdependency on the ambient temperature in this model, the SUTPP is heavily dependent on the difference between ambient temperature and the temperature inside the SUTPP system due to it being the driving force behind the hot air flow inside the tower (dos Santos Bernardes & Zhou, 2013a; Penghua Guo, Wang, Li, et al., 2016; Nizetic et al., 2008).

By design, the life cycle greenhouse gas emissions are inversely proportional to the total electricity generation. Overall, the life cycle GHG emissions for SUTPP-PV systems were higher than those of the stand-alone SUTPP systems, but not by a substantial amount. The overall average life cycle greenhouse gas emissions for the SUTPP-PV scenarios were 32.5 g CO_{2eq}/kWh, as compared to 31.86 g CO_{2eq}/kWh for the SUTPP scenarios. The locations with lower average monthly temperature (shown in Figure 20) were found to be generating higher lifetime electricity and cause lower greenhouse gas emissions as a result, even though solar PV is not influenced by ambient temperature in this model. There are slight variations in terms of weather and geographic factors like elevation, soil type, etc. among all the case study locations. Due to this variation, the amount of heat captured in the soil varied, and that is a possible reason for the differences in electric power generation (*Soils of the Southwestern US*, n.d.). Further discussion on the effects of geography on electricity generation and subsequently the life cycle GHG emission can be found in section 3.7.

For each case study with PV, scenarios were only slightly higher in electricity generation and slightly lower in life cycle greenhouse emissions. Even though the hybrid systems generate more electricity, they overall also emit more greenhouse gases due to the additional materials. So, hybridizing the SUTPP system with a 2% collector area covered by solar PV may not affect either the carbon footprint of the generated electricity or its total amount generated substantially. Future work may consider scaling up the coverage gradually to determine if higher coverage changes this conclusion. Still, studying the optimal amount of solar PV coverage is out of the scope of this current study due to the limitations of the electricity generation model which is not designed to include the effects of PV panel shading on the collector.

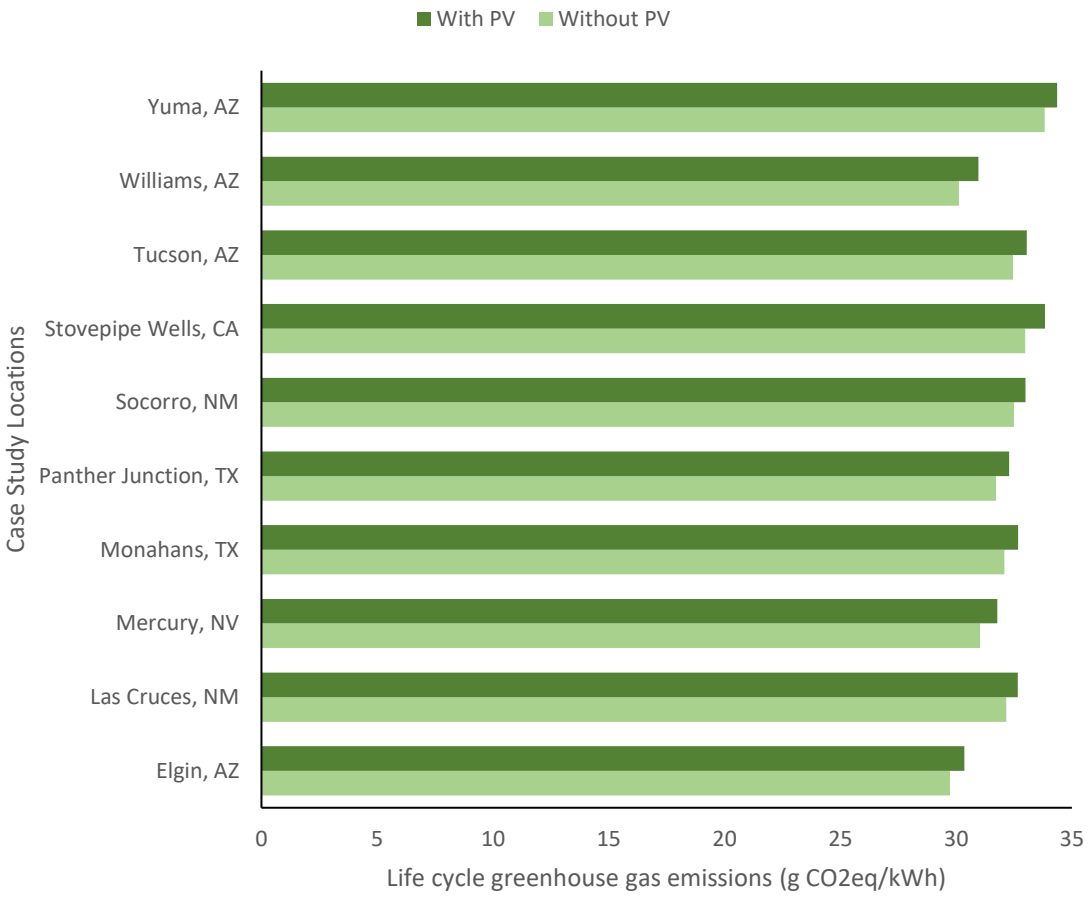

Figure 06: Comparison between life cycle greenhouse gas (GHG) emissions (in g CO_{2eq}/kWh) without and with PV at different case study locations.

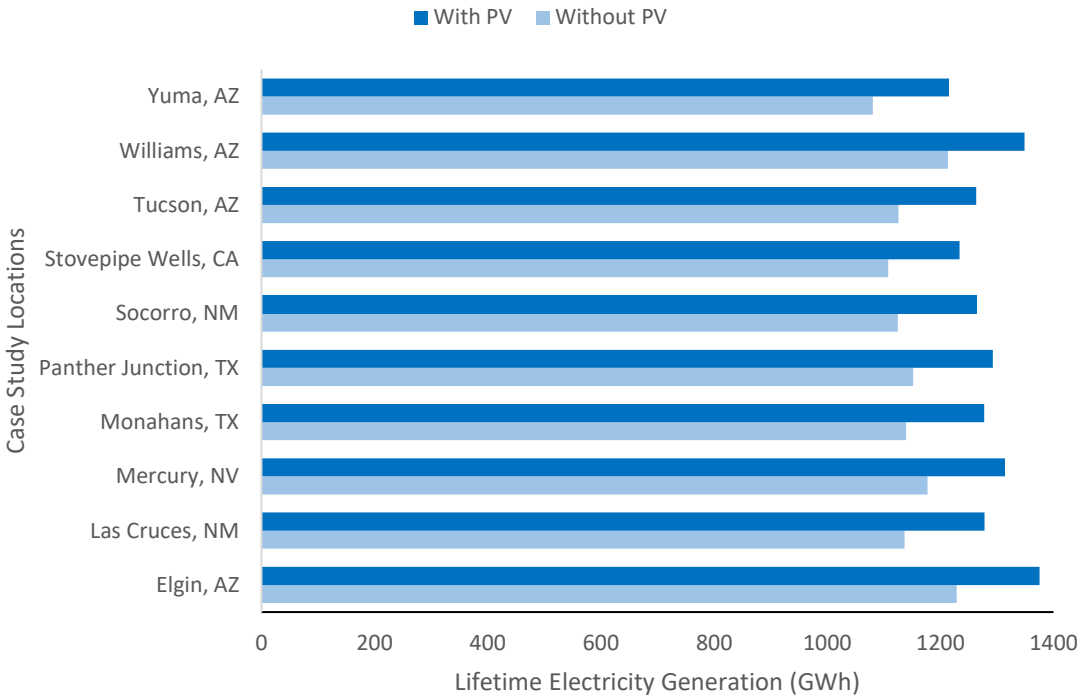

Figure 07: Comparison between lifetime electricity generation (in GWh) without and with PV at different case study locations.

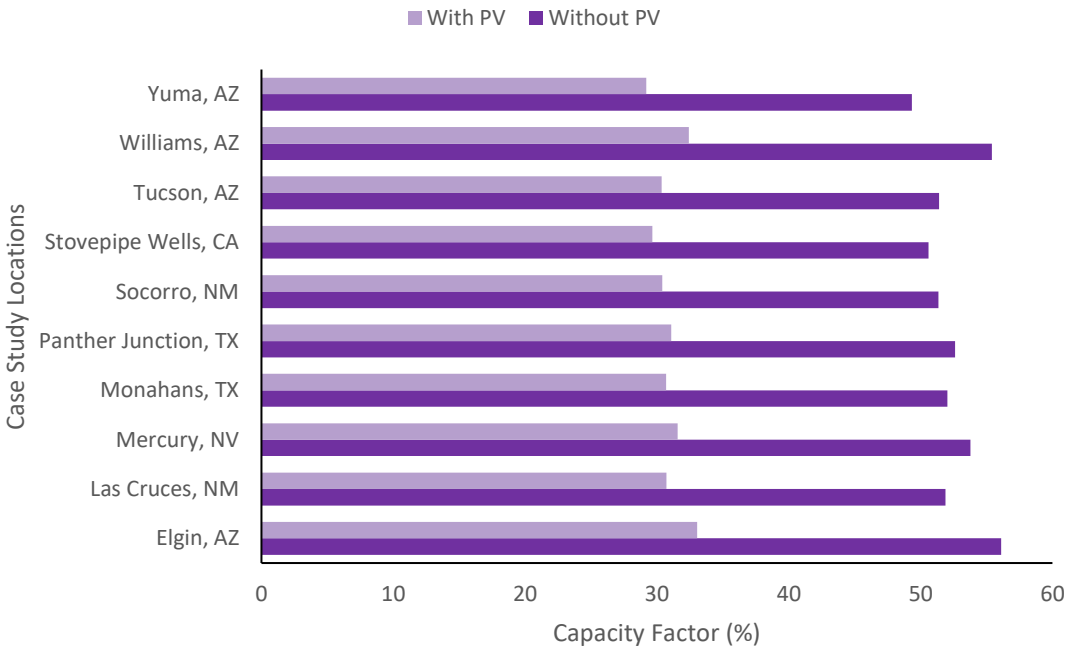

Figure 08: Comparison between Capacity Factor (%) without and with PV at different case study locations.

3.2. Performance Analysis during 24 hours

The incorporation of natural heat stored in the soil underneath the collector was necessary because the electricity generation from the solar updraft tower was not solely dependent on the instantaneous solar radiation and ambient temperature at the selected case study locations. The reason behind this is that electricity from the rotation of the central turbine caused by up-flowing hot air can still be obtained at times when there is no solar radiation. The air inside the collector still gets hot with the help of natural heat stored in the soil under the collector due to the open system having a greenhouse-like structure (Penghua Guo, Wang, Li, et al., 2016; G. Li et al., 2019; J. Li et al., 2012).

Figure 09 shows the hourly power output on a random day (24 hours) in 2020 in Elgin, Arizona. The time series plot was plotted from 1:00 am to 12:00 am the next day showing how the power output (in kW) and solar radiation (in W/m^2) are related to each other. Now this hourly distribution of power output and solar radiation may not tell the complete story because it only shows the solar radiation at an instance and the average power output during that hour. So, the plot would differ at a finer temporal resolution. Nonetheless, it shows that even though there is minimal to no solar radiation from 7:00 pm to 7:00 am, some electricity would still be generated during those hours.

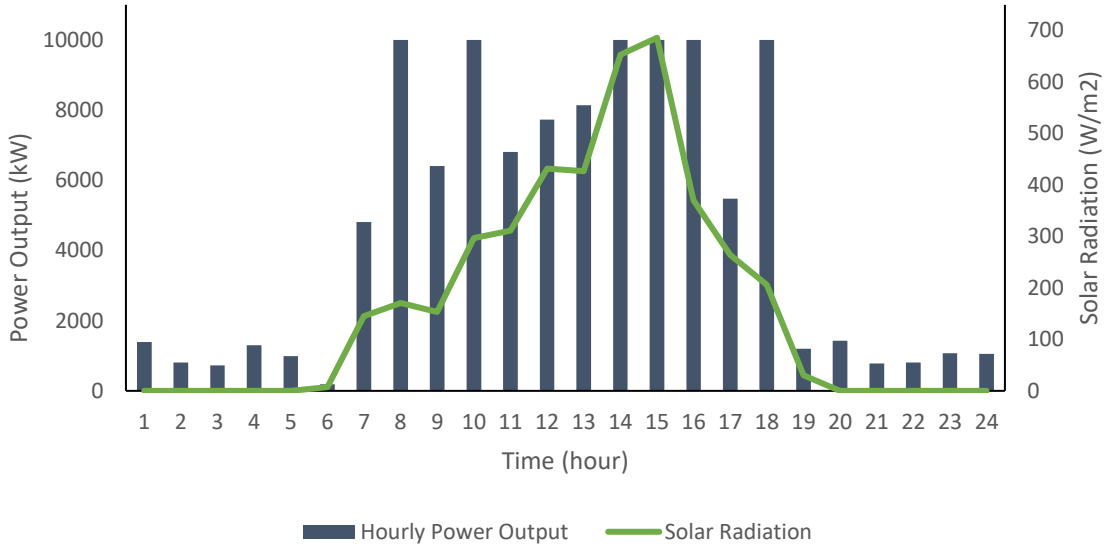

Figure 09: Time series plot showing the relationship between hourly power output (navy bars) and solar radiation (green line) throughout a random whole day in Elgin, Arizona.

Similarly, the power output is not directly proportional to ambient temperature. Figure 10 represents the relationship between the hourly power output (in kW) and ambient temperature (in K) on the same random day (24 hours) in 2020 in Elgin, Arizona. The time series plot was plotted from 1:00 am to 12:00 am the next day showing how the power output and calculated hourly average temperature are related to each other.

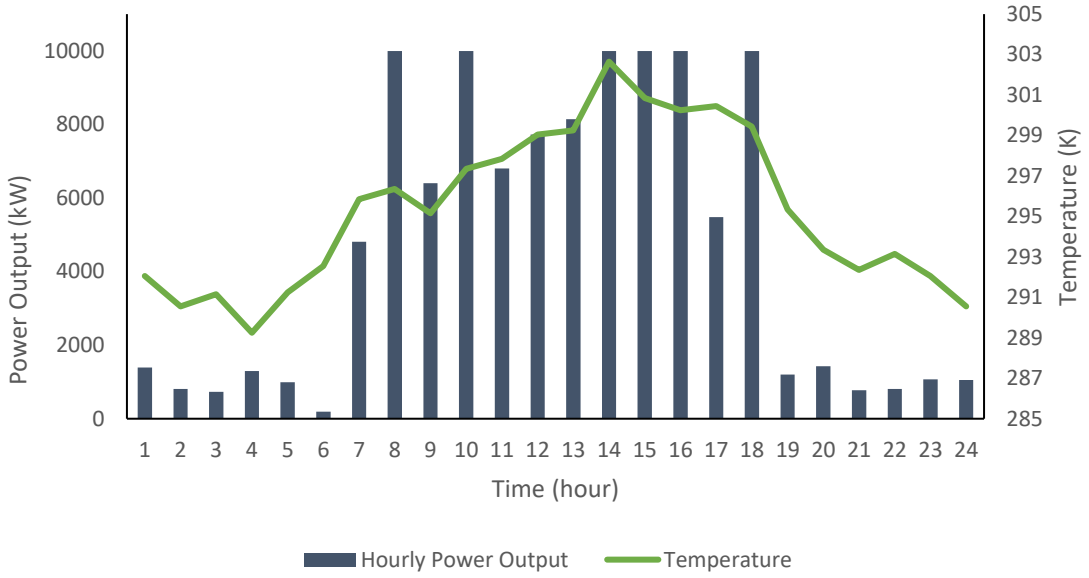

Figure 10: Time series plot showing the relationship between power output (navy bars) and ambient temperature (green line) throughout a random whole day in Elgin, Arizona.

Similarly, this hourly distribution of power output and the ambient temperature does not show the whole picture because it only shows the average ambient temperature and the average power output during that hour. So, the plot can fluctuate a bit if the data points were based on a smaller period of time than an hour. Still, it shows that even though the ambient temperature is fairly low between 7:00 pm and 7:00 am, some electricity was still being generated during those hours due to the heat captured into the soil under the collector that keeps the system warm for several hours.

3.3. Baseline LCA Scenario Analysis Results by Process and Materials

The baseline LCA results show that, without PV incorporated into the system, the total life cycle greenhouse gas emissions ranged from 29.73 g CO_{2eq}/kWh to 33.82 g CO_{2eq}/kWh for the 10 locations: Elgin, Tucson, Williams, Yuma (Arizona); Stovepipe wells (California); Las Cruces, Socorro (New Mexico); Mercury (Nevada); Monahans, Panther Junction (Texas). When 2% of the collector area was covered by solar PV panels, the total life cycle greenhouse gas emissions ranged from 30.36 g CO_{2eq}/kWh to 34.36 g CO_{2eq}/kWh. With and without solar PV, the range of total impacts was very similar, but if we compare these two cases for each of the selected sites, it was found that the impacts with solar PV were slightly higher. However, the lifetime electricity generation for solar PV cases was higher than without solar PV cases.

The baseline LCA results also show which life cycle steps are the largest contributors and which contributions were fairly negligible. When solar PV was not

incorporated into the solar updraft tower system, the largest contributors to the carbon footprint were found to be the production of 40MPa concrete (reinforced concrete) (~ 65%), glass walls (~ 14%), and sand (~ 10%). The impacts of recycling aluminum, plastic, and steel were negative due to substituting new materials and thus avoiding the impacts of their production. All the other factors were found to have minimal impacts on the total life cycle greenhouse gas emissions from the solar updraft tower power plant.

Baseline case scenario results are grouped into two categories for both the SUTPP and SUTPP-PV hybrid system: grouped by processes (Figure 11 and 13) and grouped by materials (Figure 12 and 14) to understand whether any process or any material, in particular, has a substantially higher contribution than the others. The processes include production of materials, material treatment, assembly and disassembly, material disposal, material recycling, operations, and maintenance. It was found that production of the materials has the highest contribution (~90%) in all the scenarios followed by material disposal (~6%) and operations and maintenance (~3%). These impacts from the production of materials already include the transportation impacts because they are obtained from ‘market for’ inventories from the Ecoinvent 3 life cycle inventory database in SimaPro.

The baseline scenario results are shown in Figures 12 and 14 grouped by the material to determine whether any particular material had specifically high impacts on the system. Each material impact includes the raw material extraction, production, material treatment, manufacturing, usage, and end-of-life management stages. Reinforced concrete (~65%), followed by glass walls (~14%) and sand (~10%), had the highest impact on the lifetime greenhouse gas emissions for the stand-alone SUTPP. For the SUTPP-PV hybrid power plants, reinforced concrete (~58%), sand (~10%), glass walls (~10%), and multi-Si solar PV panels (~10%) had the largest impact on the life cycle GHG emissions.

A clear relationship between the locations and the effect of processes and the materials could not be established by analyzing Figures 11-14. Yuma, AZ seems to have the highest life cycle GHG emissions, and Williams, AZ has the second-lowest values of life cycle GHG emissions, even though the differences are quite small. Yuma, AZ also happens to be the case study site with the highest average monthly temperature and one of the lowest elevations. The opposite is true for William, AZ, as seen in Figures 19 and 19. There is not a clear trend that could be observed in the relationship between elevation, average temperatures, and average solar radiation and the life cycle GHG emissions by site, and therefore, it is not clear whether there exists a correlation between geographic parameters and overall global warming potential in this LCA. The studied areas have very similar climatic conditions, however, and larger differences may be observed if the geographic area is expanded in future work.

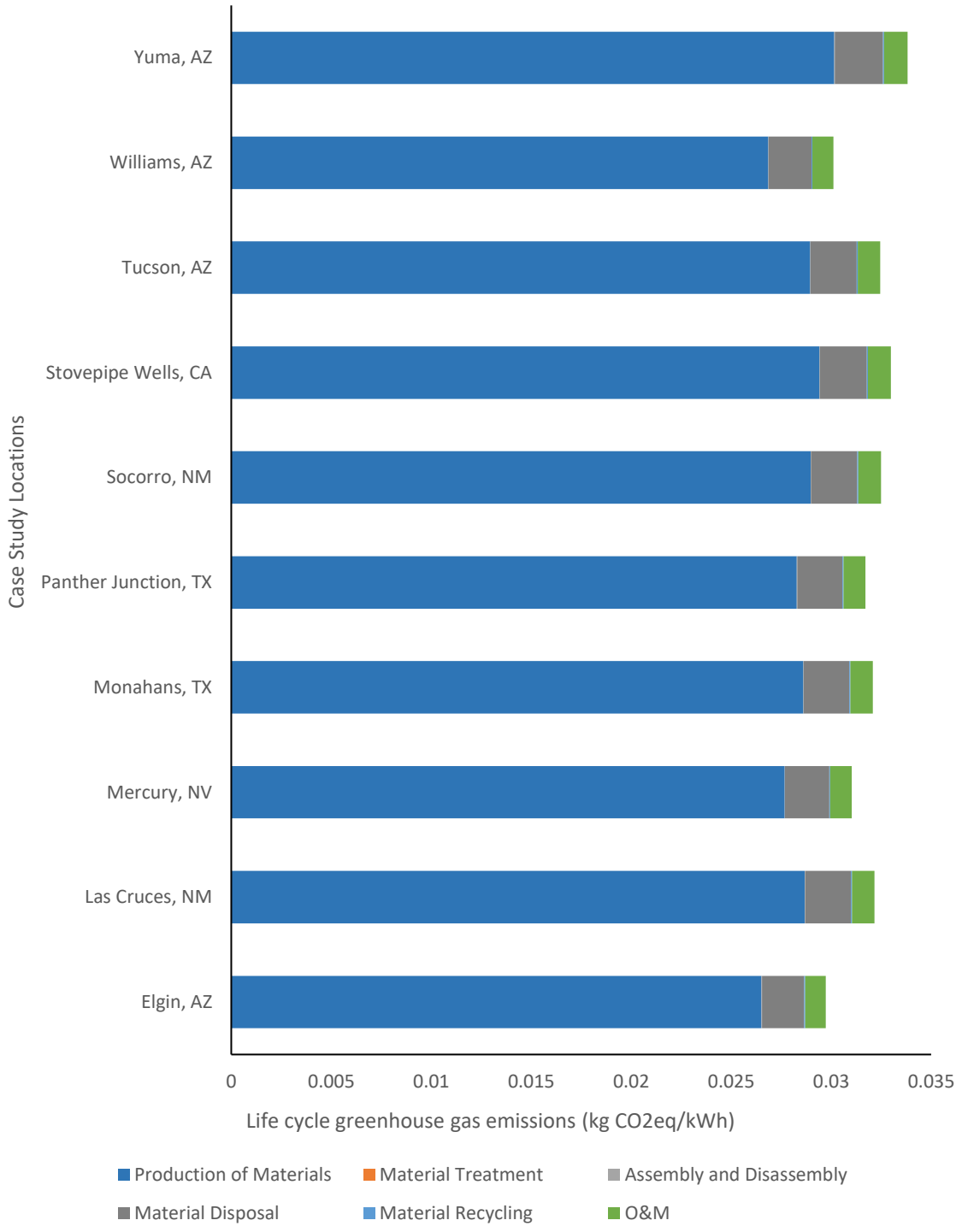

Figure 11: Life cycle GHG emissions for the baseline case scenario for different geographic case study locations for stand-alone SUTPP (grouped by processes).

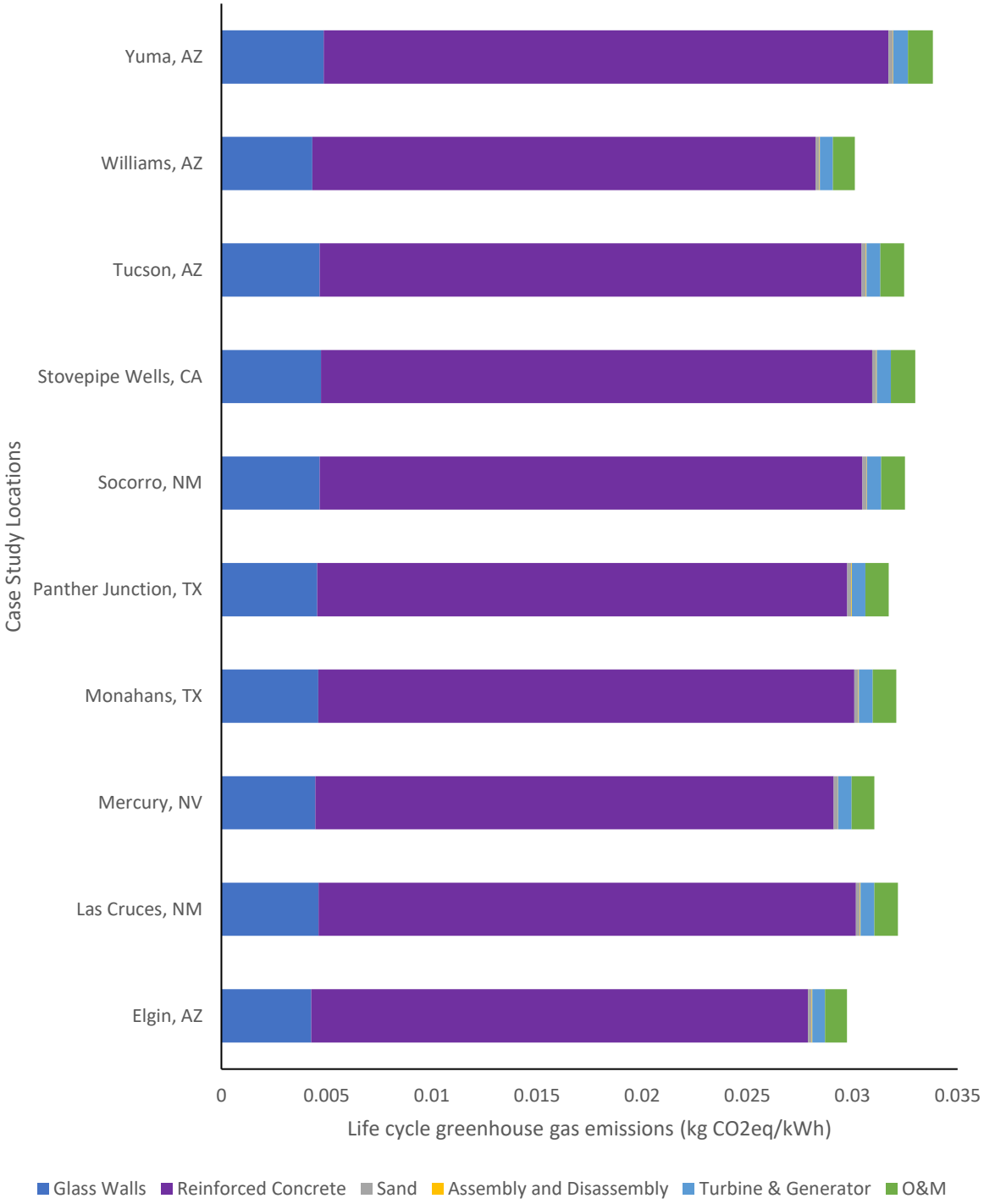

Figure 12: Life cycle GHG emissions for baseline case scenario for different geographic case study locations for stand-alone SUTPP (grouped by materials).

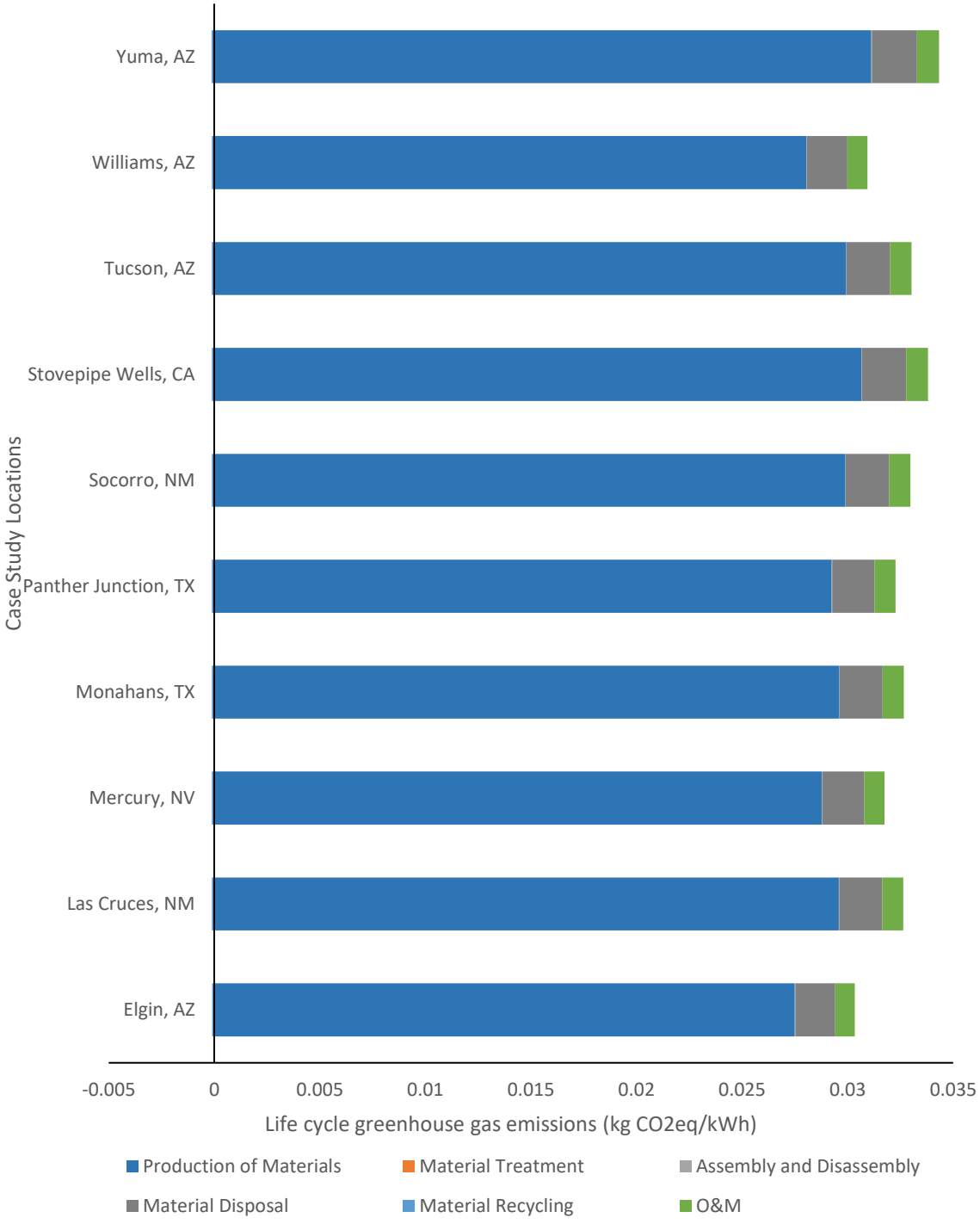

Figure 13: Life cycle GHG emissions for the baseline LCA scenarios for different geographic case study locations for SUTPP-PV hybrid power plants (grouped by processes).

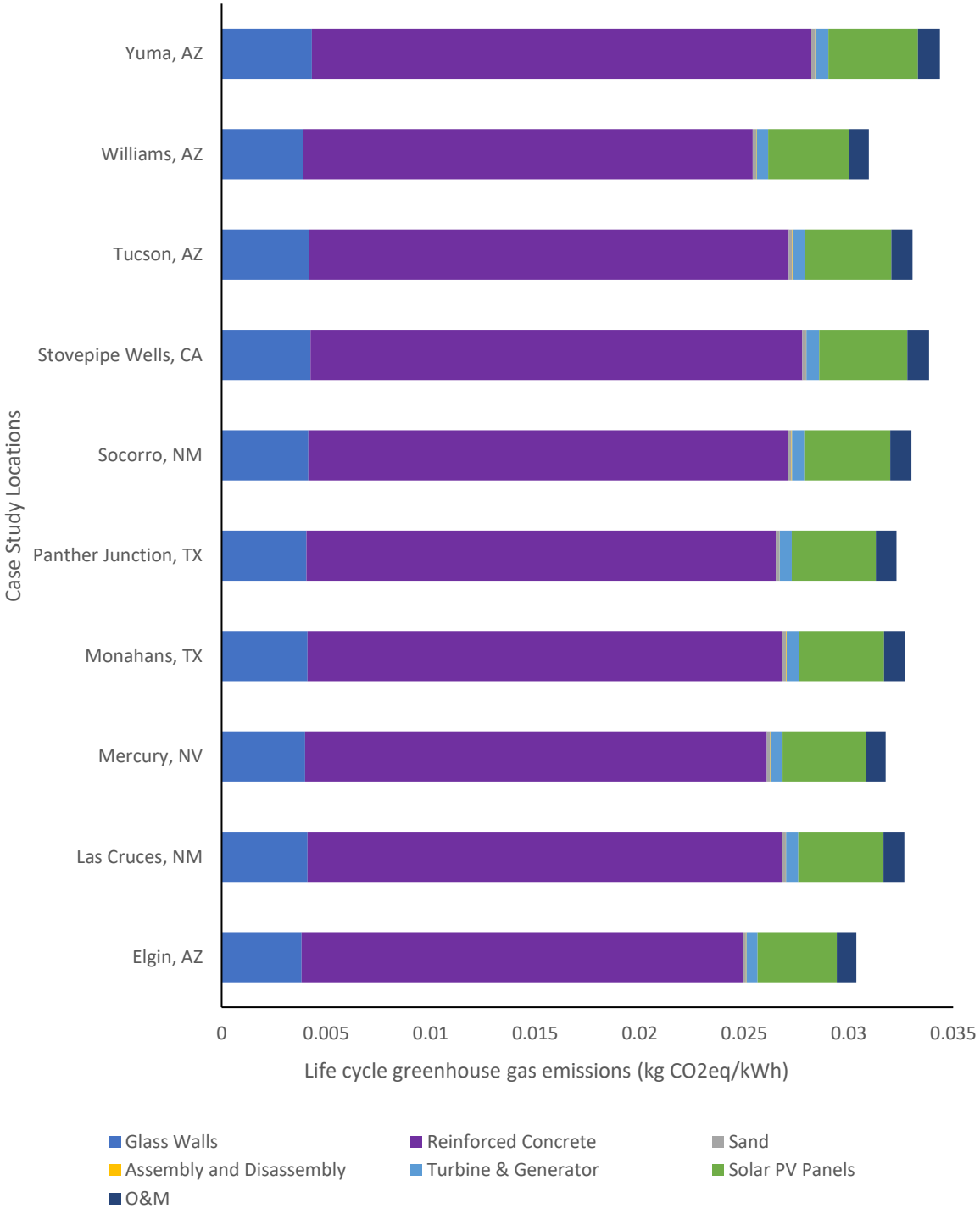

Figure 14: Life cycle GHG emissions for the baseline LCA scenarios for different geographic case study locations for SUTPP-PV hybrid power plants (grouped by materials).

3.4. Sensitivity Analysis Results:

A sensitivity analysis on mathematical models is performed to assess the sensitivity of the model outputs to the different parameter values, input variables, and calculations. Through this analysis, the parameters that should be the focus for optimization to minimize the life cycle greenhouse gas emissions could be roughly determined as well. The parameters that were altered in this analysis were: the lifetime of operation, turbine efficiency, fraction of maintenance time, a fraction of greenhouse glass walls that need replacement, the fraction of concrete for collector construction, hours of cable yarder operation for assembly, hours of cable yarder operation for disassembly, hours of construction, hours of construction machine operation, the fraction of 40mpa reinforcing concrete recycled, the fraction of steel recycled, the fraction of plastic recycled, the fraction of epoxy recycled, the fraction of glass fiber recycled, and the fraction of aluminum recycled.

The same sensitivity analysis was performed for all 10 locations for the stand-alone SUTPP and SUTPP-PV hybrid system with a 2% collector area covered with PV panels. The only difference with PV was there were some additional parameters when PV was considered: performance ratio, the annual degradation rate of solar PV panels, and the fraction of solar PV panels recycled. Some of the values of the parameters like hours of cable yarder operation for assembly, hours of cable yarder operation for disassembly, hours of construction, and hours of construction machine operation might be estimated to have some changes because, with 2% of the collector area covered by solar PV, additional hours would be needed. However, the values of maintenance time were the same for both without and with PV scenarios because it was assumed that the maintenance for both these systems was done during the same window of time.

Figures 15 and 16 represent the sensitivity analysis for the two locations with the lowest (Elgin, AZ) and highest (Yuma, AZ) life cycle GHG emissions. It shows how much the total impact deviates from the baseline values when an individual parameter was altered while keeping all the others constant. The sensitivity analysis results indicated that the modeled systems both with and without PV were particularly sensitive to the lifetime of operation. Shorter lifespans lead to higher overall life cycle GHG emissions. The lifetime of both the SUTPP and SUTPP-PV systems was the most sensitive parameter to the system followed by turbine efficiency. For SUTPP-PV systems, the performance ratio also seemed to have a notable influence on the LCA results. The systems seemed to be very minimally sensitive to all the other parameters, and so only the top five parameters with the highest sensitivity were included here. Both Elgin, AZ and Yuma, AZ along with all the other 8 case study sites show an almost identical trend in the sensitivity analysis and therefore only 2 locations were shown as a representation of all the 10 case study locations.

The sensitivity analysis performed in this study suggested that the system is highly sensitive to the lifetime of Solar Updraft Tower Power Plants. The minimum and maximum sensitivity results varied between -24 to 25% and 16 to 17% respectively from

the baseline value. This was by far the most sensitive parameter for both the stand-alone SUTPP and the SUTPP-solar PV Hybrid system. On the other hand, the system is moderately sensitive to the turbine efficiency of the Solar Updraft Tower Power Plants. The minimum and maximum sensitivity results varied between -3.0% and 3.0% respectively from the baseline value. This was the second most sensitive parameter for both the stand-alone SUTPP and the SUTPP-solar PV Hybrid system.

The same is true for the turbine efficiency of Updraft Tower Power Plants. The minimum and maximum sensitivity results varied between -3.0% and 3.0% respectively from the baseline value when the efficiencies were changed from minimum to its maximum value. Performance ratio was a sensitive parameter only for the SUTPP-solar PV Hybrid system where the minimum and maximum sensitivity results varied between -4.0% and 4.0%. But for the annual degradation rate, the minimum and maximum sensitivity results varied only between -0.4% and +0.4% respectively that suggests the system is not very sensitive to the system.

The Solar PV panel recycling rate is a quite minimally sensitive parameter (± 0.009%). The system is not very sensitive to the fraction of maintenance time (± 1.0 %) either and so it is not crucial to assess a very precise range of values for these parameters. The system was very minimally sensitive (± 0.75%) to the fraction of greenhouse glass walls that need replacement. The same is true for construction time, assembly and disassembly time, and the duration of cable yarding operation. The changes in turbine material recycling rate had quite notable impacts on the system according to the sensitivity study performed. The maximum and the minimum changes in the recycling rate of glass-fiber and epoxy from the baseline values were approximately ±7.5% and ±4.0% for the stand-alone SUTPP power plant and ±6.5 % and ±3.5% for the SUTPP-solar PV Hybrid system respectively. All of the other parameters that are not specifically mentioned had a very negligible impact (< 0.009%) on the sensitivity of the system studied in this paper.

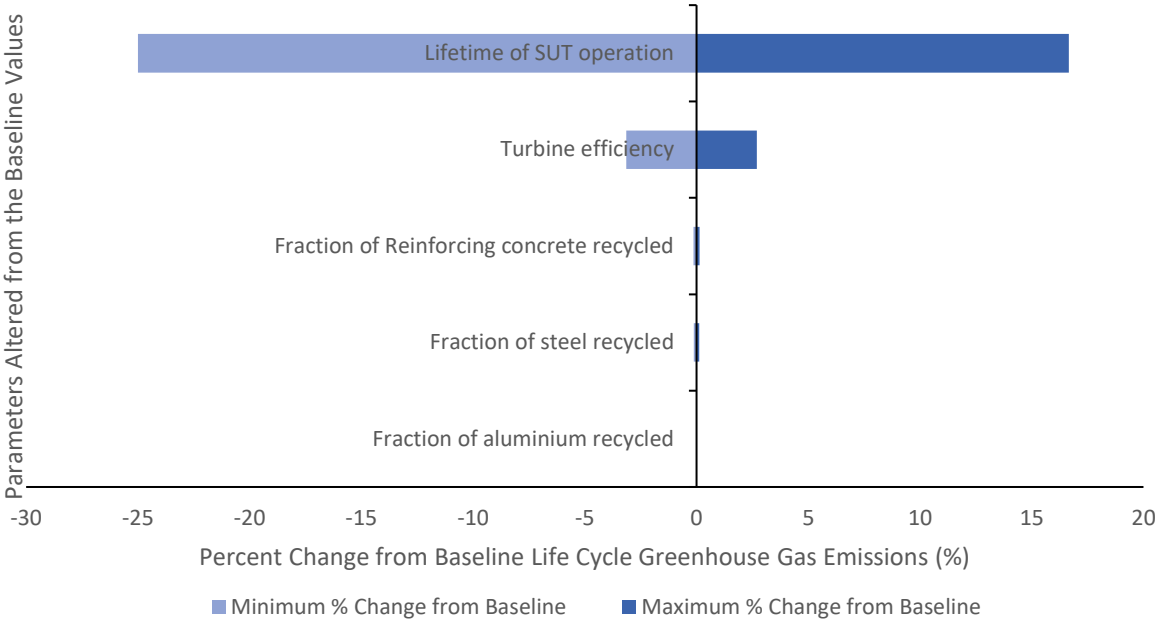

(a)

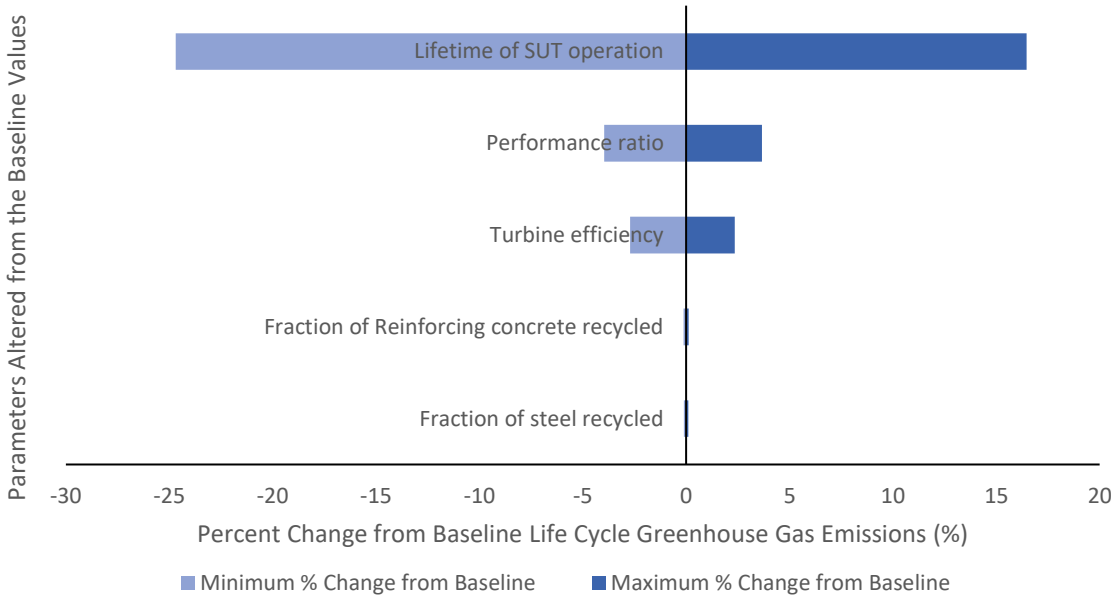

(b)

Figure 15: Sensitivity analysis for the modeled parameters of the solar updraft tower (a) without PV and (b) with PV in Elgin, Arizona. The span difference of the bars shows the life cycle greenhouse gas emissions difference for the solar updraft tower system when a parameter is changed from its minimum to its maximum value while keeping all the other parameters fixed.

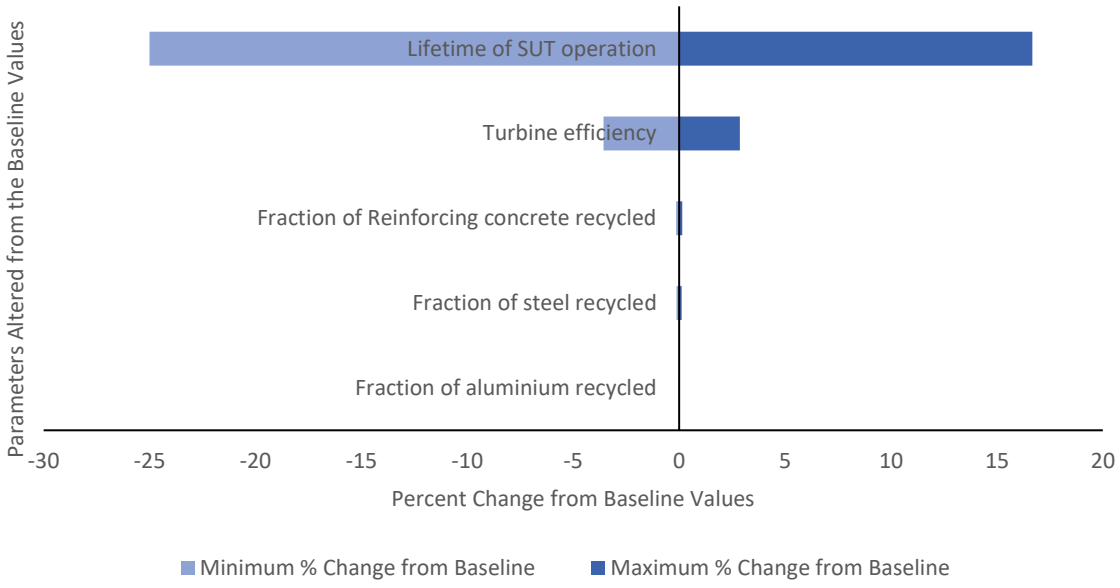

(a)

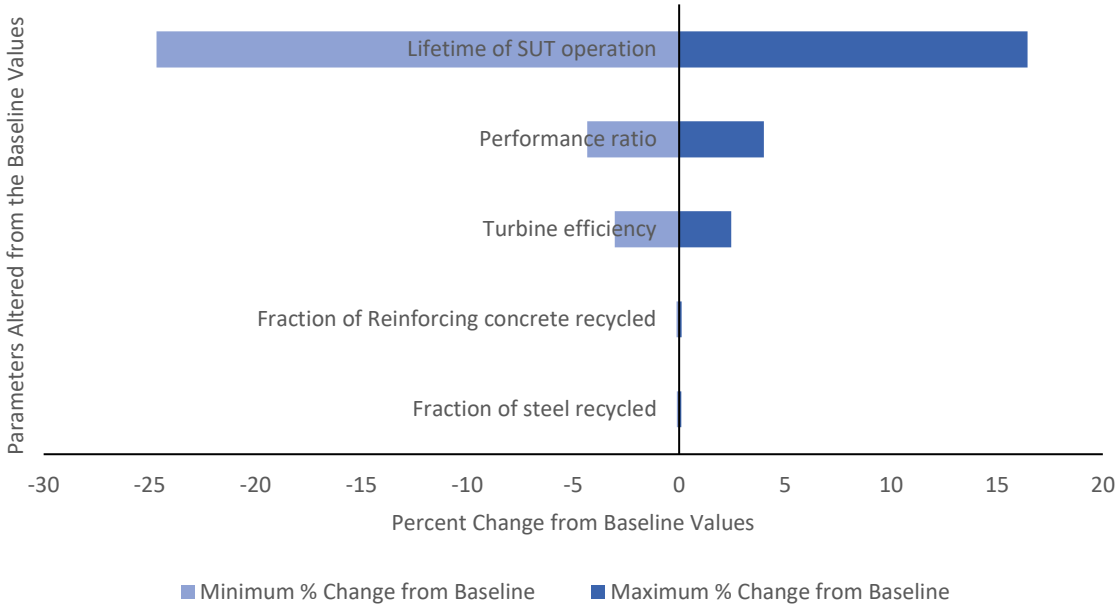

(b)

Figure 16: Sensitivity analysis for the modeled parameters of Solar Updraft Tower (a) without PV and (b) with PV in Yuma, Arizona. The span difference of the bars shows the life cycle greenhouse gas emissions from the Solar Updraft Tower system when a parameter is changed from its minimum to its maximum value keeping all the other parameters fixed.

3.5. Monte Carlo Analysis Interpretations:

Monte Carlo analysis provides statistical data for possible LCA results by combining random parameter values within specified ranges and input probability distributions. Because of the lack of available data on input parameter probability distributions for this modeled system, Monte Carlo analyses were performed by assigning all parameters to each of the three most widely used statistical distributions (uniform, normal and triangular) in order to examine if the probability distribution types have a significant effect on the Monte Carlo analysis results. The normal distribution is symmetric and the values in the middle near the mean are most likely to occur, whereas, for the uniform distribution, all the values have the same probability of occurring. Similar to the normal distribution, triangular distribution values closer to the baseline values are more likely to occur (Heijungs, 2020).

The resulting Monte Carlo plots differ substantially, indicating that further investigation of the system is needed to determine which parameter values follow what particular distributions. The results of Monte Carlo analysis for this study are inconclusive and further investigation is needed in this regard. Figures 17 and 18 represent Monte Carlo simulation for the location Elgin, Arizona without solar PV (stand-alone SUTPP system) and with solar PV (SUTPP-PV hybrid system) showing the uniform, normal and triangular distribution (n=10,000). The mean life cycle GHG emissions of all the three types of distribution for the stand-alone SUTPP system were relatively similar at 30.16 g CO_{2eq}/kWh using a uniform distribution, 29.84 g CO_{2eq}/kWh using a normal distribution, and 29.92 g CO_{2eq}/kWh using a triangular distribution.

However, the values of standard deviation varied more for these three types of distribution for Elgin, Arizona. The standard deviations were 3.56, 2.83, and 2.48 g CO_{2eq}/kWh for uniform, normal and triangular distributions, respectively. Similarly, the mean for all the three types of distribution for the SUTPP-PV hybrid system was nearly identical at 30.83 g CO_{2eq}/kWh using uniform distributions, 30.42 g CO_{2eq}/kWh using normal distributions, and 30.55 kg CO_{2eq}/kWh using triangular distributions. However, the values of standard deviation varied slightly more for these three types of distributions for Elgin, Arizona. The standard deviations were 3.66, 2.89, and 2.52 g CO_{2eq}/kWh for uniform, normal and triangular distributions, respectively.

However, not all of these resulting distributions depict normal distributions that would be defined using standard deviations (Figures 17 and 18). Despite showing similar means across Monte Carlo analysis results, the probability distributions show different shapes relative to each other. The variation in the skewness of the Monte Carlo results from the use of different input parameter distribution types (normal, uniform, and triangular) suggests that it is necessary to determine the individual parameters' probability distributions in order to obtain more accurate Monte Carlo results.

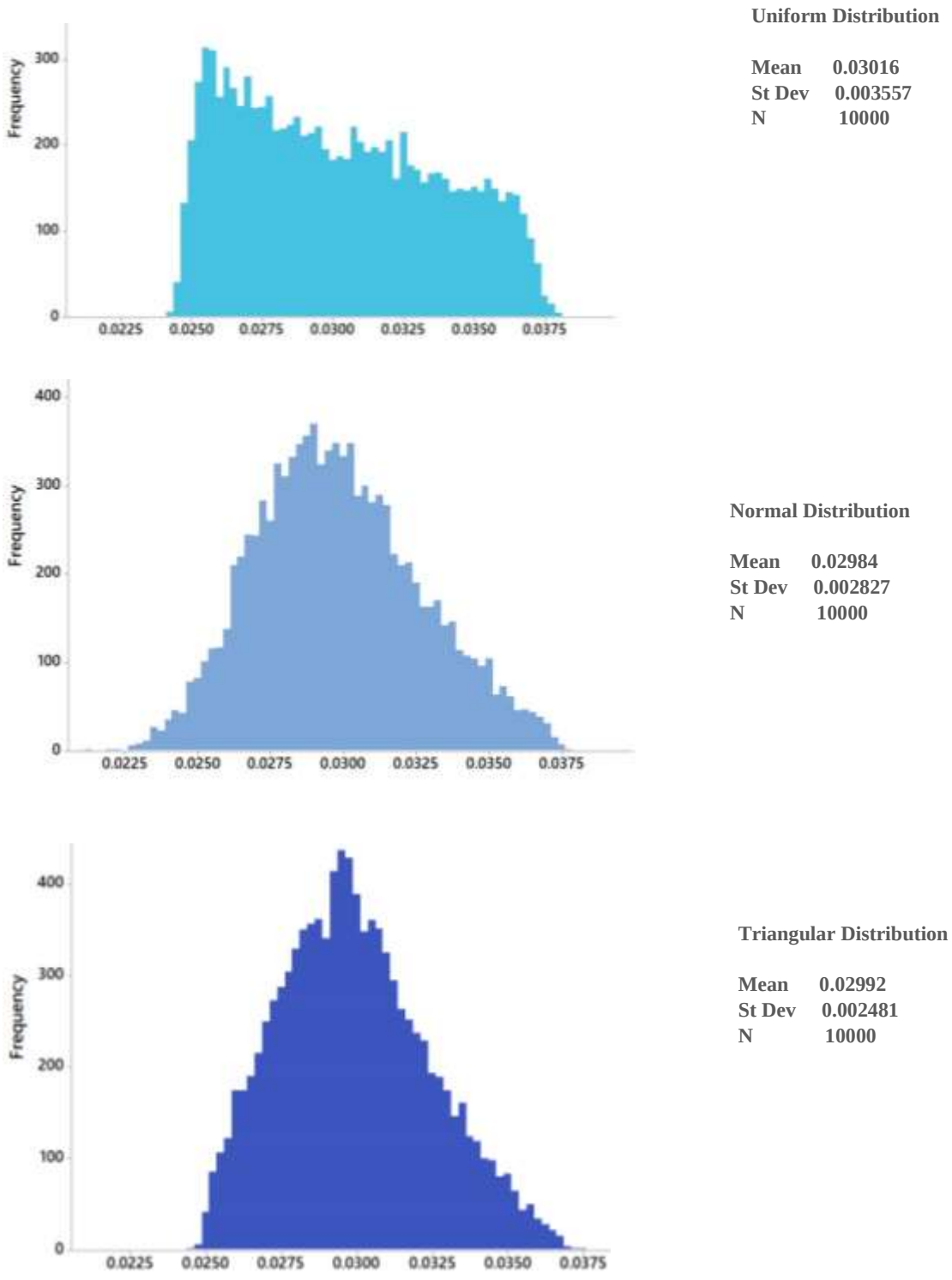

Figure 17: Monte Carlo analysis for Elgin, Arizona showing uniform, normal and triangular distributions for input parameters to obtain the probabilities of life cycle GHG emission (in kg CO_{2eq}/kWh) without solar PV (stand-alone SUTPP) scenarios.

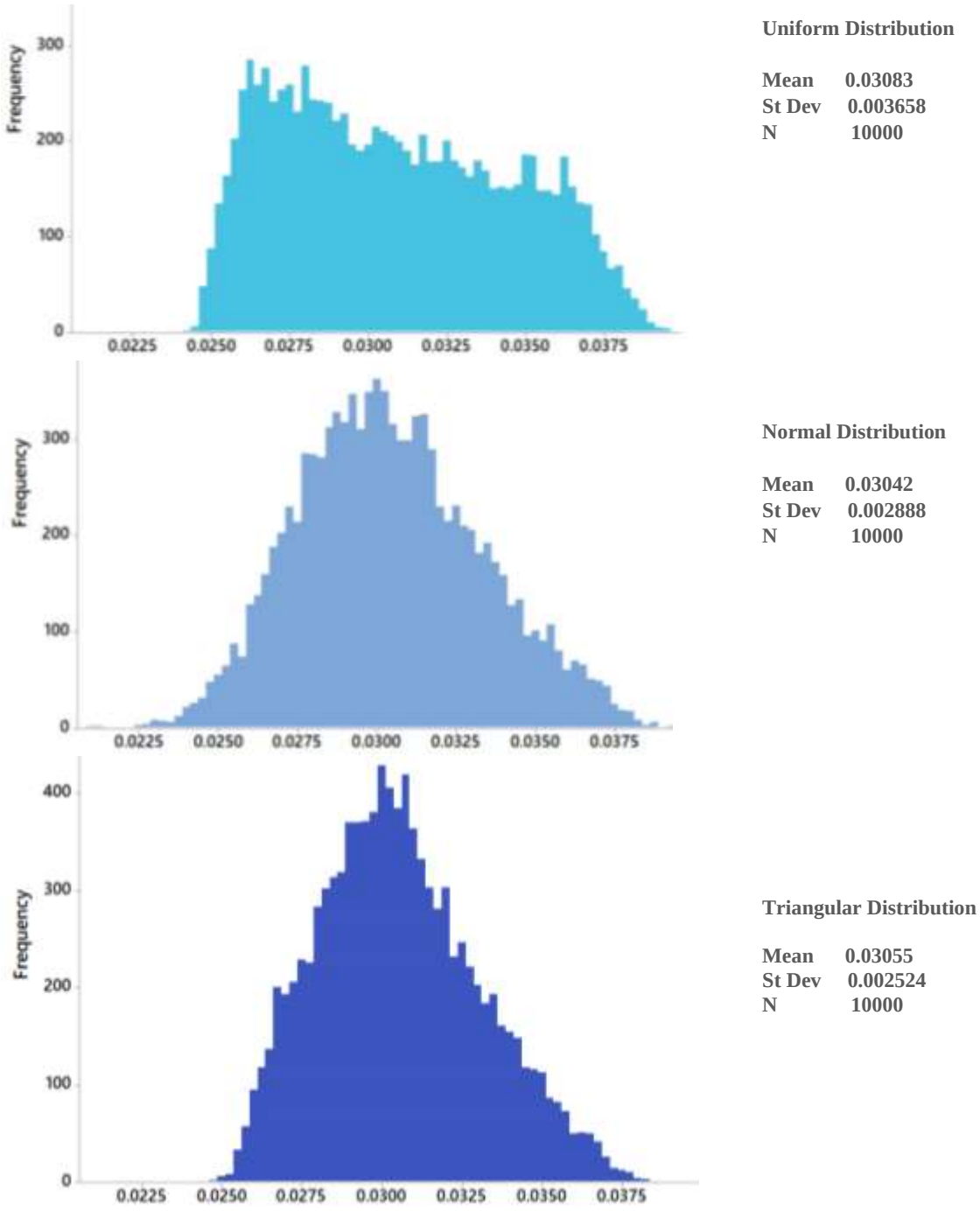

Figure 18: Monte Carlo analysis for Elgin, Arizona using uniform, normal and triangular distributions for input parameters to obtain the probabilities life cycle GHG emissions (in kg CO_{2eq}/kWh) with solar PV (SUTPP-PV hybrid) scenarios.

3.6. Geographic Effects:

Figure 19 shows the comparison of the elevation of the case study locations with the lifetime electricity generation from the stand-alone SUTPP along with SUTPP-PV hybrid power plants in the case study locations. In this plot, the elevation in feet is represented in descending order. Williams and Elgin located in Arizona have the highest elevation among the case study site that are respectively 6772 and 4731 feet. All the other sites have a moderate elevation that ranges from 2500-4600 feet except for only Yuma, AZ, and Stovepipe Wells, CA. Yuma has an elevation of only 203 feet and Stovepipe Wells has an elevation of only 62 feet making them the sites with the lowest elevation above sea level (*Weather Atlas | Weather forecast and Climate information for cities all over the Globe*, n.d.).

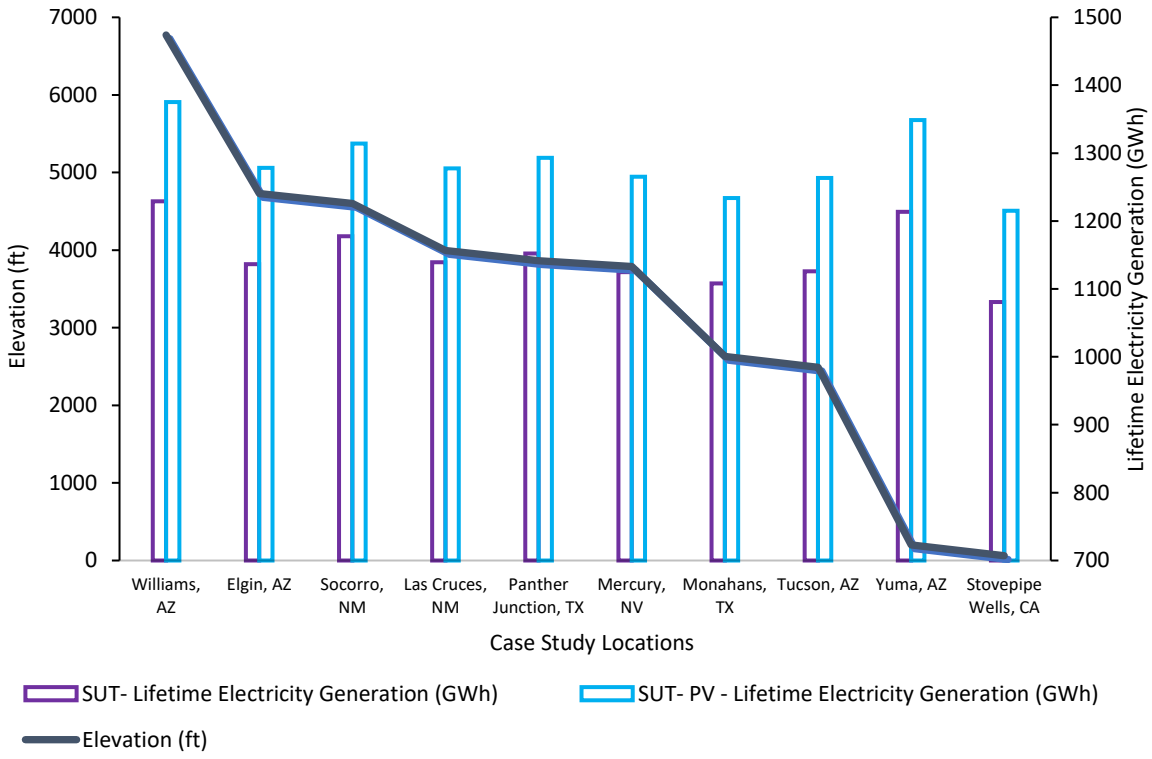

Figure 19: Comparison between elevation and lifetime electricity generation for the case study locations for the stand-alone SUTPP scenarios and SUTPP-PV hybrid scenarios. (Weather Atlas | Weather forecast and Climate information for cities all over the Globe, n.d.).

With higher elevation, the temperature tends to decrease especially more drastically for the locations with dry weather, and Figures 19 and 20 depict this (McGuire et al., 2012). However, it is not clear from Figure 19 whether temperature and elevation have any correlation with lifetime electricity generation. Locations like Elgin, AZ, Las Cruces, NM, and Mercury, NV generated a higher amount of electricity than their lower-

elevation counterparts within a 25-year lifetime. Despite having massive differences in elevation (~ 6000 ft), Yuma, AZ, and Stovepipe Wells, CA generated almost the same amount of electricity throughout their operational lifetime. Therefore, a relationship between electricity generation and elevation above sea level as well as ambient temperature could not be established.

It should be remembered that the average temperature for a month does not mean that it was the only temperature that the site had throughout that whole month. In reality, the temperature fluctuates every day, every hour, and even every minute, even though elevation stays the same for a location (McGuire et al., 2012). Although temperature increase and decrease can be driven by many different factors, overall it seemed to follow an increasing trend with decreasing elevation (McGuire et al., 2012).

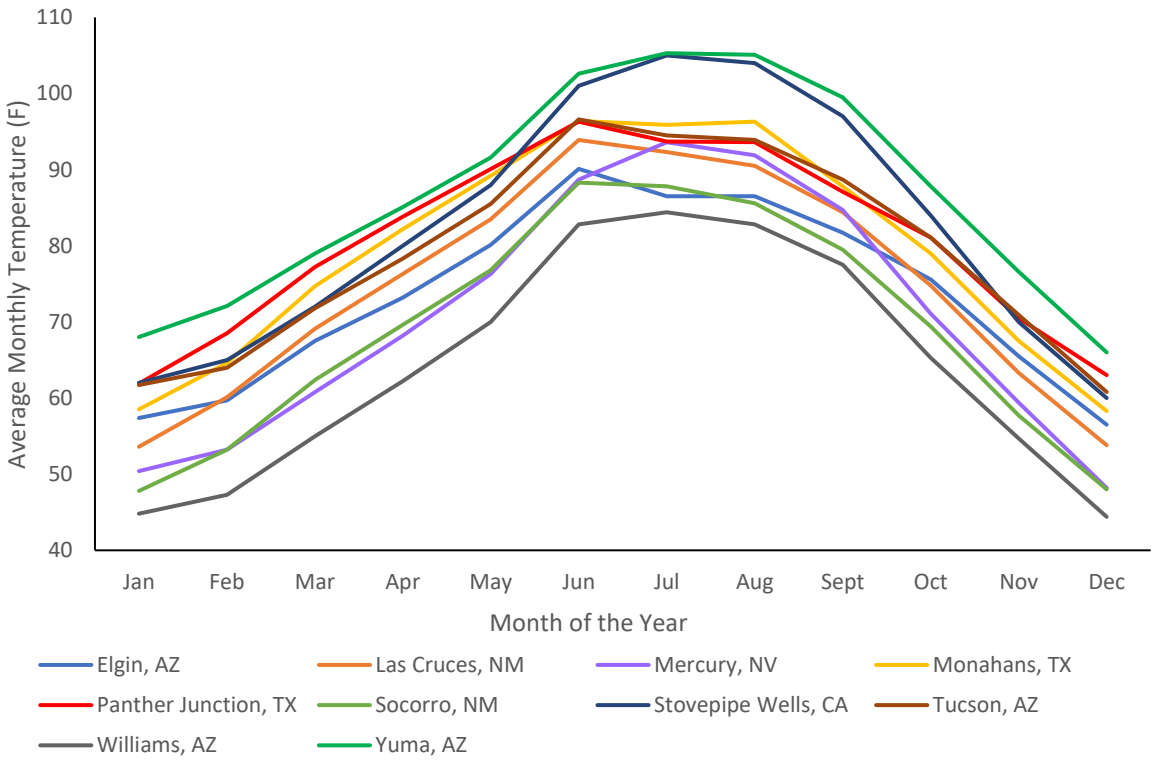

Figure 20: Average monthly temperature distribution for the case study locations. (*Weather Atlas | Weather forecast and Climate information for cities all over the Globe*, n.d.).

From Equation (14), electricity generation from a SUTPP depends on the ambient temperature, solar radiation, and ground temperature which is heavily dependent on the soil composition and humidity of the case study sites. Solar radiation is directly dependent on the hours of daylight in a day and the angle of the sun or latitude (Muneer, 2007). The latitude of the selected case study locations vary as follows: Mercury, NV

(36.66^{o}N); Stovepipe Wells, CA (36.61^{o}N); Williams, AZ (35.25^{o}N); Socorro, NM (34.1^{o}N); Yuma, AZ (32.7^{o}N); Las Cruces, NM (32.32^{o}N); Tucson, AZ (32.22^{o}N); Elgin, AZ (31.66^{o}N); Monahans, TX; (31.6^{o}N); and Panther Junction, TX (29.32^{o}N) (*Weather Atlas | Weather forecast and Climate information for cities all over the Globe*, n.d.). Still, a clear relationship between latitude and lifetime electricity generation could not be determined. The same goes for the monthly average daylight in a day in hours because all the case study locations follow a very similar trend.

3.7. Comparison of SUTPP LCA with other energy systems in the US:

Renewable energy sources provide a more sustainable long-term solution to energy usage worldwide. Despite that, all the energy systems have some overall impact on climate change. However, the effects of renewable energy sources on climate change are considered to be typically much lower than those of fossil fuel sources like natural gas, crude oil, and coal, which together still provide more than 80% of the US primary energy supply (Sayed et al., 2020). Figure 21 graphically represents the life cycle GHG emissions from various energy systems, including the results from this LCA of SUTPPs.

(Lamnatou & Chemisana, 2017) found that on average, the life cycle greenhouse gas emissions from concentrated solar power (CSP) technologies in the US vary from 22 to 40 g CO_{2eq}/kWh. Overall, this is similar to the impact of electricity from SUTPPs determined in this study. Still, in practice, the carbon footprint of CSP would vary slightly across the US because an accurate depiction would be to perform a site-specific LCA for a specific design of a utility-scale CSP plant (Burkhardt III et al., 2012). CSP technologies require additional facilities like water cooling or other cooling methods, and in some cases, molten salt for energy storage (Bukhary et al., 2018).

The life cycle climate change impact associated with solar PV is around 40 g CO_{2eq}/kWh for multi-crystalline solar PV panels in the US, whereas, for wind, nuclear, and geothermal energy sources, the approximate life cycle greenhouse emissions are 12, 220, and 126 g CO_{2eq}/kWh, respectively (Dolan & Heath, 2012; Eberle et al., 2017; Stages, 2012; Warner & Heath, 2012). Other renewable energy sources like hydropower, ocean renewable energy, biogas, biofuel are being excluded from this comparison because these sources are not the most appropriate technologies to be implemented in the arid climates of southwestern United States (Bukhary et al., 2018).

Figure 21 shows that the life cycle impact of the SUTPP and SUTPP-PV falls within the range for renewable energy in the specific climate of the southwest United States. The average life cycle GHG emissions for both these systems are around 32.9 g CO_{2eq}/kWh. This is at least 30 times lower than coal, and even half of the geothermal energy carbon footprint, and slightly lower than solar photovoltaic energy systems, which are well-established renewable energy technologies (Eberle et al., 2017; Sayed et al., 2020).

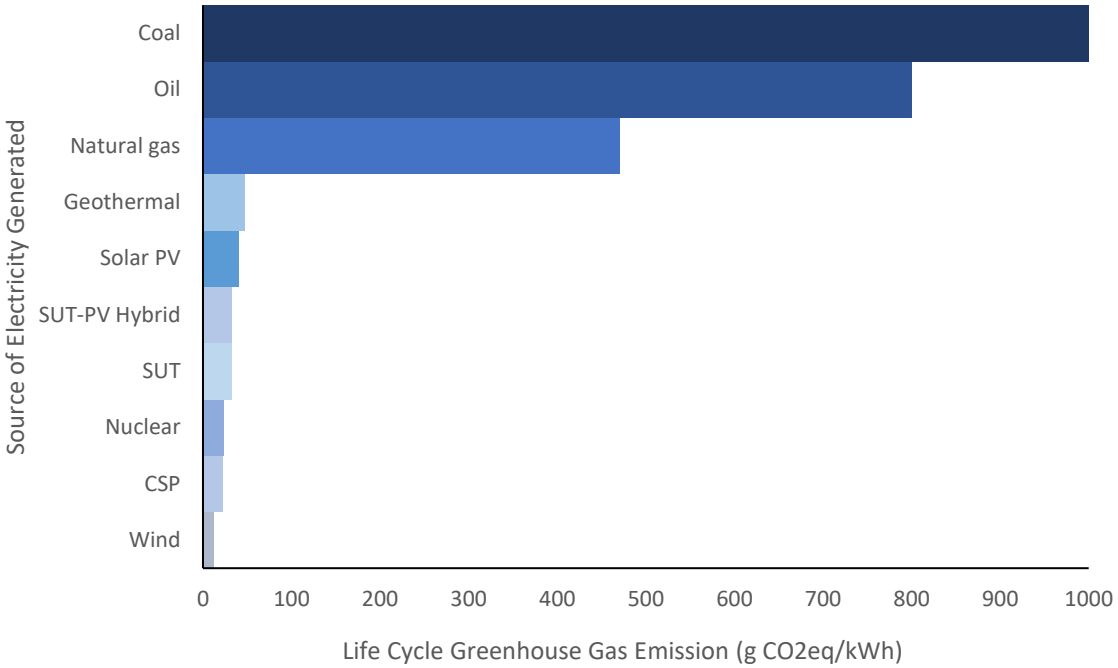

Figure 21: Comparison of average greenhouse gas emission from various energy sources. (Bukhary et al., 2018; Burkhardt III et al., 2012; Dolan & Heath, 2012; Eberle et al., 2017; Lamnatou & Chemisana, 2017; Sayed et al., 2020; Stages, 2012; Turconi et al., 2013; Warner & Heath, 2012).

Approximately 100 g CO_{2eq}/kWh is considered to be the acceptable upper limit of greenhouse gas emission from a new renewable energy system (Pehl et al., 2017). The GHG emissions from wind and nuclear energy are still notably lower than most other energy sources, and they can be established under a wider range of geographic and climatic conditions. However, a major advantage of solar updraft towers is that they can utilize the barren desert lands while needing little to no water (Al-Kayiem & Aja, 2016; Nizetic et al., 2008; Warner & Heath, 2012). The supposedly lower GHG emissions from the solar updraft tower system for the southwest US represent strong potential for SUTPP technology to be established in appropriate locations in the future along with more well-known and established renewable energy technologies.

3.8 Limitations and potential for future work:

The environmental data obtained from NOAA were limited to only very specific available locations (Bell et al., 2013; Diamond, Karl, Palecki, Baker, Bell, Leeper, Easterling, Lawrimore, Meyers, Helfert, et al., 2013). The soil temperature datasets that were used for the incorporation of soil heat storage were only available to 10 cm deep into the soil for all 10 locations. There were other options like temperatures 5 cm, 20 cm,

50 cm, and 100 cm deep into the soil, but these values were not consistently available for all the locations. The sub-hourly data sets (5 minutes interval data) available from the same source also did not have the minimum and maximum values of temperature on the surface and temperature deeper into the ground that were crucial for the calculations (Diamond, Karl, Palecki, Baker, Bell, Leeper, Easterling, Lawrimore, Meyers, Helfert, et al., 2013). That is why the usage of hourly data instead of the 5-minutes interval data was necessary. The finer-scale data may have provided different results for this current analysis.

The upper and lower limits of a few variable parameters could not be concluded from previous studies, and therefore there was a need to assume by how much the parameters vary above and below their baseline values. However, most of these parameters had a very negligible impact on the total life cycle GHG emission from the system, as was determined from the sensitivity analysis and so, investigation of issues and making major changes accordingly in those areas is not worthwhile.

Not including direct land-use change may have affected the overall life cycle GHG emissions (Fortier et al., 2017). The greenhouse-like roof may have a different surface albedo than the desert land upon which it would be installed, which could lead to either a cooling or a warming effect. The impacts of the system on the existing vegetation are unknown, and thus the contributions of carbon emissions or sequestration from effects on plant life to the life cycle GHG emissions of SUTPPs are unknown.

Due to many shared similarities in the climatic conditions of the 10 case study sites, a clear relationship between the geographic factors (like elevation, latitude, solar radiation, daylight hours, ambient temperature) and the total global warming impact of electricity from SUTPPs could not be established. Comparison with the same systems located in very different climatic conditions might give a stronger interpretation of the results in that regard (Nizetic et al., 2008).

Reinforced concrete and glass walls – the two most crucial elements of the construction of the system -- are also the two highest contributors to the total life cycle GHG emissions. Technological advancement can decrease the carbon intensity of their production processes in the future. The incorporation of a very small amount of solar PV into the system did make a moderate difference in lifetime electricity generation and life cycle GHG emissions. Increasing the coverage of solar PV along with modifying the electricity generation model might give us a clearer picture of the effects of hybridization in the future. Other areas to explore can be a combination of combined heat and power (CHP), solid oxide fuel cell, and nuclear energy systems with SUTPP system (Fathi et al., 2018; Fei et al., 2019; Joneydi Shariatzadeh et al., 2015; Tian et al., 2020). The utilization of secondary heat from SUTPPs can revolutionize this technology (Fathi et al., 2018).

CHAPTER-04

CONCLUSION

Conclusion:

This geospatial LCA of solar updraft tower power plants was the first of its kind. This study was a starting point to assess the climate change impacts of this system at a commercial scale for arid climates and potential installation in the US. The comparison between a stand-alone SUTPP system and a SUTPP-PV hybrid system was also novel. The scenarios represented in this study measured the geographic life cycle greenhouse gas emissions of SUTPP and SUTPP-PV hybrid systems for the arid climates of the southwest, analyzed the trends among case study locations, and interpreted the results in the context of the carbon footprints of other energy systems. The resulting low greenhouse gas emissions can be an indication that these two systems could be recommended for locations with similar climatic conditions and adequate land availability in the southwest US as a source of low GHG-emission electricity. The hybrid SUTPP-PV system with 2% of the collector area covered by solar PV panels showed little difference in its life cycle GHG emissions relative to the stand-alone SUTPP system.

The lifetime of the SUTPP had the largest impact on the life cycle GHG emissions of electricity generated from this technology. In terms of processes, the production of reinforced concrete and glass walls that are crucial for the construction of the long-standing central tower has the largest contribution to the overall climate change impact, according to the baseline LCA scenario analysis performed in this study. However, there are uncertainties within the systems that may also be driven by many factors like construction time, operation time, recycling rate, etc. even though individually they contributed very little to the overall life cycle impact. Because the usage of reinforced concrete was the largest source of GHG emissions that also affects the lifespan of the SUTPP towers, future enhancement of the system may benefit from considering alternative materials with higher durability and lower life cycle impacts.

Moreover, it is possible to apply the LCA model developed in this study to other suitable regions of the US and other parts of the world using appropriate geographic data and applicable inventories. The developed model is designed in a way so that it can easily be scaled up or scaled-down as well for its intended use. Therefore, this study provides the first step towards multiple directions of future research into the sustainability of SUTPPs.

CHAPTER-05

REFERENCES

References:

• *U.S. metal recycling rates by type 2019 | Statista*. (n.d.). Retrieved August 19, 2021, from https://www.statista.com/statistics/251345/percentage-of-recycled-metals-in-the-us-by-metal/

Abdulla, S. A. A., Al-Rizzo, H. M., & Cyril, M. M. (1988). Particle-size distribution of Iraqi sand and dust storms and their influence on microwave communication systems. *IEEE Transactions on Antennas and Propagation*, *36*(1), 114–126.

Adarsh, S., & Menon, A. (2014). Numerical simulation on the performance evaluation of a solar updraft tower. *Int. J. Mech. Eng. & Rob. Res.*, *3*(4).

Adedeji, A., Aweda, J., & Lasode, O. (2010). Estimation of Service Life for a Solar Chimney-Collector System. *Lecture Notes in Engineering and Computer Science*, *2184*.

Afonso, C., & Oliveira, A. (2000). Solar chimneys: simulation and experiment. *Energy and Buildings*, *32*(1), 71–79.

Al-Dabbas, M. A. (2012). The first pilot demonstration: solar updraft tower power plant in Jordan. *International Journal of Sustainable Energy*, *31*(6), 399–410.

Al-Kayiem, H. H., & Aja, O. C. (2016). Historic and recent progress in solar chimney power plant enhancing technologies. *Renewable and Sustainable Energy Reviews*, *58*, 1269–1292. https://doi.org/https://doi.org/10.1016/j.rser.2015.12.331

Alhaj, M., & Al-Ghamdi, S. G. (2019). Integrating concentrated solar power with seawater desalination technologies: a multi-regional environmental assessment. *Environmental Research Letters*, *14*(7), 74014.

Andersen, P. D., Bonou, A., Beauson, J., & Brøndsted, P. (2014). Recycling of wind turbines. *DTU International Energy Report*, *2014*, 92–97.

Anderson, K. R., Shafahi, M., McNamara, C., Schroeder, W., Owen, D., & Castillo, I. (2015). Analysis of a solar updraft tower utilizing compost waste heat. *ASME 2015 Power Conference Collocated with the ASME 2015 9th International Conference on Energy Sustainability, the ASME 2015 13th International Conference on Fuel Cell Science, Engineering and Technology, and the ASME 2015 Nuclear Forum*.

Ardente, F., Latunussa, C. E. L., & Blengini, G. A. (2019). Resource efficient recovery of critical and precious metals from waste silicon PV panel recycling. *Waste Management*, *91*, 156–167.

Ashfaq, H., Hussain, I., & Giri, A. (2017). Comparative analysis of old, recycled and new PV modules. *Journal of King Saud University-Engineering Sciences*, *29*(1), 22–28.

Attig Bahar, F., Guellouz, S., Sahraoui, M., & Kaddeche, S. (2016). *Economic and Cost Effective Analysis of Solar Chimney Power Plants in the South of Tunisia*.

Aurybi, M. A., Al-Kayeim, H. H., Gilani, S. I. U., & Ismaeel, A. A. (2006). *Mathematical modeling to evaluate the performance enhancement of solar updraft power plant by external heat source*.

Ayub, F., Akhand, S., Khan, A. S., & Saklayen, G. (2018). Design and Fabrication of Solar Updraft Tower and Estimation of Power Generation; Initially Focused on Bangladesh. *IOP*

Conference Series: Earth and Environmental Science, *150*(1), 12023.

Baker, J. W., & Lepech, M. D. (2009). Treatment of uncertainties in life cycle assessment. *Intl. Congress on Structral Safety and Reliability*.

Barou, L., Oikonomopoulou, F., Bristogianni, T., Veer, F., & Nijsse, R. (2018). Structural glass: A new remedial tool for the consolidation of historic structures. *Heron*, *63*(1–2), 159–197.

Beauson, J., Laurent, A., Rudolph, D. P., & Pagh Jensen, J. (2021). The complex end-of-life of wind turbine blades: A review of the European context. *Renewable and Sustainable Energy Reviews*, 111847. https://doi.org/https://doi.org/10.1016/j.rser.2021.111847

Bell, J. E., Palecki, M. A., Baker, C. B., Collins, W. G., Lawrimore, J. H., Leeper, R. D., Hall, M. E., Kochendorfer, J., Meyers, T. P., Wilson, T., & Diamond, H. J. (2013). U.S. climate reference network soil moisture and temperature observations. *Journal of Hydrometeorology*, *14*(3), 977–988. https://doi.org/10.1175/JHM-D-12-0146.1

Berardy, A., & Chester, M. V. (2017). Climate change vulnerability in the food, energy, and water nexus: concerns for agricultural production in Arizona and its urban export supply. *Environmental Research Letters*, *12*(3), 35004. https://doi.org/10.1088/1748-9326/aa5e6d

Bernardes, M. (2004). Life Cycle Assessment of Solar Chimneys, World Renewable Energy congress VIII. *Proceedings of the World Renewable Energy Congress VIII, Denver, USA*.

Bonate, P. L. (2001). A brief introduction to Monte Carlo simulation. *Clinical Pharmacokinetics*, *40*(1), 15–22.

Bowyer, J., Bratkovich, S., Fernholz, K., Frank, M., Groot, H., Howe, J., & Pepke, E. (2015). Understanding steel recovery and recycling rates and limitations to recycling. *Dovetail Partners Report*.

Breyer, C. (2020). A global overview of future energy. *Future Energy*, 727–756.

Bukhary, S., Ahmad, S., & Batista, J. (2018). Analyzing land and water requirements for solar deployment in the Southwestern United States. *Renewable and Sustainable Energy Reviews*, *82*, 3288–3305.

Burkhardt III, J. J., Heath, G., & Cohen, E. (2012). Life cycle greenhouse gas emissions of trough and tower concentrating solar power electricity generation: Systematic review and harmonization. *Journal of Industrial Ecology*, *16*, S93–S109.

Chaichan, M. T., Abass, K. I., & Kazem, H. A. (2018). Dust and pollution deposition impact on a solar chimney performance. *International Research Journal of Advanced Engineering and Science*, *3*(1), 127–132.

Chang, D., Lee, C. K. M., & Chen, C.-H. (2014). Review of life cycle assessment towards sustainable product development. *Journal of Cleaner Production*, *83*, 48–60.

Chen, J., Wang, J., & Ni, A. (2019). Recycling and reuse of composite materials for wind turbine blades: An overview. *Journal of Reinforced Plastics and Composites*, *38*(12), 567–577.

Chi, M., Gay-Balmaz, F., Putkaradze, V., & Vorobieff, P. (2015). Dynamics and optimal control of flexible solar updraft towers. *Proceedings of the Royal Society A: Mathematical, Physical and Engineering Sciences*, *471*(2173), 20140539.

Choi, Y. J., Kim, Y. J., Song, S. L., & Park, Y. (2015). Development of a mathematical analysis model for solar updraft tower plant (SUTP) system. *ISES Conference Proceedings*.

Chowdhury, M. S., Rahman, K. S., Chowdhury, T., Nuthammachot, N., Techato, K., Akhtaruzzaman, M., Tiong, S. K., Sopian, K., & Amin, N. (2020). An overview of solar photovoltaic panels' end-of-life material recycling. *Energy Strategy Reviews*, *27*, 100431.

Cohen, G. E., Kearney, D. W., & Kolb, G. J. (1999). *Final report on the operation and maintenance improvement program for concentrating solar power plants*. Sandia National Laboratories (SNL), Albuquerque, NM, and Livermore, CA ….

Corona, B., San Miguel, G., & Cerrajero, E. (2014). Life cycle assessment of concentrated solar power (CSP) and the influence of hybridising with natural gas. *The International Journal of Life Cycle Assessment*, *19*(6), 1264–1275.

Cousins, D. S., Suzuki, Y., Murray, R. E., Samaniuk, J. R., & Stebner, A. P. (2019). Recycling glass fiber thermoplastic composites from wind turbine blades. *Journal of Cleaner Production*, *209*, 1252–1263.

Curran, M. A. (2017). Overview of goal and scope definition in life cycle assessment. In *Goal and scope definition in life cycle assessment* (pp. 1–62). Springer.

Deline, C., Macalpine, S., Marion, B., Toor, F., Asgharzadeh, A., & Stein, J. S. (2016). *Evaluation and Field Assessment of Bifacial Photovoltaic Module Power Rating Methodologies Preprint Evaluation and Field Assessment of Bifacial Photovoltaic Module Power Rating Methodologies*. http:/www.osti.gov/scitech

Diamond, H. J., Karl, T. R., Palecki, M. A., Baker, C. B., Bell, J. E., Leeper, R. D., Easterling, D. R., Lawrimore, J. H., Meyers, T. P., & Helfert, M. R. (2013). US Climate Reference Network after one decade of operations: Status and assessment. *Bulletin of the American Meteorological Society*, *94*(4), 485–498.

Diamond, H. J., Karl, T. R., Palecki, M. A., Baker, C. B., Bell, J. E., Leeper, R. D., Easterling, D. R., Lawrimore, J. H., Meyers, T. P., Helfert, M. R., Goodge, G., & Thorne, P. W. (2013). U.S. climate reference network after one decade of operations status and assessment. *Bulletin of the American Meteorological Society*, *94*(4), 485–498. https://doi.org/10.1175/BAMS-D-12-00170.1

Dolan, S. L., & Heath, G. A. (2012). Life cycle greenhouse gas emissions of utility-scale wind power: Systematic review and harmonization. *Journal of Industrial Ecology*, *16*, S136–S154.

dos Santos Bernardes, M. A. (2013). On the heat storage in solar updraft tower collectors–influence of soil thermal properties. *Solar Energy*, *98*, 49–57.

dos Santos Bernardes, M. A., & Zhou, X. (2013a). On the heat storage in solar updraft tower collectors–Water bags. *Solar Energy*, *91*, 22–31.

dos Santos Bernardes, M. A., & Zhou, X. (2013b). Strategies for solar updraft tower power plants control subject to adverse solar radiance conditions. *Solar Energy*, *98*, 34–41.

Eberle, A., Heath, G. A., Carpenter Petri, A. C., & Nicholson, S. R. (2017). *Systematic Review of Life Cycle Greenhouse Gas Emissions from Geothermal Electricity*.

Eryener, D., & Kuscu, H. (2018). Hybrid transpired solar collector updraft tower. *Solar Energy*, *159*, 561–571.

Fathi, N., McDaniel, P., Aleyasin, S. S., Robinson, M., Vorobieff, P., Rodriguez, S., & de Oliveira, C. (2018). Efficiency enhancement of solar chimney power plant by use of waste heat from nuclear power plant. *Journal of Cleaner Production*, *180*, 407–416.

Fei, X., Xuejun, R., & Razmjooy, N. (2019). Optimal configuration and energy management for combined solar chimney, solid oxide electrolysis, and fuel cell: a case study in Iran. *Energy Sources, Part A: Recovery, Utilization, and Environmental Effects*, 1–21.

Fenton, M. D. (2003). *Iron and steel recycling in the United States in 1998*. US Department of the interior, US Geological survey.

Finkbeiner, M., Inaba, A., Tan, R., Christiansen, K., & Klüppel, H.-J. (2006). The new international standards for life cycle assessment: ISO 14040 and ISO 14044. *The International Journal of Life Cycle Assessment*, *11*(2), 80–85.

Fluri, T. P., & von Backström, T. W. (2008). Comparison of modelling approaches and layouts for solar chimney turbines. *Solar Energy*, *82*(3), 239–246.

Fonte, R., & Xydis, G. (2021). Wind turbine blade recycling: An evaluation of the European market potential for recycled composite materials. *Journal of Environmental Management*, *287*, 112269.

Fortier, M.-O. P. (2021). *The GERLCA Parametric LCA Package. GitHub Repository* . https://github.com/GERLCA/GERLCA_parametric_LCA (2021).

Fortier, M.-O. P., Roberts, G. W., Stagg-Williams, S. M., & Sturm, B. S. M. (2017). Determination of the life cycle climate change impacts of land use and albedo change in algal biofuel production. *Algal Research*, *28*, 270–281.

Gannon, A. J., & von Backstro¨ m, T. W. (2000). Solar chimney cycle analysis with system loss and solar collector performance. *J. Sol. Energy Eng.*, *122*(3), 133–137.

Gannon, A. J., & von Backstro¨ m, T. W. (2003). Solar chimney turbine performance. *J. Sol. Energy Eng.*, *125*(1), 101–106.

Gathorne-Hardy, A. (2013a). *A Newcomer's Guide to Life Cycle Assessment-Baselines and Boundaries*.

Gathorne-Hardy, A. (2013b). Greenhouse gas emissions from rice. *Harriss-White, B.(Ed.)*.

Göğüş, Y. A. (n.d.). *ENERGY STORAGE*.

Góralczyk, M. (2003). Life-cycle assessment in the renewable energy sector. *Applied Energy*, *75*(3–4), 205–211.

Gresser, P. A. (1985). *Operating and Maintaining the Greenhouse*.

Guinée, J. B., & Lindeijer, E. (2002). *Handbook on life cycle assessment: operational guide to the ISO standards* (Vol. 7). Springer Science & Business Media.

Guo, Peng-hua, Li, J., & Wang, Y. (2014). Numerical simulations of solar chimney power plant with radiation model. *Renewable Energy*, *62*, 24–30.

Guo, Penghua, Wang, Y., Li, J., & Wang, Y. (2016). Thermodynamic analysis of a solar chimney power plant system with soil heat storage. *Applied Thermal Engineering*, *100*, 1076–1084.

Guo, Penghua, Wang, Y., Meng, Q., & Li, J. (2016). Experimental study on an indoor scale solar chimney setup in an artificial environment simulation laboratory. *Applied Thermal Engineering*, *107*, 818–826.

Guo, Penghua, Zhai, Y., Xu, X., & Li, J. (2017). Assessment of levelized cost of electricity for a 10-MW solar chimney power plant in Yinchuan China. *Energy Conversion and Management*, *152*, 176–185.

Guo, Penghua, Zhou, Y., Zhang, D., Xu, B., & Li, J. (2021). Numerical investigation and multi-objective thermo-economic optimization of a solar chimney power plant. *International Journal of Energy Research*, *45*(7), 10317–10331.

Haaf, W., Friedrich, K., Mayr, G., & Schlaich, J. (1983). Solar chimneys part I: principle and construction of the pilot plant in Manzanares. *International Journal of Solar Energy*, *2*(1), 3–20.

Habibollahzade, A., Houshfar, E., Ashjaee, M., Behzadi, A., Gholamian, E., & Mehdizadeh, H. (2018). Enhanced power generation through integrated renewable energy plants: solar chimney and waste-to-energy. *Energy Conversion and Management*, *166*, 48–63.

Hatti, M. (2014). Operation and maintenance methods in solar power plants. *Use, Operation and Maintenance of Renewable Energy Systems*, 61–93.

Heijungs, R. (2020). On the number of Monte Carlo runs in comparative probabilistic LCA. *The International Journal of Life Cycle Assessment*, *25*(2), 394–402.

Heller, M. C., Mazor, M. H., & Keoleian, G. A. (2020). Plastics in the US: toward a material flow characterization of production, markets and end of life. *Environmental Research Letters*, *15*(9), 94034.

Hoffmann, S., Jaeger, D., Lingenfelder, M., & Schoenherr, S. (2016). Analyzing the efficiency of a start-up cable yarding crew in Southern China under new forest management perspectives. *Forests*, *7*(9), 188.

Huijbregts, M. A. J., Norris, G., Bretz, R., Ciroth, A., Maurice, B., von Bahr, B., Weidema, B., & de Beaufort, A. S. H. (2001). Framework for modelling data uncertainty in life cycle inventories. *The International Journal of Life Cycle Assessment*, *6*(3), 127–132.

Igos, E., Benetto, E., Meyer, R., Baustert, P., & Othoniel, B. (2019). How to treat uncertainties in life cycle assessment studies? *The International Journal of Life Cycle Assessment*, *24*(4), 794–807.

Jacobson, M. Z., & Jadhav, V. (2018). World estimates of PV optimal tilt angles and ratios of sunlight incident upon tilted and tracked PV panels relative to horizontal panels. *Solar Energy*, *169*, 55–66.

Janajreh, I., Alshrah, M., & Zamzam, S. (2015). Mechanical recycling of PVC plastic waste streams from cable industry: A case study. *Sustainable Cities and Society*, *18*, 13–20.

Jensen, J. P. (2019). Evaluating the environmental impacts of recycling wind turbines. *Wind Energy*, *22*(2), 316–326.

Jiang, W., Gong, J., De Schutter, G., Huang, Y., & Yuan, Y. (2012). Time-dependent analysis during construction of concrete tube for tower high-rise building. *Structural Concrete*, *13*(4), 236–247.

Jiang, Y., Shen, H., Pu, T., Zheng, C., Tang, Q., Gao, K., Wu, J., Rui, C., Li, Y., & Liu, Y. (2017). High efficiency multi-crystalline silicon solar cell with inverted pyramid nanostructure. *Solar Energy*, *142*, 91–96.

Jolliet, O., Margni, M., Charles, R., Humbert, S., Payet, J., Rebitzer, G., & Rosenbaum, R. (2003). IMPACT 2002+: a new life cycle impact assessment methodology. *The International Journal of Life Cycle Assessment*, *8*(6), 324–330.

Joneydi Shariatzadeh, O., Refahi, A. H., Abolhassani, S. S., & Rahmani, M. (2015). Modeling and optimization of a novel solar chimney cogeneration power plant combined with solid oxide electrolysis/fuel cell. *Energy Conversion and Management*, *105*, 423–432. https://doi.org/https://doi.org/10.1016/j.enconman.2015.07.054

Jordan, D. C., & Kurtz, S. R. (2013). Photovoltaic degradation rates—an analytical review. *Progress in Photovoltaics: Research and Applications*, *21*(1), 12–29.

Jordan, D. C., Silverman, T. J., Sekulic, B., & Kurtz, S. R. (2017). PV degradation curves: non-linearities and failure modes. *Progress in Photovoltaics: Research and Applications*, *25*(7), 583–591.

Jordan, D. C., Silverman, T. J., Wohlgemuth, J. H., Kurtz, S. R., & VanSant, K. T. (2017). Photovoltaic failure and degradation modes. *Progress in Photovoltaics: Research and Applications*, *25*(4), 318–326.

Kafka, J. L., & Miller, M. A. (2019). A climatology of solar irradiance and its controls across the United States: Implications for solar panel orientation. *Renewable Energy*, *135*, 897–907.

Kamali, M., & Hewage, K. (2016). Life cycle performance of modular buildings: A critical review. *Renewable and Sustainable Energy Reviews*, *62*, 1171–1183.

Kasaeian, A. B., Molana, S., Rahmani, K., & Wen, D. (2017). A review on solar chimney systems. *Renewable and Sustainable Energy Reviews*, *67*, 954–987. https://doi.org/https://doi.org/10.1016/j.rser.2016.09.081

Khalid, A. M., Mitra, I., Warmuth, W., & Schacht, V. (2016). Performance ratio–Crucial parameter for grid connected PV plants. *Renewable and Sustainable Energy Reviews*, *65*, 1139–1158.

Kim, B., Azzaro-Pantel, C., Pietrzak-David, M., & Maussion, P. (2019). Life cycle assessment for a solar energy system based on reuse components for developing countries. *Journal of Cleaner Production*, *208*, 1459–1468.

Kiwan, S., & Salim, I. (2020). A hybrid solar chimney/photovoltaic thermal system for direct electric power production and water distillation. *Sustainable Energy Technologies and Assessments*, *38*, 100680.

Ko, N., Lorenz, M., Horn, R., Krieg, H., & Baumann, M. (2018). Sustainability Assessment of Concentrated Solar Power (CSP) Tower Plants–Integrating LCA, LCC and LCWE in One Framework. *Procedia CIRP*, *69*, 395–400.

Kraetzig, W. B., HARTE, R., MONTAG, U., & WOERMANN, R. (2009). From large natural draft cooling tower shells to chimneys of solar upwind power plants. *Symposium of the International Association for Shell and Spatial Structures (50th. 2009. Valencia). Evolution and Trends in Design, Analysis and Construction of Shell and Spatial Structures: Proceedings*.

Kunieda, M., Ueda, N., & Nakamura, H. (2014). Ability of recycling on fiber reinforced concrete. *Construction and Building Materials*, *67*, 315–320.

Lamnatou, C., & Chemisana, D. (2017). Concentrating solar systems: Life Cycle Assessment (LCA) and environmental issues. *Renewable and Sustainable Energy Reviews*, *78*, 916–932.

Lave, M., & Kleissl, J. (2011). Optimum fixed orientations and benefits of tracking for capturing solar radiation in the continental United States. *Renewable Energy*, *36*(3), 1145–1152.

Li, G., Huang, H., Zhang, J., & Zhang, H. (2019). Study on the performance of a solar collector with heat collection and storage. *Applied Thermal Engineering*, *147*, 380–389.

Li, J., Guo, P., & Wang, Y. (2012). Effects of collector radius and chimney height on power output of a solar chimney power plant with turbines. *Renewable Energy*, *47*, 21–28.

Li, S. (2017). *Nonlinear analysis of the solar updraft tower under static wind action*.

Liu, P., & Barlow, C. Y. (2016). The environmental impact of wind turbine blades. *IOP Conference Series: Materials Science and Engineering*, *139*(1), 12032.

Ludin, N. A., Mustafa, N. I., Hanafiah, M. M., Ibrahim, M. A., Teridi, M. A. M., Sepeai, S., Zaharim, A., & Sopian, K. (2018). Prospects of life cycle assessment of renewable energy from solar photovoltaic technologies: a review. *Renewable and Sustainable Energy Reviews*, *96*, 11–28.

Luo, W., Khoo, Y. S., Kumar, A., Low, J. S. C., Li, Y., Tan, Y. S., Wang, Y., Aberle, A. G., & Ramakrishna, S. (2018). A comparative life-cycle assessment of photovoltaic electricity generation in Singapore by multicrystalline silicon technologies. *Solar Energy Materials and Solar Cells*, *174*, 157–162.

Lupi, F, Borri, C., Harte, R., Krätzig, W. B., & Niemann, H.-J. (2015). Facing technological challenges of Solar Updraft Power Plants. *Journal of Sound and Vibration*, *334*, 57–84. https://doi.org/https://doi.org/10.1016/j.jsv.2014.03.010

Lupi, Francesca, Borri, C., Krätzig, W. B., & Niemann, H.-J. (2011). Solar Updraft Power Plant technology: basic concepts and structural design". *Encyclopedia Online of Life Support Systems (EOLSS) Developed under the Auspices of the UNESCO, Eolss Publishers, Oxford, UK*.

Manufacturing Process | Powerline :: Kirloskar Green Generator Manufacturer in North East India. (n.d.). Retrieved July 14, 2021, from http://powerlinegenset.com/manufacturing-process

Mazzeo, D., Baglivo, C., Matera, N., Congedo, P. M., & Oliveti, G. (2020). A novel energy-economic-environmental multi-criteria decision-making in the optimization of a hybrid renewable system. *Sustainable Cities and Society*, *52*, 101780.

McCormick, E., Simmonds, C., Glenza, J., & Gammon, K. (2019). Americans' plastic recycling

is dumped in landfills, investigation shows. *The Guardian*, *21*, 2019.

McGuire, C. R., Nufio, C. R., Bowers, M. D., & Guralnick, R. P. (2012). *Elevation-dependent temperature trends in the Rocky Mountain Front Range: changes over a 56-and 20-year record*.

Mehla, N., Kumar, K., & Kumar, M. (2019). Thermal analysis of solar updraft tower by using different absorbers with convergent chimney. *Environment, Development and Sustainability*, *21*(3), 1251–1269.

Mehta, P. K. (1991). Durability of concrete--fifty years of progress? *Special Publication*, *126*, 1–32.

Mehta, P. K. (1999). Advancements in concrete technology. *Concrete International*, *21*(6), 69–76.

Merli, R., Preziosi, M., Acampora, A., Lucchetti, M. C., & Petrucci, E. (2020). Recycled fibers in reinforced concrete: A systematic literature review. *Journal of Cleaner Production*, *248*, 119207.

MHI Vestas Offshore V164-10.0MW - 10,00 MW - Wind turbine. (n.d.). Retrieved July 15, 2021, from https://en.wind-turbine-models.com/turbines/1912-mhi-vestas-offshore-v164-10.0mw

Ming, T.-Z., Liu, W., Xu, G.-L., Huang, S.-Y., Peng, S.-W., & Pan, Y. (2007). Analysis of the performance of the solar chimney power plant systems [J]. *Renewable Energy Resources*, *1*.

Mishnaevsky Jr, L., & Favorsky, O. (2011). Composite materials in wind energy technology. *Thermal to Mechanical Energy Conversion: Engines and Requirements, EOLSS Publishers: Oxford, UK*.

Mishnaevsky, L., Branner, K., Petersen, H. N., Beauson, J., McGugan, M., & Sørensen, B. F. (2017). Materials for wind turbine blades: an overview. *Materials*, *10*(11), 1285.

Morelli, B., Hawkins, T. R., Niblick, B., Henderson, A. D., Golden, H. E., Compton, J. E., Cooter, E. J., & Bare, J. C. (2018). Critical review of eutrophication models for life cycle assessment. *Environmental Science & Technology*, *52*(17), 9562–9578.

Muneer, T. (2007). *Solar radiation and daylight models*. Routledge.

Mustafa, A. T., Al-Kayiem, H. H., & Gilani, S. I. G. (2014). A survey on performance enhancement of solar updraft tower power plants. *Int. J. of Eng. And Technical Research*, *2*(7), 34–39.

Niemann, H.-J., Lupi, F., Hoeffer, R., Hubert, W., & Borri, C. (2009). The Solar Updraft Power Plant: Design and Optimization of the Tower for Wind Effects. *5th European and African Conference on Wind Engineering, EACWE 5, Proceedings*.

Nizetic, S., Ninic, N., & Klarin, B. (2008). Analysis and feasibility of implementing solar chimney power plants in the Mediterranean region. *Energy*, *33*(11), 1680–1690. https://doi.org/https://doi.org/10.1016/j.energy.2008.05.012

Noguchi, T., Kitagaki, R., & Tsujino, M. (2011). Minimizing environmental impact and maximizing performance in concrete recycling. *Structural Concrete*, *12*(1), 36–46.

Omar, N. S., Hatem, W. A., & Najy, H. I. (2019). Predictive Modeling for Developing

Maintenance Management in Construction Projects. *Civil Engineering Journal*, *5*(4), 892–900.

Ong, K. S., & Chow, C. C. (2003). Performance of a solar chimney. *Solar Energy*, *74*(1), 1–17.

Ortiz, O., Castells, F., & Sonnemann, G. (2009). Sustainability in the construction industry: A review of recent developments based on LCA. *Construction and Building Materials*, *23*(1), 28–39.

Padki, M. M., & Sherif, S. A. (1999). On a simple analytical model for solar chimneys. *International Journal of Energy Research*, *23*(4), 345–349.

Papaelias, M., Márquez, F. P. G., & Ramirez, I. S. (2018). Concentrated solar power: Present and future. In *Renewable energies* (pp. 51–61). Springer.

Papageorgiou, C. (2011). Floating solar chimney with multi-pole generators. *Proceedings of the IASTED International Conference on Power and Energy System, Crete, Greece*, 22–24.

Pehl, M., Arvesen, A., Humpenöder, F., Popp, A., Hertwich, E. G., & Luderer, G. (2017). Understanding future emissions from low-carbon power systems by integration of life-cycle assessment and integrated energy modelling. *Nature Energy*, *2*(12), 939–945.

Pfister, S., Koehler, A., & Hellweg, S. (2009). Assessing the environmental impacts of freshwater consumption in LCA. *Environmental Science & Technology*, *43*(11), 4098–4104.

Quansah, D. A., & Adaramola, M. S. (2019). Assessment of early degradation and performance loss in five co-located solar photovoltaic module technologies installed in Ghana using performance ratio time-series regression. *Renewable Energy*, *131*, 900–910.

Rahimi, A., & García, J. M. (2017). Chemical recycling of waste plastics for new materials production. *Nature Reviews Chemistry*, *1*(6), 1–11.

Raychaudhuri, S. (2008). Introduction to monte carlo simulation. *2008 Winter Simulation Conference*, 91–100.

Reheis, M. C., & Urban, F. E. (2011). Regional and climatic controls on seasonal dust deposition in the southwestern US. *Aeolian Research*, *3*(1), 3–21.

Reich, N. H., Mueller, B., Armbruster, A., Van Sark, W. G., Kiefer, K., & Reise, C. (2012). Performance ratio revisited: is PR> 90% realistic? *Progress in Photovoltaics: Research and Applications*, *20*(6), 717–726.

Ruppert, S., Ross, A., Vlassak, J., & Elvis, M. (2021). Towers on the Moon: 1. Concrete. *ArXiv Preprint ArXiv:2103.00612*.

Ryberg, M., Vieira, M. D. M., Zgola, M., Bare, J., & Rosenbaum, R. K. (2014). Updated US and Canadian normalization factors for TRACI 2.1. *Clean Technologies and Environmental Policy*, *16*(2), 329–339.

Ryberg, M. W., Owsianiak, M., Richardson, K., & Hauschild, M. Z. (2016). Challenges in implementing a planetary boundaries based life-cycle impact assessment methodology. *Journal of Cleaner Production*, *139*, 450–459.

Sayed, E. T., Wilberforce, T., Elsaid, K., Rabaia, M. K. H., Abdelkareem, M. A., Chae, K.-J., & Olabi, A. G. (2020). A critical review on environmental impacts of renewable energy

systems and mitigation strategies: Wind, hydro, biomass and geothermal. *Science of The Total Environment*, 144505.

Schiel, W., & Schlaich, J. (1996). *The Solar Chimney Electricity from the sun*.

Schlaich, J., Bergermann, R., Schiel, W., & Weinrebe, G. (2005). Design of Commercial Solar Updraft Tower Systems—Utilization of Solar Induced Convective Flows for Power Generation . *Journal of Solar Energy Engineering*, *127*(1), 117–124. https://doi.org/10.1115/1.1823493

Sethuraman, L., Maness, M., & Dykes, K. (2017). Optimized generator designs for the DTU 10-MW offshore wind turbine using GeneratorSE. *35th Wind Energy Symposium*, 922.

Shirvan, K. M., Mirzakhanlari, S., Mamourian, M., & Abu-Hamdeh, N. (2017). Numerical investigation and sensitivity analysis of effective parameters to obtain potential maximum power output: A case study on Zanjan prototype solar chimney power plant. *Energy Conversion and Management*, *136*, 350–360.

Singh, A. P., Kumar, A., & Singh, O. P. (2020). Performance enhancement strategies of a hybrid solar chimney power plant integrated with photovoltaic panel. *Energy Conversion and Management*, *218*, 113020.

Sissakian, V., Al-Ansari, N., & Knutsson, S. (2013). Sand and dust storm events in Iraq. *Journal of Natural Science*, *5*(10), 1084–1094.

Soils of the Southwestern US. (n.d.). Retrieved July 9, 2021, from http://geology.teacherfriendlyguide.org/index.php/25-southwestern/620-soils-sw

Southwest USA Landscapes - Deserts. (n.d.). Retrieved July 14, 2021, from https://www.americansouthwest.net/deserts.html

Spinelli, R., Visser, R., Magagnotti, N., Lombardini, C., & Ottaviani-Almo, G. (2020). The effect of partial automation on the productivity and cost of a mobile tower yarder. *Annals of Forest Research*, *63*(2), 3–14.

Stages, L. C. (2012). Life Cycle Greenhouse Gas Emissions from Solar Photovoltaics. *J. Ind. Ecol.*

Standardization, I. O. for. (2006). *Environmental Management: Life Cycle Assessment; Principles and Framework* (Vol. 14044). ISO.

Subramanian, P. M. (2000). Plastics recycling and waste management in the US. *Resources, Conservation and Recycling*, *28*(3–4), 253–263. https://doi.org/10.1016/S0921-3449(99)00049-X

Tian, M.-W., Yan, S.-R., Han, S.-Z., Nojavan, S., Jermsittiparsert, K., & Razmjooy, N. (2020). New optimal design for a hybrid solar chimney, solid oxide electrolysis and fuel cell based on improved deer hunting optimization algorithm. *Journal of Cleaner Production*, *249*, 119414.

Topham, E., McMillan, D., Bradley, S., & Hart, E. (2019). Recycling offshore wind farms at decommissioning stage. *Energy Policy*, *129*, 698–709.

Turconi, R., Boldrin, A., & Astrup, T. (2013). Life cycle assessment (LCA) of electricity generation technologies: Overview, comparability and limitations. *Renewable and*

Sustainable Energy Reviews, *28*, 555–565.

Van Blommestein, B., & Mbohwa, C. (2013). Life Cycle Assessment of Solar Chimneys. In *Re-engineering Manufacturing for Sustainability* (pp. 535–541). Springer.

Venkatachary, S. K., Samikannu, R., Murugesan, S., Dasari, N. R., & Subramaniyam, R. U. (2020). Economics and impact of recycling solar waste materials on the environment and health care. *Environmental Technology & Innovation*, *20*, 101130.

von Allwörden, H., Gasser, I., & Kamboh, M. J. (2018). Modeling, simulation and optimization of general solar updraft towers. *Applied Mathematical Modelling*, *64*, 265–284. https://doi.org/https://doi.org/10.1016/j.apm.2018.07.023

Von Backström, T. W., & Gannon, A. J. (2004). Solar chimney turbine characteristics. *Solar Energy*, *76*(1–3), 235–241.

Wang, E., & Shen, Z. (2013). A hybrid Data Quality Indicator and statistical method for improving uncertainty analysis in LCA of complex system–application to the whole-building embodied energy analysis. *Journal of Cleaner Production*, *43*, 166–173.

Warner, E. S., & Heath, G. A. (2012). Life cycle greenhouse gas emissions of nuclear electricity generation: Systematic review and harmonization. *Journal of Industrial Ecology*, *16*, S73–S92.

Weather Atlas | Weather forecast and Climate information for cities all over the Globe. (n.d.). Retrieved August 5, 2021, from https://www.weather-atlas.com/en

Williams, O., & Waterson, N. (2008). *Aerothermal Performance of a Solar Updraft Tower*.

Yadav, S. (n.d.). *CALCULATIONS OF SOLAR ENERGY OUTPUT*. Retrieved July 14, 2021, from https://www.academia.edu/9005661/CALCULATIONS_OF_SOLAR_ENERGY_OUTPUT

Zhou, X., Wang, F., & Ochieng, R. M. (2010). A review of solar chimney power technology. *Renewable and Sustainable Energy Reviews*, *14*(8), 2315–2338. https://doi.org/https://doi.org/10.1016/j.rser.2010.04.018

Zhou, X., & Xu, Y. (2016). Solar updraft tower power generation. *Solar Energy*, *128*, 95–125. https://doi.org/https://doi.org/10.1016/j.solener.2014.06.029

Zhou, X., Yang, J., Xiao, B., Hou, G., & Xing, F. (2009). Analysis of chimney height for solar chimney power plant. *Applied Thermal Engineering*, *29*(1), 178–185.

Zongker, J. D. (2013). *Life cycle assessment of Solar Updraft Tower Power Plant: EROEI and GWP as a design tool*. Wichita State University.

CHAPTER-05

SUPPLEMENTAL INFORMATION

Supplemental Information (SI):

Table SI 01: Data quality of the quality-controlled datasets obtained from the National Oceanic and atmospheric administration (NOAA). In 2020, for each location and each weather parameter, there were 8784 hourly data points and 105,408 sub-hourly (5-minute interval) data points in the NOAA dataset.

Case Study Locations	Level 3 ecoregions	Level 2 Ecoregions
Elgin, AZ	Madrean Archipelago	Western Sierra Madre Piedmont
Tucson, AZ	Sonoran Desert	Warm Desert
Williams, AZ	Arizona/New Mexico Mountains	Upper Gila Mountains
Yuma, AZ	Sonoran Desert	Warm Desert
Las Cruces, NM	Chihuahuan Desert	Warm Desert
Socorro, NM	Chihuahuan Desert	Warm Desert
Mercury, NV	Mojave Basin and Range	Warm Deserts
Monahans, TX	Chihuahuan Desert	Warm Desert
Panther Junction, TX	Chihuahuan Desert	Warm Desert
Stovepipe Wells, CA	Mojave Basin and Range	Warm desert

Table SI 02: Life cycle greenhouse gas emissions (in kg CO_{2eq}/kWh electricity) generated from different processes for stand-alone SUTPP system in Elgin, AZ; Las Cruces, NM; Mercury, NV; Monahans, TX; Panther Junction, TX.

Processes	Elgin, AZ	Las Cruces, NM	Mercury, NV	Monahans, TX	Panther Junction, TX
Production of steel	0.000263	0.000284432	0.000274499	0.000283723	0.00028055
Production of iron	8.22×10^{-5}	8.89×10^{-5}	8.58×10^{-5}	8.86×10^{-5}	8.76×10^{-5}
Production of greenhouse glass walls	0.004147525	0.004485506	0.004328866	0.004474329	0.004424281
Production of 40MPa concrete	0.021484023	0.023234753	0.022423361	0.023176858	0.02291761
Production of epoxy	1.22×10^{-5}	1.32×10^{-5}	1.27×10^{-5}	1.32×10^{-5}	1.30×10^{-5}
Production of sand	0.000182642	0.000197526	0.000190628	0.000197034	0.00019483
Production of permanent magnet	1.41×10^{-10}	1.53×10^{-10}	1.47×10^{-10}	1.52×10^{-10}	1.51×10^{-10}
Production of cable	8.29×10^{-12}	8.96×10^{-12}	8.65×10^{-12}	8.94×10^{-12}	8.84×10^{-12}
Production of glassfibre	0.000312401	0.000337859	0.00032606	0.000337017	0.000333247
Production of copper	3.11×10^{-5}	3.36×10^{-5}	3.25×10^{-5}	3.36×10^{-5}	3.32×10^{-5}
Cable yarding	1.93×10^{-5}	2.08×10^{-5}	2.01×10^{-5}	2.08×10^{-5}	2.06×10^{-5}
Diesel for construction machine operation	1.23×10^{-6}	1.33×10^{-6}	1.28×10^{-6}	1.33×10^{-6}	1.31×10^{-6}
Steel treatment	2.58×10^{-10}	2.79×10^{-10}	2.69×10^{-10}	2.78×10^{-10}	2.75×10^{-10}
Copper treatment	1.37×10^{-11}	1.48×10^{-11}	1.43×10^{-11}	1.48×10^{-11}	1.46×10^{-11}
40MPa reinforcing concrete recycling	0.000140627	0.000152086	0.000146775	0.000151707	0.00015001

40MPa reinforcing concrete disposal	0.001990129	0.002152304	0.002077142	0.002146941	0.002122926
Waste glass disposal	0.000126147	0.000136427	0.000131663	0.000136087	0.000134565
Steel recycling	-5.52×10^{-5}	-5.97×10^{-5}	-5.77×10^{-5}	-5.96×10^{-5}	-5.89×10^{-5}
Steel disposal	1.08×10^{-12}	1.16×10^{-12}	1.12×10^{-12}	1.16×10^{-12}	1.15×10^{-12}
Iron recycling	-3.66×10^{-5}	-3.96×10^{-5}	-3.82×10^{-5}	-3.95×10^{-5}	-3.90×10^{-5}
Iron disposal	6.28×10^{-14}	6.79×10^{-14}	6.56×10^{-14}	6.78×10^{-14}	6.70×10^{-14}
Plastic recycling	-5.06×10^{-8}	-5.47×10^{-8}	-5.28×10^{-8}	-5.45×10^{-8}	-5.39×10^{-8}
Plastic disposal	8.81×10^{-10}	9.53×10^{-10}	9.20×10^{-10}	9.51×10^{-10}	9.40×10^{-10}
Epoxy recycling	1.28×10^{-18}	1.39×10^{-18}	1.34×10^{-18}	1.38×10^{-18}	1.37×10^{-18}
Epoxy disposal	3.51×10^{-14}	3.80×10^{-14}	3.67×10^{-14}	3.79×10^{-14}	3.75×10^{-14}
Glassfibre recycling	2.43×10^{-17}	2.63×10^{-17}	2.54×10^{-17}	2.63×10^{-17}	2.60×10^{-17}
Glassfibre disposal	6.67×10^{-13}	7.22×10^{-13}	6.97×10^{-13}	7.20×10^{-13}	7.12×10^{-13}
Aluminium recycling	-1.30×10^{-6}	-1.41×10^{-6}	-1.36×10^{-6}	-1.41×10^{-6}	-1.39×10^{-6}
Aluminium disposal	5.76×10^{-15}	6.22×10^{-15}	6.01×10^{-15}	6.21×10^{-15}	6.14×10^{-15}
Copper End of the Life	3.33×10^{-8}	3.60×10^{-8}	3.47×10^{-8}	3.59×10^{-8}	3.55×10^{-8}
O&M	0.001036881	0.001121377	0.001082216	0.001118582	0.00110607
Total Impact	0.02973619	0.032159388	0.031036335	0.032079255	0.031720428
The lifetime electricity generation	1229048445	1136440107	1177562317	1139278909	1152166636
The capacity factor	0.561209336	0.518922423	0.537699688	0.52021868	0.526103487

Table SI 03: Life cycle greenhouse gas emissions (in kg CO_{2eq}/kWh electricity) generated from different processes for stand-alone SUTPP system in Socorro, NM; Stovepipe Wells, CA; Tucson, AZ; Williams, AZ; Yuma, AZ.

Processes	Socorro, NM	Stovepipe Wells, CA	Tucson, AZ	Williams, AZ	Yuma, AZ
Production of steel	0.000287397	0.000291709	0.000287084	0.000266356	0.000299101
Production of iron	8.98×10^{-5}	9.11×10^{-5}	8.97×10^{-5}	8.32×10^{-5}	9.34×10^{-5}
Production of greenhouse glass walls	0.004532266	0.004600255	0.00452732	0.004200442	0.004716839
Production of 40MPa concrete	0.02347697	0.023829146	0.023451347	0.021758133	0.024433048
Production of epoxy	1.33×10^{-5}	1.35×10^{-5}	1.33×10^{-5}	1.24×10^{-5}	1.39×10^{-5}
Production of sand	0.000199585	0.000202579	0.000199367	0.000184973	0.000207713
Production of permanent magnet	1.54×10^{-10}	1.57×10^{-10}	1.54×10^{-10}	1.43×10^{-10}	1.61×10^{-10}
Production of cable	9.06×10^{-12}	9.19×10^{-12}	9.05×10^{-12}	8.39×10^{-12}	9.43×10^{-12}
Production of glassfibre	0.000341381	0.000346502	0.000341008	0.000316387	0.000355283
Production of copper	3.40×10^{-5}	3.45×10^{-5}	3.39×10^{-5}	3.15×10^{-5}	3.54×10^{-5}
Cable yarding	2.11×10^{-5}	2.14×10^{-5}	2.10×10^{-5}	1.95×10^{-5}	2.19×10^{-5}
Diesel for construction machine operation	1.34×10^{-6}	1.36×10^{-6}	1.34×10^{-6}	1.25×10^{-6}	1.40×10^{-6}
Steel treatment	2.82×10^{-10}	2.86×10^{-10}	2.82×10^{-10}	2.61×10^{-10}	2.94×10^{-10}

Copper treatment	1.50 x10^{-11}	1.52 x10^{-11}	1.49 x10^{-11}	1.39 x10^{-11}	1.56 x10^{-11}
40MPa reinforcing concrete recycling	0.000153672	0.000155977	0.000153504	0.000142421	0.00015993
40MPa reinforcing concrete disposal	0.002174741	0.002207364	0.002172368	0.00201552	0.002263306
Waste glass disposal	0.000137849	0.000139917	0.000137699	0.000127757	0.000143463
Steel recycling	-6.04 x10^{-5}	-6.13 x10^{-5}	-6.03 x10^{-5}	-5.59 x10^{-5}	-6.28 x10^{-5}
Steel disposal	1.17 x10^{-12}	1.19 x10^{-12}	1.17 x10^{-12}	1.09 x10^{-12}	1.22 x10^{-12}
Iron recycling	-4.00 x10^{-5}	-4.06 x10^{-5}	-4.00 x10^{-5}	-3.71 x10^{-5}	-4.16 x10^{-5}
Iron disposal	6.86 x10^{-14}	6.97 x10^{-14}	6.86 x10^{-14}	6.36 x10^{-14}	7.14 x10^{-14}
Plastic recycling	-5.53 x10^{-8}	-5.61 x10^{-8}	-5.52 x10^{-8}	-5.12 x10^{-8}	-5.75 x10^{-8}
Plastic disposal	9.63 x10^{-10}	9.78 x10^{-10}	9.62 x10^{-10}	8.93 x10^{-10}	1.00 x10^{-9}
Epoxy recycling	1.40 x10^{-18}	1.42 x10^{-18}	1.40 x10^{-18}	1.30 x10^{-18}	1.46 x10^{-18}
Epoxy disposal	3.84 x10^{-14}	3.90 x10^{-14}	3.83 x10^{-14}	3.56 x10^{-14}	4.00 x10^{-14}
Glassfibre recycling	2.66 x10^{-17}	2.70 x10^{-17}	2.66 x10^{-17}	2.47 x10^{-17}	2.77 x10^{-17}
Glassfibre disposal	7.29 x10^{-13}	7.40 x10^{-13}	7.29 x10^{-13}	6.76 x10^{-13}	7.59 x10^{-13}
Aluminium recycling	-1.43 x10^{-6}	-1.45x10^{-6}	-1.42 x10^{-6}	-1.32 x10^{-6}	-1.48 x10^{-6}
Aluminium disposal	6.29 x10^{-15}	6.38 x10^{-15}	6.28 x10^{-15}	5.83 x10^{-15}	6.55 x10^{-15}
Copper End of the Life	3.64 x10^{-8}	3.69 x10^{-8}	3.63 x10^{-8}	3.37 x10^{-8}	3.79 x10^{-8}
O&M	0.001133067	0.001150064	0.00113183	0.001050111	0.00117921
Total Impact	0.032494642	0.032982091	0.032459177	0.030115587	0.033817956
The lifetime electricity generation	1124715231	1108092808	1125944097	1213564846	1080704528
The capacity factor	0.513568599	0.505978451	0.514129724	0.554139199	0.493472387

Table SI 04: Life cycle greenhouse gas emissions (in kg CO_{2eq}/kWh electricity) generated from different processes in baseline case scenario for stand-alone SUTPP systems (grouped by processes) in Elgin, AZ; Las Cruces, NM; Mercury, NV; Monahans, TX; Panther Junction, TX.

Processes	Elgin, AZ	Las Cruces, NM	Mercury, NV	Monahan, TX	Panther Junction, TX
Production of Materials	0.02652	0.02868	0.02767	0.0286	0.02828
Material Treatment	2.72x10^{-10}	2.94x10^{-10}	2.84x10^{-10}	2.93x10^{-10}	2.90x10^{-10}
Assembly and Disassembly	2.05x10^{-5}	2.22x10^{-5}	2.14x10^{-5}	2.21x10^{-5}	2.19x10^{-5}
Material Disposal	0.00212	0.00229	0.00221	0.00228	0.00226
Material Recycling	0.00005	0.00005	0.00005	0.00005	0.00005
O&M	0.00104	0.00112	0.00108	0.00112	0.00111

Table SI 05: Life cycle greenhouse gas emissions (in kg CO_{2eq}/kWh electricity) generated from different processes in baseline case scenario for stand-alone SUTPP systems (grouped by processes) in Socorro, NM; Stovepipe Wells, CA; Tucson, AZ; Williams, AZ; Yuma, AZ.

Materials	Socorro, NM	Stovepipe Wells, CA	Tucson, AZ	Williams, AZ	Yuma, AZ
Glass Walls	0.00467	0.00474	0.00467	0.00433	0.00486
Reinforced Concrete	0.02581	0.02619	0.02578	0.02392	0.02686
Sand	0.0002	0.0002	0.0002	0.00018	0.00021
Assembly and Disassembly	$2.24x10^{-5}$	$2.27x10^{-5}$	$2.24x10^{-5}$	$2.08x10^{-5}$	$2.33x10^{-5}$
Turbine & Generator	0.00066	0.00067	0.00066	0.00062	0.00069
O&M	0.00113	0.00115	0.00113	0.00105	0.00118

Table SI 06: Life cycle greenhouse gas emissions (in kg CO_{2eq}/kWh electricity) generated in baseline case scenario for stand-alone SUTPP systems (grouped by materials) in Elgin, AZ; Las Cruces, NM; Mercury, NV; Monahans, TX; Panther Junction, TX.

Processes	Elgin, AZ	Las Cruces, NM	Mercury, NV	Monahan, TX	Panther Junction, TX
Production of Materials	0.02652	0.02868	0.02767	0.0286	0.02828
Material Treatment	$2.72x10^{-10}$	$2.94x10^{-10}$	$2.84x10^{-10}$	$2.93x10^{-10}$	$2.90x10^{-10}$
Assembly and Disassembly	$2.05x10^{-5}$	$2.22x10^{-5}$	$2.14x10^{-5}$	$2.21x10^{-5}$	$2.19x10^{-5}$
Material Disposal	0.00212	0.00229	0.00221	0.00228	0.00226
Material Recycling	0.00005	0.00005	0.00005	0.00005	0.00005
O&M	0.00104	0.00112	0.00108	0.00112	0.00111

Table SI 07: Life cycle greenhouse gas emissions (in kg CO_{2eq}/kWh electricity) generated in baseline case scenario for stand-alone SUTPP systems (grouped by materials) in Socorro, NM; Stovepipe Wells, CA; Tucson, AZ; Williams, AZ; Yuma, AZ.

Materials	Socorro, NM	Stovepipe Wells, CA	Tucson, AZ	Williams, AZ	Yuma, AZ
Glass Walls	0.00467	0.00474	0.00467	0.00433	0.00486
Reinforced Concrete	0.02581	0.02619	0.02578	0.02392	0.02686
Sand	0.0002	0.0002	0.0002	0.00018	0.00021
Assembly and Disassembly	$2.24x10^{-5}$	$2.27x10^{-5}$	$2.24x10^{-5}$	$2.08x10^{-5}$	$2.33x10^{-5}$
Turbine & Generator	0.00066	0.00067	0.00066	0.00062	0.00069
O&M	0.00104	0.00112	0.00108	0.00112	0.00111

Table SI 08: Life cycle greenhouse gas emissions (in kg CO_{2eq}/kWh electricity) generated from different processes from SUTPP-PV hybrid systems in Elgin, AZ; Las Cruces, NM; Mercury, NV; Monahans, TX; Panther Junction, TX.

Processes	Elgin, AZ	Las Cruces, NM	Mercury, NV	Monahans, TX	Panther Junction, TX
Production of steel	0.000235048	0.000252862	0.000245979	0.000253022	0.000249978
Production of iron	7.34×10^{-5}	7.90×10^{-5}	7.68×10^{-5}	7.90×10^{-5}	7.81×10^{-5}
Production of greenhouse glass walls	0.003706721	0.003987637	0.003879099	0.003990173	0.003942159
Production of 40MPa concrete	0.019200676	0.02065581	0.020093589	0.020668945	0.020420236
Production of epoxy	1.09×10^{-5}	1.17×10^{-5}	1.14×10^{-5}	1.17×10^{-5}	1.16×10^{-5}
Production of sand	0.000163231	0.000175602	0.000170822	0.000175713	0.000173599
Production of permanent magnet	1.26×10^{-10}	1.36×10^{-10}	1.32×10^{-10}	1.36×10^{-10}	1.34×10^{-10}
Production of cable	7.41×10^{-12}	7.97×10^{-12}	7.75×10^{-12}	7.97×10^{-12}	7.88×10^{-12}
Production of glassfibre	0.000279199	0.000300358	0.000292183	0.000300549	0.000296933
Production of copper	2.78×10^{-5}	2.99×10^{-5}	2.91×10^{-5}	2.99×10^{-5}	2.96×10^{-5}
Cable yarding	1.72×10^{-5}	1.85×10^{-5}	1.80×10^{-5}	1.85×10^{-5}	1.83×10^{-5}
Diesel for construction machine operation	1.10×10^{-6}	1.18×10^{-6}	1.15×10^{-6}	1.18×10^{-6}	1.17×10^{-6}
Steel treatment	2.31×10^{-10}	2.48×10^{-10}	2.41×10^{-10}	2.48×10^{-10}	2.45×10^{-10}
Copper treatment	1.22×10^{-11}	1.32×10^{-11}	1.28×10^{-11}	1.32×10^{-11}	1.30×10^{-11}
40Mpa reinforcing concrete recycling	0.000125681	0.000135205	0.000131525	0.000135291	0.000133663
40Mpa reinforcing concrete disposal	0.001778615	0.001913409	0.001861329	0.001914626	0.001891587
Waste glass disposal	0.00011274	0.000121284	0.000117983	0.000121361	0.000119901
Steel recycling	-4.94×10^{-5}	-5.31×10^{-5}	-5.17×10^{-5}	-5.31×10^{-5}	-5.25×10^{-5}
Steel disposal	9.61×10^{-13}	1.03×10^{-12}	1.01×10^{-12}	1.03×10^{-12}	1.02×10^{-12}
Iron recycling	-3.27×10^{-5}	-3.52×10^{-5}	-3.42×10^{-5}	-3.52×10^{-5}	-3.48×10^{-5}
Iron disposal	5.61×10^{-14}	6.04×10^{-14}	5.87×10^{-14}	6.04×10^{-14}	5.97×10^{-14}
Plastic recycling	-4.52×10^{-8}	-4.86×10^{-8}	-4.73×10^{-8}	-4.86×10^{-8}	-4.81×10^{-8}
Plastic disposal	7.88×10^{-10}	8.47×10^{-10}	8.24×10^{-10}	8.48×10^{-10}	8.38×10^{-10}
Epoxy recycling	1.15×10^{-18}	1.23×10^{-18}	1.20×10^{-18}	1.23×10^{-18}	1.22×10^{-18}
Epoxy disposal	3.14×10^{-14}	3.38×10^{-14}	3.29×10^{-14}	3.38×10^{-14}	3.34×10^{-14}
Glassfibre recycling	2.18×10^{-17}	2.34×10^{-17}	2.28×10^{-17}	2.34×10^{-17}	2.31×10^{-17}
Glassfibre disposal	5.97×10^{-13}	6.42×10^{-13}	6.24×10^{-13}	6.42×10^{-13}	6.34×10^{-13}
Aluminium recycling	-1.17×10^{-6}	-1.25×10^{-6}	-1.22×10^{-6}	-1.26×10^{-6}	-1.24×10^{-6}
Aluminium disposal	5.14×10^{-15}	5.53×10^{-15}	5.38×10^{-15}	5.54×10^{-15}	5.47×10^{-15}
Copper End of the Life	2.98×10^{-8}	3.20×10^{-8}	3.11×10^{-8}	3.20×10^{-8}	3.16×10^{-8}
O&M	0.00092668	0.000996909	0.000969775	0.000997543	0.00098554
Production of PV panels	0.003607903	0.00388133	0.003775686	0.003883798	0.003837064
Solar PV inverter	0.000197477	0.000212443	0.00020666	0.000212578	0.00021002
Multi-Si PV panel recycling	-1.92×10^{-5}	-2.07×10^{-5}	-2.01×10^{-5}	-2.07×10^{-5}	-2.04×10^{-5}
Multi-Si PV panel disposal	1.58×10^{-17}	1.70×10^{-17}	1.66×10^{-17}	1.70×10^{-17}	1.68×10^{-17}

Total Impact	0.030361974	0.032662974	0.031773935	0.032683744	0.032290461
The lifetime electricity generation	1375207070	1278328219	1314096003	1277515847	1293075413
The capacity factor	0.330499176	0.307216587	0.315812546	0.307021352	0.310760734

Table SI 09: Life cycle greenhouse gas emissions (in kg CO_{2eq}/kWh electricity) generated from different processes from SUTPP-PV hybrid systems in Socorro, NM; Stovepipe Wells, CA; Tucson, AZ; Williams, AZ; Yuma, AZ.

Processes	Socorro, NM	Stovepipe Wells, CA	Tucson, AZ	Williams, AZ	Yuma, AZ
Production of steel	0.000255476	0.000261978	0.000255846	0.000239669	0.000266013
Production of iron	7.98×10^{-5}	8.18×10^{-5}	7.99×10^{-5}	7.49×10^{-5}	8.31×10^{-5}
Production of greenhouse glass walls	0.004028864	0.004131405	0.004034695	0.003779594	0.00419504
Production of 40MPa concrete	0.020869365	0.021400521	0.020899566	0.019578156	0.021730152
Production of epoxy	1.19×10^{-5}	1.22×10^{-5}	1.19×10^{-5}	1.11×10^{-5}	1.23×10^{-5}
Production of sand	0.000177417	0.000181933	0.000177674	0.00016644	0.000184735
Production of permanent magnet	1.37×10^{-10}	1.41×10^{-10}	1.37×10^{-10}	1.29×10^{-10}	1.43×10^{-10}
Production of cable	8.05×10^{-12}	8.26×10^{-12}	8.06×10^{-12}	7.55×10^{-12}	8.38×10^{-12}
Production of glassfibre	0.000303463	0.000311187	0.000303903	0.000284688	0.00031598
Production of copper	3.02×10^{-5}	3.10×10^{-5}	3.03×10^{-5}	2.83×10^{-5}	3.15×10^{-5}
Cable yarding	1.87×10^{-5}	1.92×10^{-5}	1.88×10^{-5}	1.76×10^{-5}	1.95×10^{-5}
Diesel for construction machine operation	1.19×10^{-6}	1.22×10^{-6}	1.20×10^{-6}	1.12×10^{-6}	1.24×10^{-6}
Steel treatment	2.51×10^{-10}	2.57×10^{-10}	2.51×10^{-10}	2.35×10^{-10}	2.61×10^{-10}
Copper treatment	1.33×10^{-11}	1.36×10^{-11}	1.33×10^{-11}	1.25×10^{-11}	1.38×10^{-11}
40MPa reinforcing concrete recycling	0.000136603	0.00014008	0.000136801	0.000128151	0.000142238
40MPa reinforcing concrete disposal	0.001933191	0.001982394	0.001935989	0.001813583	0.002012928
Waste glass disposal	0.000122538	0.000125657	0.000122715	0.000114956	0.000127592
Steel recycling	-5.37×10^{-5}	-5.50×10^{-5}	-5.37×10^{-5}	-5.03×10^{-5}	-5.59×10^{-5}
Steel disposal	1.04×10^{-12}	1.07×10^{-12}	1.05×10^{-12}	9.80×10^{-13}	1.09×10^{-12}
Iron recycling	-3.56×10^{-5}	-3.65×10^{-5}	-3.56×10^{-5}	-3.34×10^{-5}	-3.70×10^{-5}
Iron disposal	6.10×10^{-14}	6.26×10^{-14}	6.11×10^{-14}	5.72×10^{-14}	6.35×10^{-14}
Plastic recycling	-4.91×10^{-8}	-5.04×10^{-8}	-4.92×10^{-8}	-4.61×10^{-8}	-5.11×10^{-8}
Plastic disposal	8.56×10^{-10}	8.78×10^{-10}	8.57×10^{-10}	8.03×10^{-10}	8.91×10^{-10}
Epoxy recycling	1.24×10^{-18}	1.28×10^{-18}	1.25×10^{-18}	1.17×10^{-18}	1.30×10^{-18}
Epoxy disposal	3.41×10^{-14}	3.50×10^{-14}	3.42×10^{-14}	3.20×10^{-14}	3.55×10^{-14}
Glassfibre recycling	2.37×10^{-17}	2.43×10^{-17}	2.37×10^{-17}	2.22×10^{-17}	2.46×10^{-17}
Glassfibre disposal	6.48×10^{-13}	6.65×10^{-13}	6.49×10^{-13}	6.08×10^{-13}	6.75×10^{-13}
Aluminium recycling	-1.27×10^{-6}	-1.30×10^{-6}	-1.27×10^{-6}	-1.19×10^{-6}	-1.32×10^{-6}
Aluminium disposal	5.59×10^{-15}	5.73×10^{-15}	5.60×10^{-15}	5.24×10^{-15}	5.82×10^{-15}
Copper End of the Life	3.23×10^{-8}	3.32×10^{-8}	3.24×10^{-8}	3.03×10^{-8}	3.37×10^{-8}

O&M	0.001007216	0.001032851	0.001008674	0.000944899	0.00104876
Production of PV panels	0.003921458	0.004021265	0.003927133	0.003678833	0.004083204
Solar PV inverter	0.000214639	0.000220102	0.00021495	0.000201359	0.000223492
Multi-Si PV panel recycling	$-2.09x10^{-5}$	$-2.14x10^{-5}$	$-2.09x10^{-5}$	$-1.96x10^{-5}$	$-2.17x10^{-5}$
Multi-Si PV panel disposal	$1.72x10^{-17}$	$1.76x10^{-17}$	$1.72x10^{-17}$	$1.61x10^{-17}$	$1.79x10^{-17}$
Total Impact	0.033000666	0.033840582	0.033048424	0.030958882	0.034361827
The lifetime electricity generation	1265247211	1233844050	1263418821	1348692157	1215127506
The capacity factor	0.30407287	0.296525847	0.303633458	0.32412693	0.292027759

Table SI 10: Life cycle greenhouse gas emissions (in kg CO_{2eq}/kWh electricity) generated in baseline case scenario for SUTPP-PV hybrid power plants (grouped by processes) in Elgin, AZ; Las Cruces, NM; Mercury, NV; Monahans, TX; Panther Junction, TX.

Processes	Elgin, AZ	Las Cruces, NM	Mercury, NV	Monahans, TX	Panther Junction, TX
Production of Materials	0.0275	0.02959	0.02878	0.02961	0.02925
Material Treatment	$2.43x10^{-10}$	$2.61x10^{-10}$	$2.54x10^{-10}$	$2.62x10^{-10}$	$2.58x10^{-10}$
Assembly and Disassembly	$1.83x10^{-5}$	$1.97x10^{-5}$	$1.92x10^{-5}$	$1.97x10^{-5}$	$1.95x10^{-5}$
Material Disposal	0.00189	0.00203	0.00198	0.00204	0.00201
Material Recycling	-0.0001	-0.00011	-0.00011	-0.00011	-0.00011
O&M	0.00093	0.001	0.00097	0.001	0.00099

Table SI 11: Life cycle greenhouse gas emissions (in kg CO_{2eq}/kWh electricity) generated in baseline case scenario for SUTPP-PV hybrid power plants (grouped by processes) in Socorro, NM; Stovepipe Wells, CA; Tucson, AZ; Williams, AZ; Yuma, AZ.

Processes	Socorro, NM	Stovepipe Wells, CA	Tucson, AZ	William, AZ	Yuma, AZ
Production of Materials	0.02989	0.03065	0.02994	0.02804	0.03113
Material Treatment	$2.64x10^{-10}$	$2.71x10^{-10}$	$2.64x10^{-10}$	$2.48x10^{-10}$	$2.75x10^{-10}$
Assembly and Disassembly	$1.99x10^{-5}$	$2.04x10^{-5}$	$2.00x10^{-5}$	$1.87x10^{-5}$	$2.07x10^{-5}$
Material Disposal	0.00206	0.00211	0.00206	0.00193	0.00214
Material Recycling	-0.00011	-0.00011	-0.00011	-0.0001	-0.00012
O&M	0.00101	0.00103	0.00101	0.00094	0.00105

Table SI 12: Life cycle greenhouse gas emissions (in kg CO_{2eq}/kWh electricity) generated in baseline case scenario for SUTPP-PV hybrid power plants (grouped by materials) in Elgin, AZ; Las Cruces, NM; Mercury, NV; Monahans, TX; Panther Junction, TX.

Materials	Elgin, AZ	Las Cruces, NM	Mercury, NV	Monahans, TX	Panther Junction, TX
Glass Walls	0.00382	0.00411	0.004	0.00411	0.00406
Reinforced Concrete	0.0211	0.0227	0.02209	0.02272	0.02245
Sand	0.00016	0.00018	0.00017	0.00018	0.00017
Assembly and Disassembly	$1.83x10^{-5}$	$1.97x10^{-5}$	$1.92x10^{-5}$	$1.97x10^{-5}$	$1.95x10^{-5}$
Turbine & Generator	0.00054	0.00058	0.00057	0.00058	0.00058
Solar PV Panels	0.00379	0.00407	0.00396	0.00408	0.00403
O&M	0.00093	0.001	0.00097	0.001	0.00099

Table SI 13: Life cycle greenhouse gas emissions (in kg CO_{2eq}/kWh electricity) generated in baseline case scenario for SUTPP-PV hybrid power plants (grouped by materials) in Socorro, NM; Stovepipe Wells, CA; Tucson, AZ; Williams, AZ; Yuma, AZ.

Materials	Socorro, NM	Stovepipe Wells, CA	Tucson, AZ	William, AZ	Yuma, AZ
Glass Walls	0.00415	0.00426	0.00416	0.00389	0.00432
Reinforced Concrete	0.02294	0.02352	0.02297	0.02152	0.02389
Sand	0.00018	0.00018	0.00018	0.00017	0.00018
Assembly and Disassembly	$1.99x10^{-5}$	$2.04x10^{-5}$	$2.00x10^{-5}$	$1.87x10^{-5}$	$2.07x10^{-5}$
Turbine & Generator	0.00059	0.00061	0.00059	0.00055	0.00061
Solar PV Panels	0.00412	0.00422	0.00412	0.00386	0.00428
O&M	0.00101	0.00103	0.00101	0.00094	0.00105

Table SI 14: Monthly average temperature distribution in Fahrenheit (°F) in the selected case study locations.

Monthly Temp (°F)	Jan	Feb	Mar	Apr	May	Jun	Jul	Aug	Sept	Oct	Nov	Dec
Elgin, AZ	57.4	59.7	67.5	73.2	80.1	90.1	86.5	86.5	81.7	75.6	65.5	56.5
Las Cruces, NM	53.6	60.1	69.1	76.3	83.5	93.9	92.3	90.5	84.4	74.8	63.3	53.8
Mercury, NV	50.4	53.2	60.8	68.2	76.3	88.7	93.6	91.9	84.7	71.1	59.4	48.2
Monahans, TX	58.5	64.6	74.7	82.2	89.2	96.4	95.9	96.3	87.8	79	67.5	58.3
Panther Junction, TX	61.9	68.5	77.2	83.8	90.1	96.3	93.7	93.6	87.1	81.1	70.5	63
Socorro, NM	47.8	53.2	62.4	69.6	76.8	88.3	87.8	85.6	79.5	69.4	57.7	48
Stovepipe Wells, CA	62	65	72	80	88	101	105	104	97	84	70	60
Tucson, AZ	61.7	64	71.8	78.3	85.5	96.6	94.5	93.9	88.7	81.1	70.9	60.8
Williams, AZ	44.8	47.3	55	62.2	70	82.8	84.4	82.8	77.5	65.3	54.7	44.4
Yuma, AZ	68	72.1	79	85.1	91.6	102.6	105.3	105.1	99.5	87.8	76.6	66

Table SI 15: Average elevation (in ft) and latitude (in °N) of the selected case study locations.

Case Study Locations	Elevation (ft)	Latitude (°N)
Williams, AZ	6772	36.66
Elgin, AZ	4731	36.61
Socorro, NM	4603	35.25
Las Cruces, NM	3996	34.1
Panther Junction, TX	3862	32.7
Mercury, NV	3789	32.32
Monahans, TX	2628	32.22
Tucson, AZ	2490	31.66
Yuma, AZ	203	31.6
Stovepipe Wells, CA	62	29.32

Curriculum Vitae:

Farhana Sharmin
fsharmin@ucmerced.edu | https://farhana-sharmin.jimdosite.com/

EDUCATIONAL BACKGROUND

University of California Davis (CA, United States)
Doctor of Philosophy (Ph.D.) in Energy Systems.
September 2021 – Present

University of California Merced (CA, United States)
Master of Science in Mechanical Engineering.
August 2019 – Present
Advisor: Dr. Marie-Odile Fortier
Thesis: Life Cycle Greenhouse Gas Emissions of Electricity Generated from Solar Updraft Towers
Cumulative Grade Point Average – 4.00/4.00

Bangladesh University of Engineering and Technology (Dhaka, Bangladesh)
Bachelor of Science in Industrial and Production Engineering.
February 2014 – October 2018
Cumulative Grade Point Average – 3.01/4.00

PROJECTS

Estimation and Comparison of Harmful Emissions from the Wildland Fires in California | Developing a One- Dimensional Fuel Cell Model | Analysis of a Fuel cell system using Electrochemical Impedance Spectroscopy (EIS) | An Analysis of Biomethane Capture in California | An assessment of Solar Photo-Voltaic (PV) electricity generation policy of Bangladesh | Solar Updraft Tower Technology and Its Potential Applications to Meet Our Future Energy Demand | Sidney Harbor Bridge, SolidWorks | Automatic Roti Maker | Robotic Arm | Infusion Pump Model | Racing cycle, Catia |FarmCheck, Android Application linked with website and blog (Designed to identify farming-related illnesses and provide viable solutions to the users | Jobdroid BD, Android Application.

HONORS AND AWARDS

Grad Slam 2021 – UC Merced Campus Finalist | Graduate Dean's Advisory Council on Diversity (GDACD) Fellowship award for the Academic Year 2020-2021 | UC ANR Summer Rice Extension and Research Fellowship | School of Engineering ME Graduate Bobcat Fellowship Award | Duke of Edinburgh, Gold Award | Champion in Innovation Challenge 2016 by BUET Career Club | 2ndrunner up in inter-departmental CAD Competition, Dept. of Industrial and Production Engineering, BUET | Champion in inter-departmental CAD contest, Dept. of Mechanical Engineering, BUET| 2ndrunner up in inter-departmental CAD contest, Dept. of Mechanical Engineering, BUET

PROFESSIONAL AND RESEARCH EXPERIENCES

The University of California Merced, School of Engineering
August 2019 – December 2020
Teaching Assistant (TA)
Worked on the grading, leading discussion sessions, and helping students with conceptual problems for the following Courses taught at UC Merced.

- Fall 2019 - Engineering Economic Analysis (ENGR 155)
- Spring 2020 - Engineering Economic Analysis (ENGR 155)
- Fall 2020 - Statics and Dynamics (ENGR 057)

Geospatial Energy Resources & Life Cycle Assessment (GERLCA) Research Group
May 2020 – Present
Graduate Student Researcher (GSR)
Our lab work on modeling emerging energy systems and climate change mitigation strategies and study their environmental impacts using life cycle assessment (LCA)

- Working on efficiency analysis, global warming potential, and geospatial LCA study of the Solar Updraft tower power system and integration of Solar PV with the system in the arid climate of Southwestern United States. (Master's thesis)

International Centre for Climate Change and Development
February 2019 – July 2019
Research Assistant
The International Centre for Climate Change and Development (ICCCAD) is one of the leading research and capacity-building organizations working on climate change and development in Bangladesh. ICCCAD aims to develop a world-class institution that is closely related to local experience, knowledge, and research in one of the countries that are most affected by climate change.

- Worked on developing climate change mitigation strategies and the proper management of resources.
- Participated in several research and development projects related to disaster management and awareness building.

Organization of Islamic Cooperation (OIC)
April 2018 – May 2018
Delegation Liaison Officer (DLO)
45th Council of Foreign Ministers (CFM) of Organization of Islamic Cooperation (OIC) 2018 took place in Dhaka and 120 people were chosen from Bangladesh to help the Ministry of Foreign Affairs Dhaka to organize this great historical event.

- Worked in the Airport Protocol team and helped the VIP delegation with their necessary information, VISA, Immigration, Transportation, and services and kept a record of every delegation, arrival, departure, and updates on events for reporting to the authority.

Microsoft Bangladesh (Dhaka, Bangladesh)
January 2017 – March 2017
Intern
Microsoft Young Bangla program introduces a platform for the youths of Bangladesh to create innovations for greater change.

- Managed a team of five people to fulfill the project and Developed an Android Application for the job-seeking market called Jobdroid BD.

Global Forum on Migration and Development (GFMD)
November 2016 – December 2016
Delegation Liaison Officer (DLO)
9th Global Forum of Migration and Development (GFMD) Summit Bangladesh was organized by the United Nations in collaboration with the Ministry of Foreign Affairs and 81 people were chosen from Bangladesh to work as conference aides in this event.

- Completed the responsibilities with the invitation, Delegation management, and food committee and executed the 4 days long conference successfully.

DBL Group of Industries.
August 2017 – September 2017
Industrial Trainee
A diversified business entity that specializes in the apparel, ceramic, and semiconductor sector. It was a part of our academic degree completion.

- Created a new standard system in apparel design and completed Projects on Error Reduction & 7 Waste management of Color wastage in DBL Group of Industries.

POSTER PRESENTATION

Farhana Sharmin, Prianka B. Zaman. Optimization of Process Parameters for Turning AISI 1060 Steel Using Integrated Taguchi-Response Surface Methodology; Poster presented at 8th BSME International Conference on Thermal Engineering; Dec 19-21, 2018, Dhaka, Bangladesh.

LEADERSHIP AND EXTRACURRICULAR ACTIVITIES

Graduate Dean's Advisory Council on Diversity (GDACD), UC Merced
Council Member
May 2020 – May 2021
The Graduate Dean's Advisory Council on Diversity is dedicated to enhancing and strengthening a culture of open inquiry, pluralism, mutual respect, and engagement among UC Merced graduate students through the work of the council itself and the active advisement of the Dean.

Library and Scholarly Communication (LASC), UC Merced
August 2019 – May 2021
Graduate Student Representative
The Committee on Library and Scholarly Communications (LASC) advises the Chancellor or Chancellor's designee and the Division regarding the administration of the UC Merced Library.

- Attending meetings and discussing the agenda of scholarly needs.

BUET Career Club (BCC)
January 2016 – September 2017
Former Vice President
This club aims to help the students in different career-related matters and form an active network of alumni and students.

- Managed the whole execution of the event, Women Engineers' Congress BUET 2016 by BUET Career Club.
- Managed the whole Design and web development team of BUET Career Club.
- Coordinated the sponsorship and guest management for various events organized by BUET Career Club.

BUET Robotics Society (BRS)
January 2016 – September 2017
Former Organizing Secretary.
These robotics enthusiasts of BUET formed this club to encourage and motivate people to use robotics in research, education, development, and in our day-to-day life to design a better life.

- Organized the national chapter of the International Humanitarian Robotics Competition, Minesweepers 2017, Malaysia as the Country Ambassador under BUET Robotics Society.
- Coordinated the Media and Public relations at the BRS Robo Carnival 2016 organized by BUET Robotics Society (BRS). Prepared regular reports on the club meetings and events.

BUET Entrepreneurship Development Club (BEDC)
January 2016 – January 2017
Former Head of IT and Creative Design.
The objective of this club is to gather the students passionate about entrepreneurship and give them guidance for their life ahead.

- Coordinated the Info-graphics & contents section for the HULT PRIZE at BUET 2017 Competition under this Club.
- Managed the overall social media content and website development team.

- Managed sponsorship and guest and judges for different events

TRAINING AND WORKSHOPS

Climate Tracker Leadership Corps training, Las Vegas, USA (Moved to Virtual Platform)
7th – 9th March 2020
This event talks about the climate crisis, new ways to educate others, inspire action, leadership, and community outreach. We will learn from the Founder and Chairman, former US Vice President and Nobel Laureate Al Gore, and a diverse set of expert speakers.

RISE Youth Mentorship Program by ICCCAD, BRAC C3ER, and BCAS
8th -10th November 2018
RISE (Rethink and Innovate for a Sustainable Environment) focuses on climate change and project management. This program is part of the Climate Finance Transparency Mechanism (CFTM) project under the PROKAS program of the British Council of Bangladesh.

Climate, Culture and Art Symposium by International Centre for Climate Change and Development (ICCCAD)
15th - 17th March 2018
A creative place for the youth to engage with climate change issues, sustainable development goals, and relate with culture.

Bangladesh Youth Leadership Center (BYLC) (Dhaka, Bangladesh)

1. Office of Professional Development -17 (OPD) Workshop
6th October - 7th October 2017
The Office of Professional Development (OPD) is a new initiative of BYLC designed to support the BYLC graduates with their right careers.

2. Master Class on Leadership
15th July – 18th July 2017
Master class on leadership is designed to prepare the future facilitators of different BYLC programs so that, they can develop active skills of teaching and guiding.

3. Youth Leadership Bootcamp- 04
9th February- 12th February 2017
A 4 days long workshop took place at Sreemangal, Bangladesh with 105 participants to train them to actively exercise leadership for the greater purpose and development of the society.

ADDITIONAL SKILLS

Skills - 3D and 2D animation | 3D CAD (Motion, Animation, and Simulation) | Programming | Graphics Design | Video Editing | Logo, T-shirt, Poster, and Banner design | Proficient in Bangla, English, and Arabic speaking, writing, and listening.

Expertise in Software and Programming Language - SolidWorks | Catia | Python | C, C++| ArcGIS | Microsoft Word, Excel, PowerPoint | Adobe Photoshop | Adobe Illustrator | Adobe After Effects | Blender